รายงานการวิจัยฉบับสมบูรณ์

การศึกษาประสิทธิภาพของตัวเร่งปฏิกิริยาเพื่อเปลี่ยนเอทานอลเป็นแก๊สโซลีน

The Catalytic Conversion of Ethanol to Gasoline with High Performance.

รศ.ดร.ตะวัน สุขน้อย

ได้รับทุนสนับสนุนงานวิจัยจากงบประมาณเงินรายได้ ประจำปีงบประมาณ พ.ศ.2560 คณะวิทยาศาสตร์

สถาบันเทคโนโลยีพระจอมเกล้าเจ้าคุณทหารลาดกระบัง

ชื่อโครงการ การศึกษาประสิทธิภาพของตัวเร่งปฏิกิริยาเพื่อเปลี่ยนเอทานอลเป็นแก๊สโซลีน
แหล่งเงิน งบประมาณเงินรายได้
ประจำปีงบประมาณ 2560 จำนวนเงินที่ได้รับการสนับสนุน 150,000 บาท
ระยะเวลาทำการวิจัย 1 ปี ตั้งแต่ 1 ตุลาคม 2559 - 30 กันยายน 2560
หัวหน้าโครงการวิจัย รศ.ดร.ตะวัน สุขน้อย ภาควิชาเคมี คณะวิทยาศาสตร์

Abstract

In this project the conversion of ethanol to gasoline over metal transition loaded H-ZSM-5 zeolite catalysts was investigated. Catalysts were prepared by impregnation of copper, nickel, cobalt and sliver on suitable support, such as silica and zeolites H-ZSM-5. The influence of reaction conditions, such as contact time (5-42 g·h/mol), the effect of temperature (325-500°C), and acidic property (Si/Al ratio: 12.5 and 28) were investigated. The Cu/SiO_2 gives high conversion and selectivity for acetaldehyde, nonetheless, shows a rapid deactivation rate due to the metal sintering. Ni/SiO_2 and Co/SiO_2 exhibit lower activity and give undesired products, methane and carbon monoxide from decarbonylation of ethanol. Although Ag/SiO_2 gives a low conversion, a high acetaldehyde selectivity is obtained. The dehydrogenation activity is thermodynamically enhanced at high temperature. However, a small fraction of decarbonylation was also observed in parallel.

Over H-ZSM-5 catalyst, rate of ethylene oligomerization is relatively low, as compared to the rate of dehydration, because the reaction initially proceeds via primary carbocation. As the acidity is increased, the formation of intermediate hydrocarbons is enhanced due to the close proximity of the acid sites. The oligomerization of ethylene to higher hydrocarbons can be promoted at temperature higher than 400°C. However, the severe deactivation is observed at 425°C. The presence of silver in the catalyst can promote dehydrogenation of ethanol to acetaldehyde and conversion of both ethylene and acetaldehyde to higher hydrocarbons. Over the acid site, it is found that rate of aldol condensation seems to be faster than the rate of ethylene oligomerization, depending on the contact time.

Keywords : ethanol, aldol condensation, gasoline

กิตติกรรมประกาศ

ขอขอบคุณสมาชิกกลุ่มวิจัย Catalytic Chemistry Research Unit และเจ้าหน้าที่ นักวิทยาศาสตร์ ประจำภาควิชาเคมี คณะวิทยาศาสตร์ ทุกท่านที่ให้การช่วยเหลือในการวิจัยครั้งนี้ เป็นอย่างดี

การวิจัยครั้งนี้ได้รับทุนสนับสนุนการวิจัยจากสถาบันเทคโนโลยีพระจอมเกล้าเจ้าคุณทหารลาดกระบัง จากงบประมาณเงินรายได้ ประจำปีงบประมาณ พ.ศ.2560

รศ.ดร.ตะวัน สุขน้อย

สารบัญ

หน้า

สารบัญ (ต่อ)

หน้า

สารบัญ (ต่อ)

หน้า

สารบัญตาราง

ตารางที่ **หน้า**

สารบัญภาพ

ภาพที่ **หน้า**

บทที่ 1
บทนำ

1.1 ความเป็นมาและความสำคัญของปัญหา

For renewable fuel, gasoline can be produced from acid-catalyzed dehydration of ethanol and oligomerization over H-ZSM-5 zeolite as below. Acidic property of H-ZSM-5 is probably a main point that directly determines ethanol dehydration to ethylene and secondary reactions (i.e. oligomerization) of ethylene to gasoline or longer chain hydrocarbons [1].

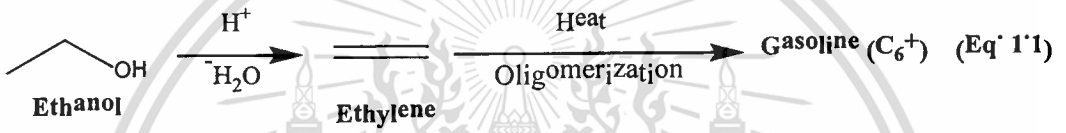

The improvement of Si/Al ratio on H-ZSM-5 framework is the common way to significantly enhance the acidic property and hence the activity [2]. Although ethanol dehydration over acid site to ethylene is more rapid and thermodynamically favored at high temperature, the oligomerization of ethylene to gasoline is highly exothermic and relatively slow [3-4]. Accordingly, dehydrogenation of ethanol to acetaldehyde followed by aldol condensation to higher aldehyde and higher alcohol is proposed to increase rate of the oligomerization. The higher alcohol can be readily dehydrated over acid catalysts into hydrocarbon as shown in (Eq. 1.2). In this approach, H-transfer plays significant role for ethanol conversion to hydrocarbons.

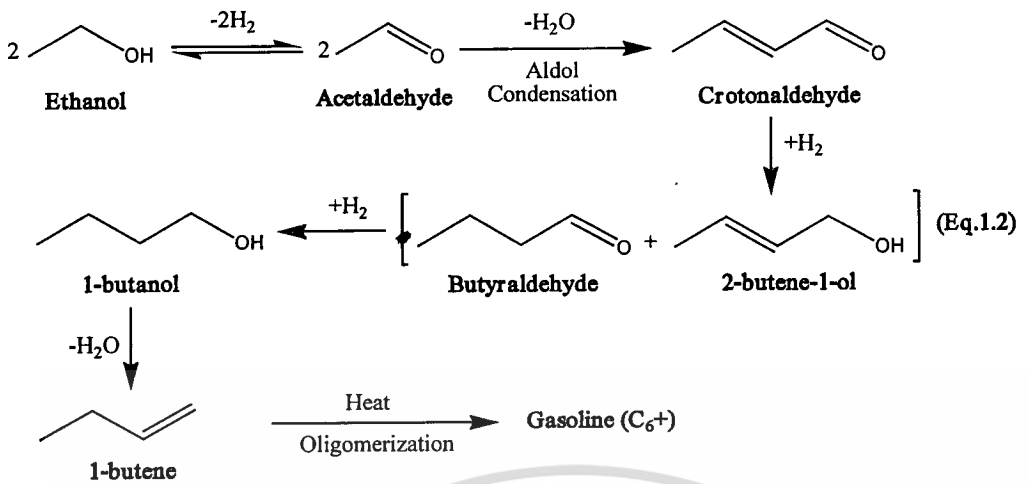

For the above concept, bi-functional catalyst is required. The dehydrogenation promoted by metal catalysts whiles the aldol condensation and dehydration can be performed over acidic part in the bi-functional catalyst. The transition metals, for example, silver, cobalt and nickel are typically used as the catalyst for dehydrogenation because they are low cost, as compared to rhodium, palladium and platinum. As aldol condensation of aldehyde is readily promoted, the metal phase indicates a key role in controlling ethanol conversion to acetaldehyde as well as higher products. Among acid catalyst, H-ZSM-5 possesses high surface area and thermal stability [5]. Moreover, H-ZSM-5 has been considered as the most selective catalysts for the ethanol to gasoline process due to its unique structural properties that selectively produce light hydrocarbon mixtures similar to motor gasoline [6]. However, dehydrogenation and dehydration is endothermic and preferred at high temperature. While aldol condensation is exothermic and generally operated at low temperature. In this work, the optimization of reaction conditions is required. In addition, types of metal and effect of contact time on both dehydrogenation and aldol condensation was studied. Moreover, acidic property of H-ZSM-5 that effects aldol condensation was investigated.

1.2 วัตถุประสงค์ของโครงการวิจัย

1. To product gasoline from ethanol via the dehydrogenation and aldol condensation approach.
2. To understand the mechanism of dehydrogenation and aldol condensation reaction over bi-functional catalyst.

3. To understand the effect of temperature, contact time, acidic property and types of metals.

1.3 ขอบเขตของโครงการวิจัย

The scopes of this special project are as follows:

1. Catalyst preparation by wetness impregnation of sliver, nickel, cobalt and copper on suitable support, such as silica and zeolites H-ZSM-5.
2. Characterization of catalyst by X-Ray Diffraction spectroscopy (XRD), X-ray Fluorescence (XRF), Temperature Programmed Reduction (TPR), Temperature Programmed Desorption (TPD), Brunauer Emmett Teller technique (BET) and Transmission Electron Microscopy (TEM).
3. Testing on ethanol dehydrogenation and subsequent aldol condensation of the products over various catalysts in a continuous fixed-bed reactor.
4. Investigation on the effect of temperature (325-500°C), contact time (5-42 g.h/mol), type of metal (silver, nickel, cobalt and copper) and acidic property (Si/Al ratio: 12.5 and 28) on dehydrogenation and aldol condensation reaction.
5. Analysis and quantification of liquid products from the reactions by online gas chromatograph equipped with a flame ionization detector (GC-FID).

1.4 วิธีดำเนินการวิจัย

1. Catalyst Preparation and modification

   1.1 Preparation of H-ZSM-5 Support

   1.2 Preparation of metal supported on silica catalysts.

   1.3 Preparation of 10%wt. Silver Supported on Silica (Ag/SiO2) physical mixed with H-ZSM-5 Catalysts (H-ZSM-5).

   1.4 Impregnation of Silver Supported on H-ZSM-5 (Ag/H-ZSM-5)

2. Characterization of catalysts

   2.1 X-ray diffraction (XRD)

   2.2 X-ray fluorescence (XRF)

   2.3 Surface area analysis

   2.4 Temperature programmed reduction (TPR)

2.5 Temperature programmed desorption (TPD)

2.6 Transmission electron microscopy (TEM)

3. Catalytic Activity testing

3.1 Investigate the effect of type of metals.

3.2 Investigate the effect of contact time of silver.

3.3 Investigate the effect of dehydrogenation temperature

3.4 Investigate the effect of contact time of H-ZSM-5 (12.5)

3.5 Investigate the effect of Si /Al of H-ZSM-5

3.6 Investigate the effect of dehydration temperature

3.7 Investigate the effect of metallic silver physical mixture and impregnation

3.8 Investigate the effect of contact time of Ag/H-ZSM-5 (28)

4. Products analysis

4.1 Determine the amount of product by gas chromatograph equipped with flame ionization detector (GC-FID).

1.5 ประโยชน์ที่คาดว่าจะได้รับ

New technology for production of gasoline from ethanol can be obtained. This technology can benefit from raw materials available in the country.

บทที่2
ทฤษฎีและงานวิจัยที่เกี่ยวข้อง

2.1 Ethanol

2.1.1 Ethanol production [7]

Ethanol is an important renewable energy as it can be produced from agricultural feedstock by fermentation in anoxic environment. In the most of the fermentation, ethanol is made from cone. However, it can be produced other agricultural raw materials such as sugarcane, potato, cassava, and cellulose. In addition, ferment garbage to ethanol was studied [8]. The fermentation of sugarcane and corn can use yeast for ethanol directly. Starches (from potato, cassava) must first be hydrolyzed by enzymes amylase to fermentable sugar. While, cellulose (from wood, paper) similar to starches must hydrolyzed by acids before fermentation. Generally the fermentation of three types can produce ethanol with 10% concentration, then the mixture is separated and purified, usually by distillation and dehydration.

2.1.2 Alcohol fuel [9]

Although fossil fuels have become dominant energy resource for the modern world and it is essential in daily life, this fossil energy is decreased and there is the pollution problem. Utilization of ethanol from fermentation of biomass gained considerable interest as fuel in the past several years. Ethanol is commonly used to power other vehicles such as farm tractor and car by mixing in gasoline, so called gasohol. There are different percentage of ethanol i.e. E10 and E85. This blending percentage of ethanol into gasoline for cleaner combustion, decreased carbon monoxide and hydrocarbon exhaust emission [10]. It is a common practice to use anhydrous ethanol (99.5% purity). However, hydrated ethanol (95% purity) for blending gasoline is also used widely. In addition, ethanol can be additive in fuel to increase octane number for engine replace methyl tertiary butyl ether (MTBE), because MTBE is more toxic chemicals that has been found to contaminate groundwater.

E10, a fuel mixture of 10% anhydrous ethanol and 90% gasoline by volume, it was used during the 1970 oil crisis due to the world energy shortage and this fuel has been

used until now [11]. In Thailand called gasohol 91 and gasohol 95, is fuel can be used in common vehicles without need for any modification on the engine or fuel system. In addition, E10 can reduce carbon monoxide (CO) 20 to 30%, increase octane number from 2 to 3 higher than regular gasoline and reduced greenhouse gas such as carbon dioxide (CO_2) emission upto 2.4 to 2.9% [10]. Also, Thailand has shown that the emission rates of benzene, toluene, and xylene are decreased in cars using E10fuel [12]. This decrease in emission is important due to the major health effect (including leukemia) of long-term inhalation of benzene and toluene [13].

E85, a blend of 85% anhydrous ethanol and 15% gasoline by volume, it is used to operate spark-ignited engines that have been modified to accept this fuel. Unlike E10, E85 cannot directly used in spark-ignited engines that have not been modification due to higher mixture ratio of ethanol per gasoline and corrosion to some material, such as fuel injection, fuel delivery system, and tank. This has led to the development of a new type of vehicle, called a Flexible Fuel Vehicle, or FFV, which can operate using various blends of alcohol from 0% (gasoline) to 85% (E85) by volume. This FFV are designed and improved using E85 compatible materials due to the different type of fuel-air mixture of gasoline and E85, for example size of the fuel delivery system to compensate the increased volumes of fuel when using E85. The ignition timing can improve engine performance.

2.2 Dehydrogenation of ethanol [14, 15]

Dehydrogenation is a chemical reaction that involves the removal of hydrogen from a molecule. It is the reverse process of hydrogenation. The first step in this process is ethanol adsorption on the catalyst surface by O atom of hydroxyl group attached on the metal surface (such as Ag) to produce η^1 (O)-alcohol species (a). After that, dissociation of O-H bond is generated alkoxide intermediate. Finally the dehydrogenation of ethanol can occur via an alkoxide intermediate to produce acetaldehyde with a metal hydride (di-hydride). In addition, η^2 (C, O)-alcohol species (b) can occur with ethanol by α-C and O atom attached on metal surface (such as Co, Ni) to form acyl intermediate (η^1 (C)-acyl) that may well desorp as acetaldehyde. However, yield of acetaldehyde obtained from

η^2 (C, O)-alcohol species is less than that from η^1 (O)-alcohol species because formation of the acyl intermediate can lead to decarbonylation to CH_4 and CO in **Figure 2.1.**

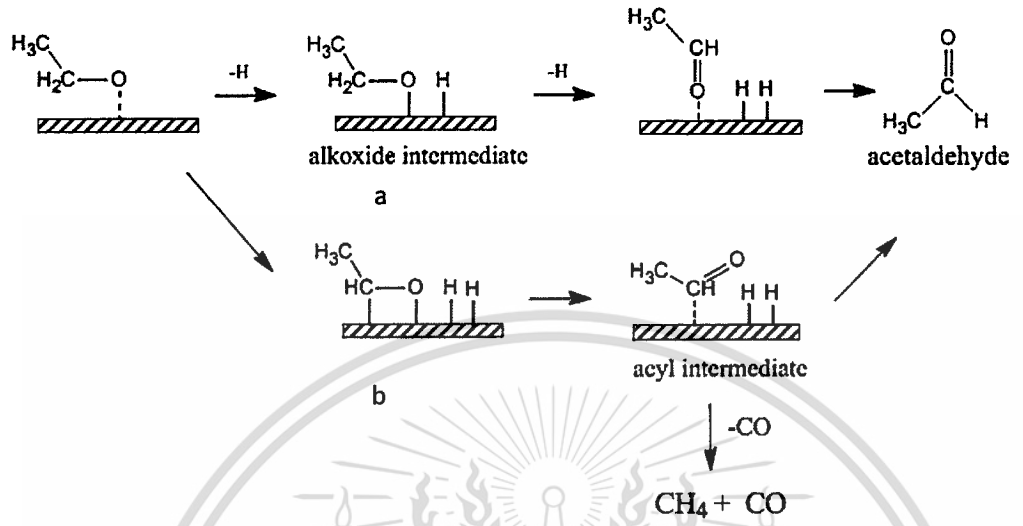

Figure 2.1 Dehydrogenation of ethanol (a) η^1 (O)-alcohol species. (b) η^2 (C, O)-alcohol species.

2.3 Aldol condensation of aldehyde [16, 17]

Aldol reactions can occur under acid catalysis, in which the reaction generally leads to the α,β- unsaturated product by direct dehydration of the β- hydroxyl aldehyde intermediate. When an acid catalyst is used, the first step in the reaction mechanism involves acid-catalyzed tautomerization of the carbonyl compound to the enol. The acid also serves to activate the carbonyl group of another molecule by protonation, rendering it highly electrophilic. The enol is nucleophilic at the α-carbon, allowing it to attack the protonated carbonyl compound, leading to the β-hydroxyl aldehyde intermediate after deprotonation. This usually dehydrates to give the unsaturated carbonyl compound. The scheme shows a typical acid-catalyzed self-condensation of an aldehyde.

Acid-catalyzed aldol mechanism

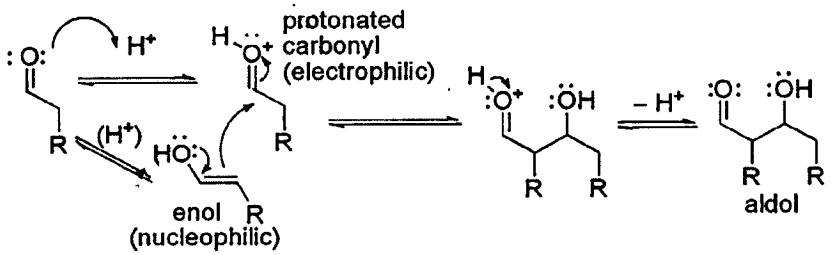

Acid-catalyzed dehydration

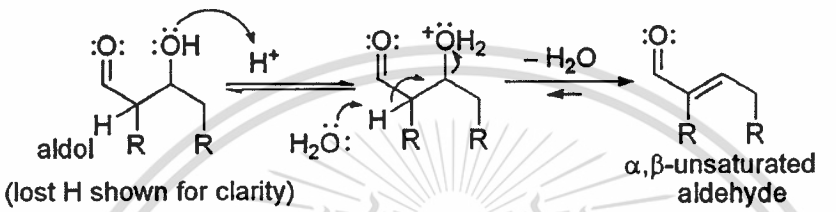

2.4 Hydrogenation [17, 18]

Hydrogenation is a chemical reaction between molecular hydrogen (H_2) and another compound, usually in the presence of a catalyst such as nickel, cobalt, palladium or platinum. The process is commonly employed to reduce or saturated organic compounds. The hydrogenation typically constitutes the addition of pairs of hydrogen atoms to a molecule, generally an alkene. The first step of alkene, C=C double bond, adsorbed on the catalyst surface and H_2 dissociates follow by an H atom bonds to one C atom. While other C atom is still attached to the surface. Finally a second C atom bonds to an H atom and then the molecule leaves the surface to alkane. Additionally, the formyl group can be readily reduced to a primary alcohol ($-CH_2OH$).

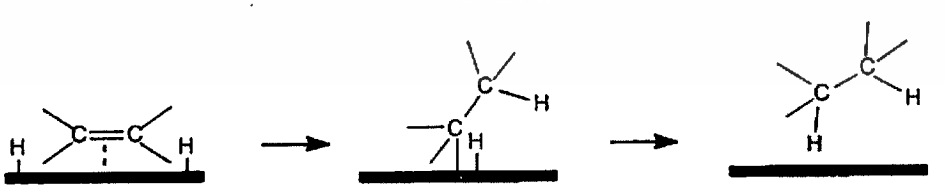

Figure 2.2 Hydrogenation of alkene.

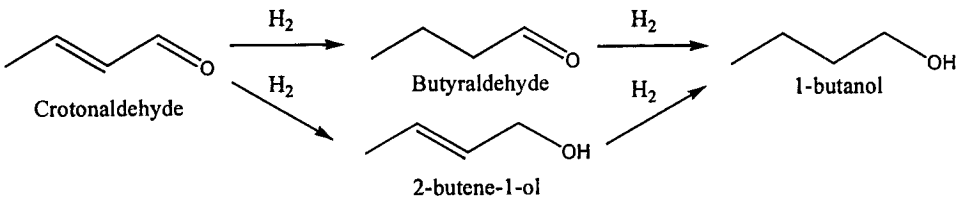

Figure 2.3 Hydrogenation of formyl group.

2.5 Dehydration of ethanol [17]

Dehydration reaction is a chemical reaction that involves the loss of a water molecule from the reacting molecule. The reverse of a dehydration reaction is a hydration reaction. The dehydration may go by either the E1 or E2 mechanism, with primary alcohols favoring the E2 mechanism, and secondary and tertiary alcohol generally reacting by the E1 mechanism. The first step of either mechanism involves protonation of the hydroxyl oxygen atom by the acid, in order to convert the -OH group into a better leaving group, $-OH_2^+$.

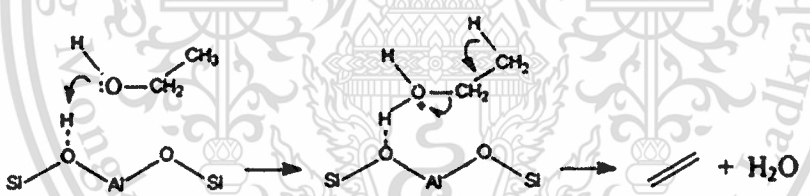

Figure 2.4 Acid catalyzed dehydration of ethanol to produce ethylene

2.6 Oligomerization [19, 20]

Oligomerization is chemical process that converts light olefins, usually propylene, butylene or their mixtures, contained in mixtures with light paraffins to higher hydrocarbon over catalysis or heat. In this process (ETG), olefins which obtained from dehydration reaction will be reacts with other olefins to forms heavier olefinic compounds follow by hydrogenation to higher hydrocarbon. For example, in previous research, the oligomerization is promoted by H-ZSM-5 as catalyst in important step of the Mobil olefin-to-distillate-and-gasoline process . When operated at relatively low temperature and high

pressure (300-200°C, 20-105 atm.), the products are higher molecular weight iso-olefins . Under these conditions light olefins are first converted to high oligomers. Subsequently, isomerization and cracking give intermediate C_4-C_7 olefins. Finally the latter participate in copolymerization to yield the product.

2.7 Catalyst

2.7.1 ZSM5 zeolite [21-28]

Zeolite ZSM-5, Zeolite Socony Mobil-5, is one type of family zenolite, it has shape selective catalysts with unique channel structures. The secondary building unit of framework of ZSM-5 including mor 8T, case 12T, mel 14T, and mfi 14T shown in **Figure 2.5** These secondary building units can be connected to form sheet and the linking of the sheet lead to a three dimensional framework structure by the chains extend along the *z*-axis. The sheets parallel to [010] and [100] are shown in **Figure 2.6** and **2.7**

mor 8T case 12T mfi 14T mel 14T

Figure 2.5 The secondary building unit of framework of ZSM-5

Figure 2.6 shows that the *x*-axis is horizontal and the *z*-axis vertical and the 10-membered ring apertures shown are the entrances to the straight channels which run parallel to [010] plane. While, Figure 2.7 shows that the *y*-axis is horizontal and the *z*-axis vertical and the circular 10-membered ring apertures shown are the entrances to channels which run parallel to [100] plane.

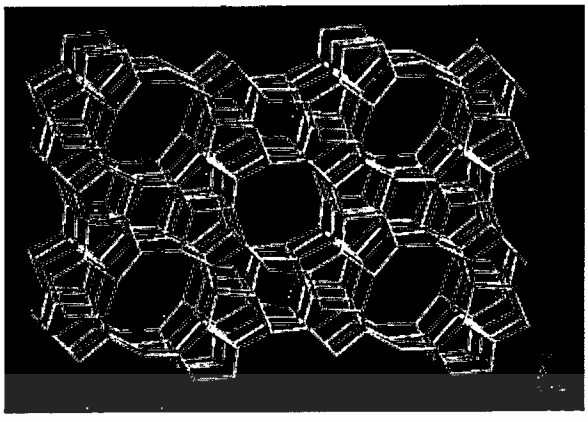

Figure 2.6 Skeletal diagram of the [010]-plane of the ZSM-5 unit cell.

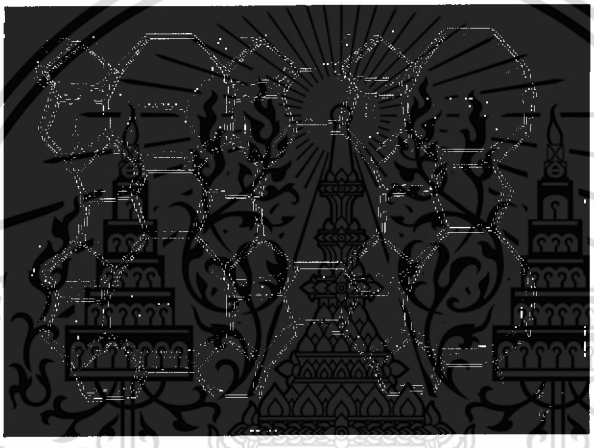

Figure 2.7 Skeletal diagram of the [100]-plane of the ZSM-5 unit cell.

ZSM-5 has chemical formula is $Na^{+}_{n}\ (H_2O)_{16}|\ [Al_nSi_{96-n}\ O_{192}]$-MFI , $n < 27$. It is widely used in many catalytic reaction of industrial interest such as xylene isomerization, benzene ethylation, and ethanol, methanol- to- gasoline conversion. Their individual catalytic properties are mainly due to their regular framework with a pore size which is intermediate to the large pore sized zeolites (for instance, zeolites X and Y) and the small pore sized zeolite (for instance the A zeolite). The shape selectivity of the pentasil zeolite is catalytically expressed by many features, such as;

1. The sieving effect, i.e. the capability of zeolite to admit in to its pores or to reject reactive molecules having a critical diameter falling within a well defined range;
2. The (reverse) sieving effect, i.e. the capability of the zeolite to allow product molecules having a certain critical diameter to diffuse out of its pores. Thus, in the case of a

product molecule having a diameter exceeding to the pore size of the zeolite, this molecule will have to undergo cracking or rearrangement into a smaller molecule before diffusing out of the zeolite

3. The effect on the reaction intermediates, i.e. the capability of certain active site to determine the length and structure of reaction intermediate secies.

ZSM5 zeolite has pore system which is believed to be significant for their low coke formation. While most industrial applications of zeolite catalyst make use of these in acid form, zeolite is also excellent support for metal species. Zeolite supported metal species called a bifuntional catalyst is an acid zeolite on which a metal species phase is deposited. The function of the metal is to catalyze dehydrogenation and hydrogenation reaction while H- ZSM- 5 possesses excellent dehyadration and oligomerization properties which bifunctional catalyst can further undergo a variety of metal species and acidity reactions to form desirable product.

2.8 งานวิจัยที่เกี่ยวข้อง

In several researches, such as ETG process (ethanol to gasoline), gasoline can be produced from dehydration of ethanol and oligomerization over H-ZSM-5 zeolite. However, ethanol dehydration to ethylene favored at high temperature while the oligomerization of ethylene to gasoline is highly exothermic relatively slow.

Nagabhatla Viswanadham et al., tested conversion of ethanol to gasoline for production of higher aromatic. The catalyst includes micro H-ZSM-5 Si/Al ratio~30, micro H-ZSM-5 Si/Al ratio~100, and nano ZSM-5 Si/Al ratio~30. The acidity, porosity and catalytic performance were compared, at 450 and 500°C. It found that nano H-ZSM-5 catalyst having high acidity and mesoporosity showed higher production of aromatics yields for gasoline, as compared to micro H-ZSM-5 with Si/Al ratio~30 and micro H-ZSM-5 with Si/Al ratio~100. The aromatic yield is increased from 38.6 wt% to 50.6 wt% when temperature is increased from 450°C to 500°C over nano H-ZSM5 catalyst [5].

Xianlong Zhang et al., studied hydrothermal synthesis of 1-butanol from ethanol over metal with $NaHCO_3$ as catalyst. The different metal (Fe, Co, Ni, Raney Cu, copper chromite, $CoCO_3$, and Co_2O_3), effect of ethanol concentration (0.10-0.25 mol), $NaHCO_3$ (0.005-0.025 mol), and cobalt powder (0.005-0.015 mol) were compared at 200°C for 3 days. It was found that the optimized hydrothermal reaction conditions were 0.15 mol of ethanol, 0.01 mol of $NaHCO_3$, and 0.005 mol of Co powder. After that, the effects of the reaction time (1-30 days) and reaction temperature (140-240 °C) were also investigated. It was found that the yield of 1-butanol is increased with reaction time and then remained constant the maximum (9.8 mol %) after 20 days. However, the selectivity to 1-butanol decreased from 74% to 62% when the reaction time changed from 1 to 30 days. In addition, the variation of reaction temperature showed that the yield of 1-butanol is increased from 1.2 to 5.5 mol % with temperature (from 140 to 240°C). The selectivity to 1-butanol is increased from 50% to 74% when the reaction temperature is increased from 140 to 180°C and then remained constant (around 70%) even at a higher reaction temperature up to 240°C [29].

S. Totong et al., studied the hydrogen production from catalytic dehydrogenation of ethanol through at low temperature (<500°C). Copper (Cu) silver (Ag) and bimetallic metal (Ag-Cu) supported on silica (SiO_2) were compared at 300-375°C. The hydrogen production from ethanol dehydrogenation using bimetallic catalyst (Ag-Cu/SiO_2) was found to be higher (40%) when compared to the monometallic (Cu/SiO_2 and Ag/SiO_2) at low temperature (300°C). However, the yield hydrogen is decreased due to ethanol cracking to other hydrocarbon compound such as C_2H_6 and C_2H_4 at higher temperature over Ag-Cu/SiO_2 [30]

บทที่ 3
วิธีดำเนินการวิจัย

3.1 Chemical reagents

Chemical reagents	Grade of purity	Manufacturers
1. Silver nitrate ($AgNO_3$)	99.6%	BAKER ANALYZED (A.C.S. REAGENT)
2. Nickel nitrate hexahydrate ($Ni(NO_3)_2{\cdot}6H_2O$)	99%	CARLO ERBA
3. Cobalte nitrate hexahydrate ($Co(NO_3)_2{\cdot}6H_2O$)	98.0%	LABORATORY REAGENT (RANKEM)
4. Copper nitrate trihydrate ($Cu(NO_3)_2{\cdot}3H_2O$)	99.5%	QREC New Zealand
5. Absolute ethanol (CH_3CH_2OH)		
6. Sillicon dioxide (SiO_2)	99.0%	CARLO ERBA
7. NH_4-ZSM-5 (Si/Al = 28)		ZEOLYST INTERNATIONAL
8. NH_4-ZSM-5 (Si/Al = 180)		ZEOLYST INTERNATIONAL
9. Deionized water		
10. Air zero gas, high purity	99.99%	PRAXAIR
11. Hydrogen gas, high purity	99.99%	PRAXAIR
12. Nitrogen gas, high purity	99.99%	PRAXAIR

3.2 Apparatus and instruments

1. Catalytic testing rig
2. Mass flow controller (BROOKS INSTRUMENT LLC)
3. Hot air oven
4. Tube furnace with a programmed temperature controller (CARBOLITE)
5. Heating rod with a programmed temperature controller
6. Clamp
7. Gas chromatograph (Model 910, BUCK SCIENTIFIC)
8. Laboratory glassware
9. Laboratory plastic ware
10. Trap condenser
11. Syringe (5 ml)
12. Syringe pump
13. Vial
14. Sieve (U.S.A standard sieve, AASHO N-92)
15. X-ray powder diffractometer (D8 Advance, Bruker AG)
16. X- ray fluorescence spectrometer (Wavelength Dispersive, Philips, PW2400, Scientific and Technological Research Equipment Centre 2- 3 Building, Chulalongkorn University) and (Energy Dispersive, Oxford, ED- 2000, Scientific and Technological Research Equipment Centre 2-3 Building, Chulalongkorn University)
17. Gas adsorption analysis (Autosorb-1C, Quantachrome)
18. Temperature programmed reduction (TPR, Model TCD2-NIFED)
19. Temperature programmed desorption (TPD, Model TCD2-NIFED)
20. Transmission electron microscopy (JEM-2100, JEOL, Japan)

3.3 Catalyst Preparation and modification

3.3.1 Preparation of H-ZSM-5 Support

A powder of NH_4-ZSM-5 with Si/Al ratio of 12.5 and 28 were calcined in the tube furnace with programmable temperature controller at 500°C for 5 h to make a proton form.

3.3.2 Metal Supported on Silica Catalysts (M/SiO_2).

The metal supported silica (SiO_2) catalysts (10 grams) with different type of loaded metals (Co, Ag, Ni and Cu) were prepared by wet impregnation method.

In the first step, 10 %wt. Co supported on SiO_2 (Co/SiO_2) was impregnated using cobalt nitrate hexahydrate ($Co(NO_3)_2{\cdot}6H_2O$) solution as a metal precursor as the preparation shown in Table 3.1.

In a similar procedure, 10% wt. Ag, 10% wt. Ni and 10% wt. Cu on SiO_2 was subsequently impregnated using $AgNO_3$, $Ni(NO_3)_2{\cdot}6H_2O$ and $Cu(NO_3)_2{\cdot}3H_2O$ solution respectively. After that, the solid was dried in an oven at 70°C for 24 hours. The prepared catalyst was calcined in a horizontal tube furnace under a flow of air zero (60 ml/min) at 450°C with a heating rate of 2°C/min and hold at that temperature for 5 hours. Finally, the catalyst was pressed, crushed, and sieved into 600-850 μm.

Table 3.1 Preparation of metal supported on silica catalysts

Catalyst	Metal precursor	Weight of metal procure (g)	Deionization Water (ml)	SiO_2 (g)
10%wt.Co/SiO_2	$Co(NO_3)_2{\cdot}6H_2O$	4.9648	16.9	9.10
10%wt.Ag/SiO_2	$AgNO_3$	1.6083	9.3	9.08
10%wt.Ni/SiO_2	$Ni(NO_3)_2{\cdot}6H_2O$	5.0571	17	9.03
10%wt.Cu/SiO_2	$Cu(NO_3)_2{\cdot}3H_2O$	2.8	15.6	9.0

3.3.3 10%wt. Silver Supported on Silica (Ag/SiO_2) physical mixed with H-ZSM-5 Catalysts (H-ZSM-5).

The 10%wt silver supported on silica was physical mixed with H-ZSM-5 (Si/Al ratio 28) at the mass ratio of Ag/SiO_2 : H-ZSM-5 = 0.074 : 0.085 and then the catalyst has ground. Finally, the catalyst was pressed, crushed, and sieved into 600-850 μm.

3.3.4 Impregnation of Silver Supported on H-ZSM-5 (Ag/H-ZSM-5)

The 10 g of silver supported on H-ZSM-5 (Si/Al ratio 28) catalyst was prepared by wet impregnation method. In the first step, 1.2481 g. of silver nitrate ($AgNO_3$) was dissolved in 7.3 ml deionized water and used as metal precursor. After that 9.76 g of H-ZSM-5 was impregnated by this solution. The solid was dried in an oven at 70°C for 24 hours. Then, the dried catalyst was calcined in a horizontal tube furnace under a flow of air zero (60 ml/min) at 550°C for 5 hours with a heating rate at 5°C /min.

3.4 Characterization of catalysts

3.4.1 X-ray diffraction (XRD)

X-ray diffraction (XRD) is the technique used for determined crystal structure of the catalysts. CuK_α was used as analytical X-ray source at 30 kV and 40 mA. The sample is prepared by spreading catalyst over sample holder and placed into the instrument. The XRD analysis was scanned from 2θ = 5 to 90°C with 1 sec/step time and 0.04 2θ/step increment.

3.4.2 X-ray fluorescence (XRF)

X-ray fluorescence (XRF) is the emission of characteristic "secondary x-ray" (or fluorescent), which is x-rays from a material that has been excited by bombarding with high-energy X-rays. Each element has electronic orbitals of characteristic energy. The removal of an inner electron by an energetic photon was provided by a primary radiation source, following by the moving of an electron from an outer shell into that vacancy and released energy call secondary electron or fluorescent. The released energy is a characteristic

radiation that tells the composition of the sample. This technique can be done according to the following procedure: 0.5 g of catalyst sample was mixed with 4.5 g boric acid, and compressed into alumina pan before bring into the XRF sample holder in XRF instrument.

3.4.3 N_2-Gas adsorption analysis

Gas adsorption analysis is the technique generally used for determining surface area and pore size distribution of a solid catalyst. This technique can be done according to the following procedure: the catalyst sample was weighed about 100 mg and transferred to a cleaned, dried sample cell. This sample cell was attached to the outgassing station. Then, a heating mantle was installed with the sample cell and the temperature was raised to 300 °C for 12 h. After the residual gas was removed by heating under vacuum, nitrogen adsorbate was filled by opening the gas inlet valve. The sample cell was attached to the sample station. Initially, a dewar flask of liquid nitrogen was placed around the sample cell. Nitrogen adsorbate pressure can be regulated by 1 torr transducer with 3 minutes equilibration time and 0 scaled tolerances. .

3.4.4 Temperature programmed reduction (TPR)

Temperature-programmed reduction (TPR) provides information on the active site species of the catalysts by monitoring their reducibility. Temperature programmed reduction was measured using thermal conductivity detector (TCD). The sample weighed 1.0 g was placed into a quartz tube reactor, which was located inside a temperature-regulated furnace. Prior to the H_2-TPR, each sample was heated to its calcinations temperature in air zero for 3 h (25 mL/min) and cooled to 50°C. The heating rate of 2°C/min, the 5% H_2 in Ar flow of 25 mL/min was applied for TPR analysis. Water produced during the reduction process will be removed in a U-shape glass trap at -70°C (vapor of liquid N_2) before entering the TCD.

3.4.5 Temperature programmed desorption (TPD)

Ammonia is probably the most frequently used probe molecule for acidity assessment. Its small molecular size allows one to probe almost all acid sites of both micro and mesoporous materials. NH_3 - temperature- programmed desorption (NH_3 - TPD) experiments was carried out using a TCD detector. Before adsorption, the sample (2.0 g) as heated to its calcinations temperature in air zero for 2 h (30 mL/min) and cooled to 30°C. The adsorption of NH_3 was performed at 30°C. After saturation, the sample will be flushed with He at this temperature for 1 h. TPD measurements was done from 35 to 800°C with a heating rate of 10°C/min, using He as a carrier gas.

3.4.6 Transmission electron microscopy (TEM)

Transmission electron microscope (TEM) was used to study the morphology of catalyst and dispersion of metal supported catalyst. TEM uses a beam of highly energetic electron (voltage 80–120 kV) and signals from TEM depending on the sample density and thickness. Electrons that pass through the sample without energy loss it shows bright filed image and electrons are diffracted (scattered) by particles obtain dark-field images at magnification of 100,000–120,000x.

3.5 Catalytic Activity testing

Gas phase catalytic conversion of Ethanol was investigated at atmospheric pressure in a continuous fixed-bed reactor made with glass tube (8.0 mm O.D.). Schematic of the catalytic testing rig is shown in **Figure 3.1.** The catalyst bed was packed in the middle of the reactor and topped with glass wool and glass beads. The reactor was then installed inside a temperature-controlled electrical furnace. The gas flows were controlled by the mass flow controllers and checked by bubble flow meter. Before the catalytic testing, the catalyst was activated by heating at 2°C/min to its calcinations temperature (450°C) and was hold at that temperature for 1 hour under the stream of air zero (30 ml/min). Then N_2 was flowed to eliminate the remaining air zero in the line. Finally, the gas stream was switched to a flow of H_2 gas for reduction with a heating of 2°C/min to 400°C and hold for 5 hours.

After that the reaction was run at 400±5°C for 6 hour. In each run, ethanol was passed through the catalyst bed under a 30 ml/min flow of N_2. The catalytic testing was continued for at least 6 hours on stream. The reacted gaseous mixture was flowed out of the reactor and passed through a gas sampling loop. In order to prevent condensation of products, the line after reactor was heated by heating rods. Description of the reactor set up and the reaction conditions are summarized in Table 3.2

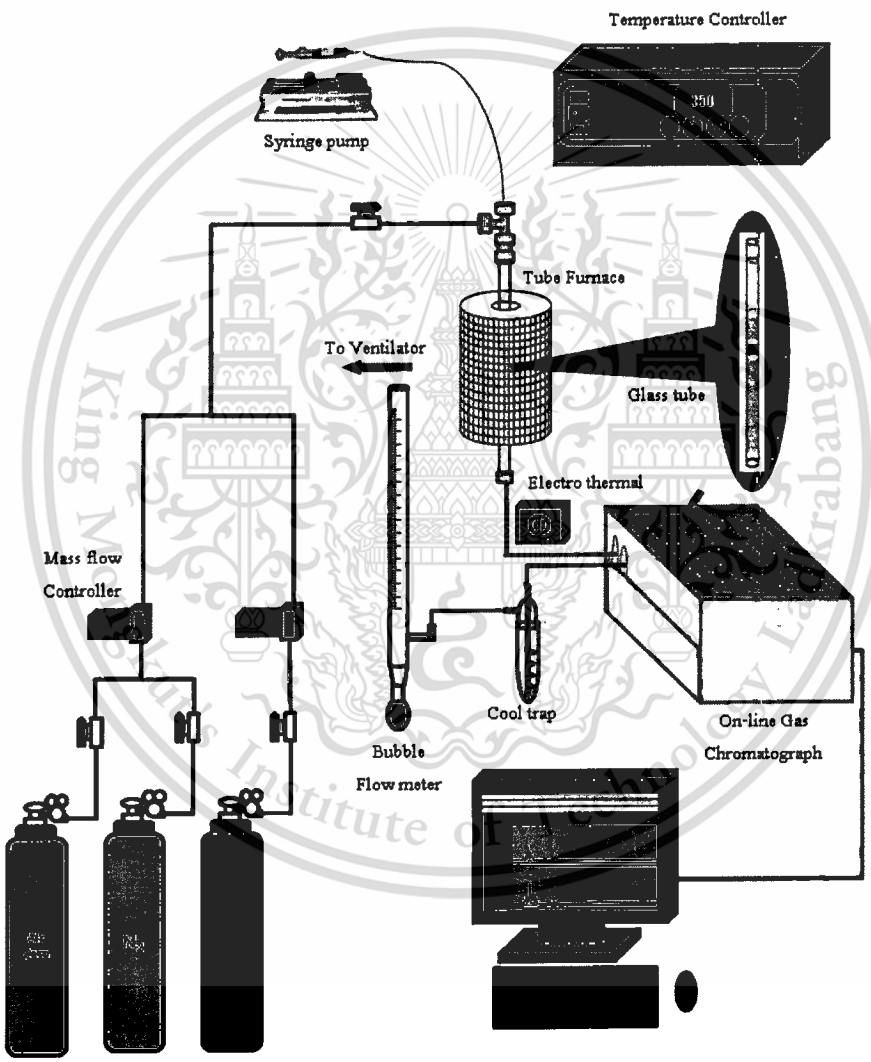

Figure 3.1 Schematic of the catalytic testing rig.

Table 3.2 Description of the reactor set up and the reaction condition

Parameters	Value
Reactor outside diameter (mm)	8
Bed length (mm)	5-25
Total flow (ml/min)	30
Catalyst weight (g)	0.04-0.36
Contact time: W/F (g.h/mol)	5-42
Catalyst pallet size (μm)	600-850
Catalyst activation (before reaction)	Heating rate: 2°C/min Calcination temperature: 450°C Gas: air zero (30 ml/min)
Catalyst reduction (before reaction)	Heating rate: 2°C/min Reduction temperature: 400°C Gas: Hydrogen (100 ml/min)
Reaction temperature (°C)	325-500
Total reaction pressure	Atmospheric pressure (1 atm)

3.6 Products analysis

The product analysis was generally performed using an online gas chromatograph. The gas sample was collected in gas sampling loop, then periodically injected into GC column (HP-5, 30 m length, 0.32 mm internal diameter, 0.25μm film thickness) connected to flame ionized detectors (FID). The following temperature program was used for the analysis: holding at 35°C for 5 min, followed by the ramping to 85°C at the rate of 15°C/min. holding for 2 min., then ramping to 220°C at rate of 10°C/min., before a final holding at that temperature for 3 min. N_2 gas was used as a carrier gas. Each component was separated as passed though the column with an inert carrier N_2 gas and their presence in the effluent were recorded as a chromatogram. Each peak areas from the chromatogram was measured

and calculated. Then each peak was identified by comparing with standard and the composition of each product was determined by calibration of standard.

บทที่ 4
ผลการวิจัย

4.1 Catalyst characterization

4.1.1 X-ray diffraction (XRD)

The catalysts prepared by wetness impregnation method after calcined at 450 °C were determined by X-ray power diffraction technique (XRD). In order to identify the crystal structure, 2θ angle in XRD diffraction pattern of each catalyst were compared with those of the reference diffraction pattern. The catalysts were scanned over the angle range (2θ) from 5° to 90°. The X-ray powder diffraction patterns of the metal oxide supported on silica catalysts are shown in **Figure 4.1**.

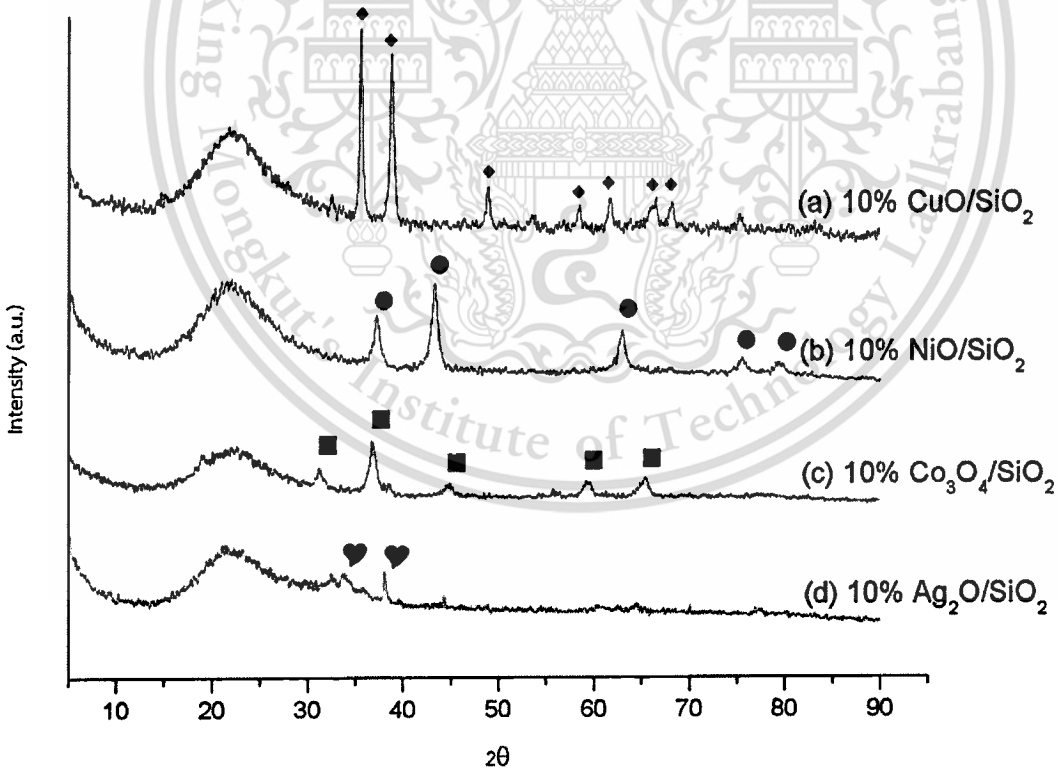

Figure4.1 XRD patterns of CuO/SiO_2 (a), NiO/SiO_2 (b), Co/SiO_2 (c), and Ag/SiO_2 (d) catalysts.

All catalysts show a broad peak at 2θ around 22° attributed to amorphous silica. In addition, the catalysts showed the diffraction peak at 35.5°, 38.7°, 48.9°, 58.5°, 61.8°, 66.4°, 68.1° for CuO, at 37.2°, 43.4°, 63°, 75.4°, 79.5° for NiO, at 31.3°, 36.9°, 44.7°, 59.4°, 65.4° for Co_3O_4 and at 33.6° and 38.1° for Ag_2O crystalline phase after calcination at 450 °C [30-32]. It is clear that the oxide of Cu, Ni, Co and Ag is incorporated on silica. In addition, the intensity of these diffraction peaks describes the crystallinity of metal oxide phase. The high intensity reviews the larger crystallite size of metal oxide. This suggests the weak interaction of metal oxide and silica support. It is clear that the intensity of metal oxide is in order this: CuO/SiO_2> NiO/SiO_2 > Co_3O_4/SiO_2> Ag_2O/SiO_2 catalyst. Accordingly, the metal oxide dispersion should be in order of: Ag_2O/SiO_2 > Co_3O_4/SiO_2 >NiO/SiO_2 > CuO/SiO_2 catalyst.

4.1.2 Elemental Analysis and Gas Adsorption

The elemental composition of the catalysts was determined by X- ray fluorescence spectroscopy (XRF). The specific surface area of the catalysts was determined by N_2 gas adsorption using BET method. The results are shown in **Table4.1**.

Table 4.1 Elemental analysis and gas adsorption characteristics of catalysts.

Catalysts	*S_{BET} (m^2/g)	% Metal loading
SiO_2	363	-
Co/SiO_2	242	10.0
Ni/SiO_2	239	11.4
Cu/SiO_2	229	7.8
Ag/SiO_2	206	12.9
H-ZSM-5 (12.5)	404	-
H-ZSM-5 ((28	479	-
Ag/H-ZSM-5 ((28	322	2.1

* Determined by BET

It can be seen that metal content in the catalysts is similar to the expected loading; that is 10% wt. Variation of the loading obtained may be accounted for the deviated concentration of metal precursor during preparation.

Silica support shows relatively high surface area of 363 m^2/g. The surface area of all 10% wt. metal supported catalysts is obviously decreased upon metal loading. Again, 2% wt. Ag/H-ZSM-5 (28) shown lower surface area (322 m^2/g), as compared with H-ZSM-5 (28) (479 m^2/g). However, all catalysts prepared by wetness impregnation method exhibits comparatively high surface area.

4.1.3 Temperature Program Reduction (TPR)

Temperature programmed reduction profiles of Co/SiO_2, Ni/SiO_2, Ag/SiO_2 and Cu/SiO_2 catalysts were investigated by H_2-temperature programmed reduction (H_2-TPR). The H_2- TPR profiles of those catalysts prepared by impregnation method are shown in **Figure** 4.2.

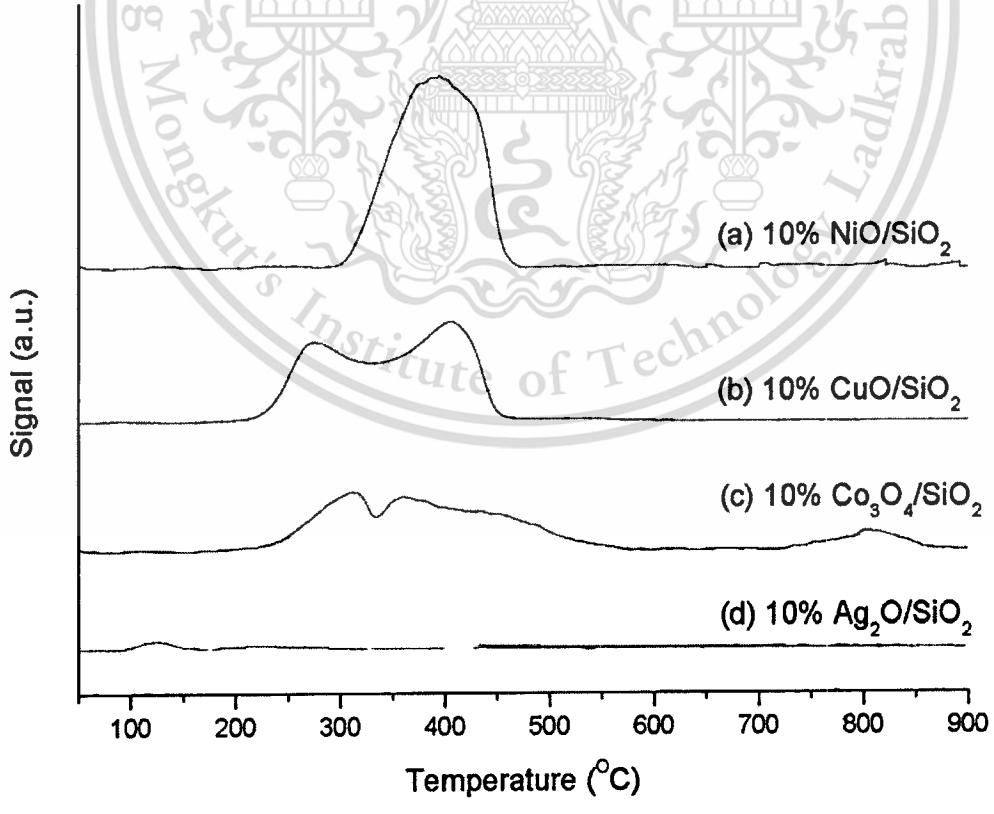

Figure 4.2 TPR profiles of Ni/SiO_2 (a), Cu/SiO_2 (b), Co/SiO_2(c), and Ag/SiO_2 (d) catalysts

As seen from **Figure 4.2**, the reduction of Ni^{2+} to metallic Ni take places as a broad peak at 400°C. For Cu/SiO_2 catalyst, two peaks at 275°C and 400°C are attributed to the reduction of Cu^{2+} to Cu^{1+} species and Cu^{1+} species to metallic Cu, respectively. For Co/SiO_2 catalyst, two main reduction peaks at 300°C and 350°C are observed. The first peak is assigned to the reduction of Co_3O_4 to CoO, and the other is the subsequent reduction of CoO to metallic Co [33]. Moreover, the reduction peak around 750-850°C is observed, which suggests the reduction of cobalt silicate species that requires high reduction temperature. In the case of Ag/SiO_2, the peak at 125°C and 220°C represents the reduction of Ag^{+} to metallic Ag [34].

4.1.4 NH_3-Temperature Programmed Desorption (NH_3-TPD)

Acid site in the catalysts has been investigated using NH_3-TPD. **Figure 4.3** shows the NH_3-TPD profiles for the H-ZSM-5 catalysts.

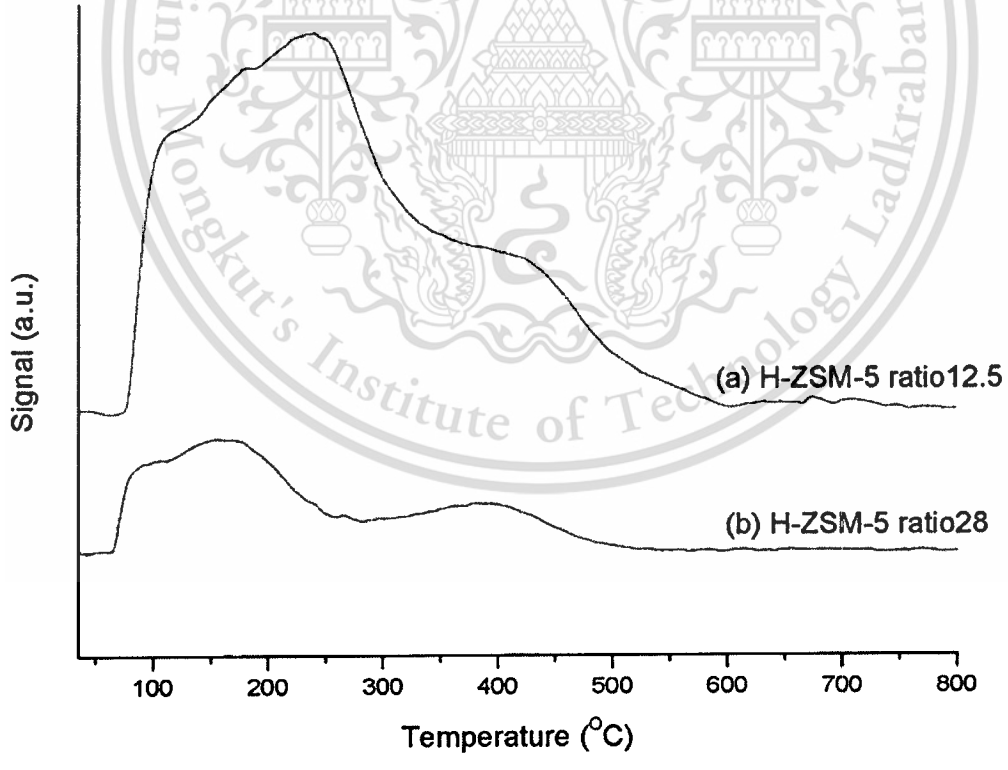

Figure 4.3 NH_3-TPD profiles of H-ZSM-5 (Si/Al ratio = 12.5 and 28) catalysts

The thermal desorption of physisorbed ammonia on the surfaces was observed at 100°C for all catalysts. The low-temperature broaden peak (150-200°C) is attributed to the desorption of weakly bound ammonia on weak acid sites. The concentration of these sites was of no catalytic importance [35-36]. While, the peak around 300-800 °C was the ammonia desorption from the defect framework of alumina in the structure [37]. This is probably due to the bridging hydroxyl (BrØnsted acid) of the zeolite. In **Figure 4.3,** intensity of the acid sites of H-ZSM-5 (12.5) was higher than that of H-ZSM-5 (28). This is because H-ZSM-5 (12.5) consists of relatively higher aluminum content in the framework; number of acid sites of H-ZSM-5 (12.5) is therefore greater than that in H-ZSM-5 (28) as shown in **Table** 4.2.

Table 4.2. Number of acid site over various catalysts.

Catalyst	Number of acid site (mmol of NH_3/g)		
	Weak	Strong	Total
H-ZSM-5 (12.5)	1.7	0.8	2.5
H-ZSM-5 (28)	0.4	0.3	0.7
Ag/H-ZSM-5 (28)	0.4	0.3	0.7

The Ag/H-ZSM-5 (28) catalyst prepared by wetness impregnation method also shows NH_3-TPD as seen in **Figure 4.4.**

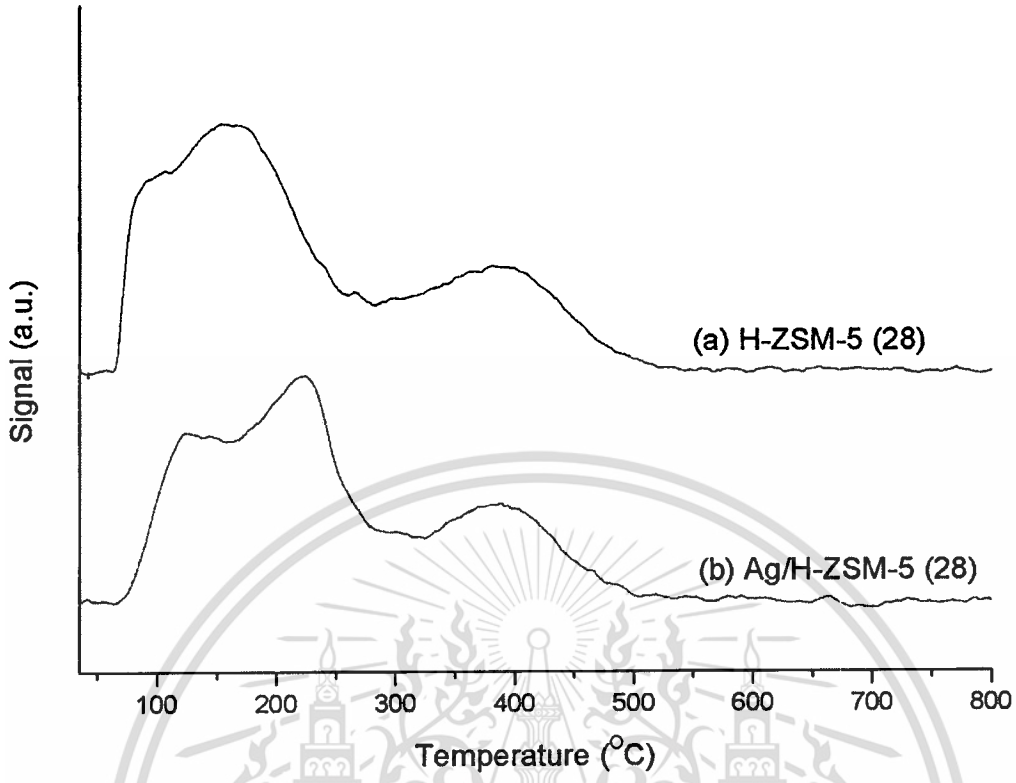

Figure 4.4 NH_3-TPD profiles of H-ZSM-5 (28) and Ag/H-ZSM-5 (28) catalysts

It was observed that acid sites of silver impregnated H-ZSM-5 are similar to H-ZSM-5 with Si/Al ratio of 28 (**Table 4.2**). However, the ammonia desorption profile slightly shifts to higher temperature indicating a higher acid strength in this sample. This is presumably because the interaction of the BrØnsted acid sites with the nearby metallic sliver.

4.2 Ethanol dehydrogenation over metal supported catalysts

4.2.1 The effect of metal supported SiO_2

The product distributions from the dehydrogenation of ethanol to acetaldehyde over Co/SiO_2, Ni/SiO_2, Ag/SiO_2 and Cu/SiO_2 catalysts were shown in **Table 4.3**

Table 4.3 Product distributions from ethanol conversion over various metal catalysts

Catalyst	Surface Area (m^2/g)	% Conversion	% Yields		% Selectivity	
			CH_4	Acetaldehyde	CH_4	Acetaldehyde
Cu/SiO_2	229	36	0	36	0	100
Ni/SiO_2	239	10.5	7.2	3.3	68	32
Ag/SiO_2	206	5.5	0.4	5.1	7.8	92
Co/SiO_2	242	2.1	1.0	1.1	48	52

(Reaction temperature: 325°C, Feed rate: 0.3889 g/h of absolute ethanol, W/F; 12 g.h/mol, Carrier gas; nitrogen)

It can be seen that Cu/SiO_2 gives a relatively high conversion and high selectivity to acetaldehyde, as compared to those over the other metals. However, a severe deactivation is observed as shown in **Figure 4.5**.

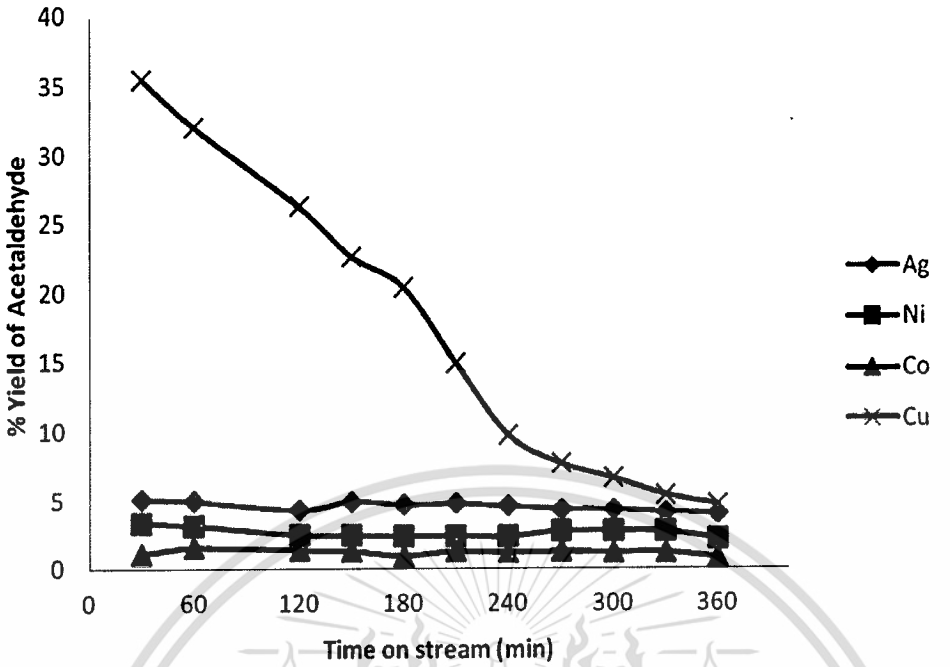

Figure 4.5 Yield of acetaldehyde over various metal catalysts.

(Reaction temperature: 325°C, Feed rate: 0.3889 g/h of absolute ethanol, W/F; 12 g.h/mol, Carrier gas; nitrogen)

The observed deactivation of Cu/SiO_2 catalyst is presumably due to sintering of copper particles at high temperature. This is because Cu possesses weak interaction with silica support, as suggested by high intensity of CuO phase in XRD pattern and low reduction temperature in the TPR profile. TEM also reviews sintering of copper particles as shown below.

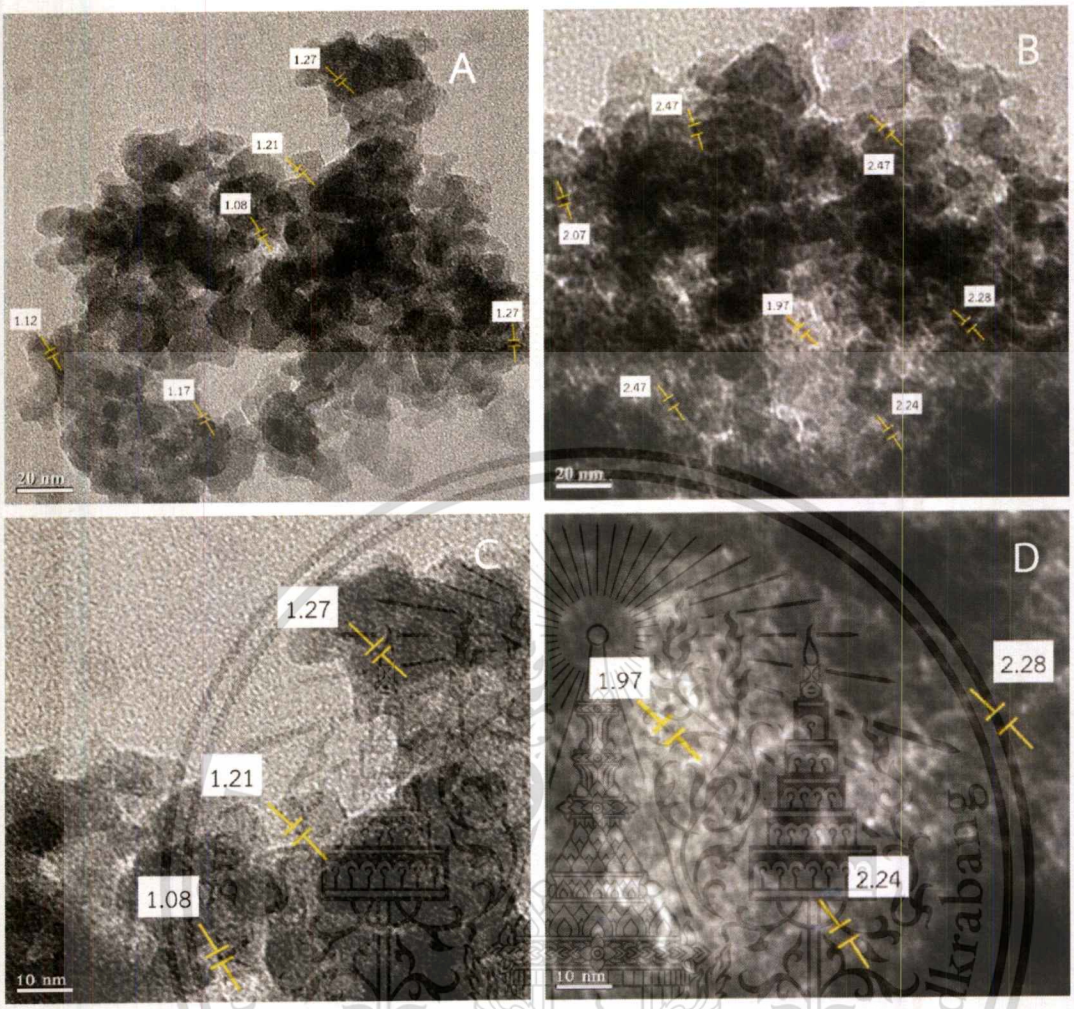

Figure 4.6 TEM images of the Cu/SiO_2: (A) fresh catalyst (20 nm), (B) spent catalyst (20 nm), (C) fresh catalyst (10 nm), (D) spent catalyst (10 nm)

From **Figure 4. 6**, the spent catalyst (B, D) shows copper particle size of approximately 2 nanometers diameter, as compared to 1 nanometer diameter of the fresh catalyst (A, C). Therefore, it is clear that the increased copper particles support in line with the observed decay of catalytic activity for Cu/SiO_2 [38]. For Ni/SiO_2 catalyst, ethanol conversion was higher than that of Ag/SiO_2 and Co/SiO_2. However, a significant yield of methane was obtained presumably due to the hydrogenolysis activity of nickel metal. It is possible that, over Ni/SiO_2 catalyst, ethanol could be dissociated on nickel surface forming acyl intermediate that lead to decarbonylation to methane and carbon monoxide as shown below.

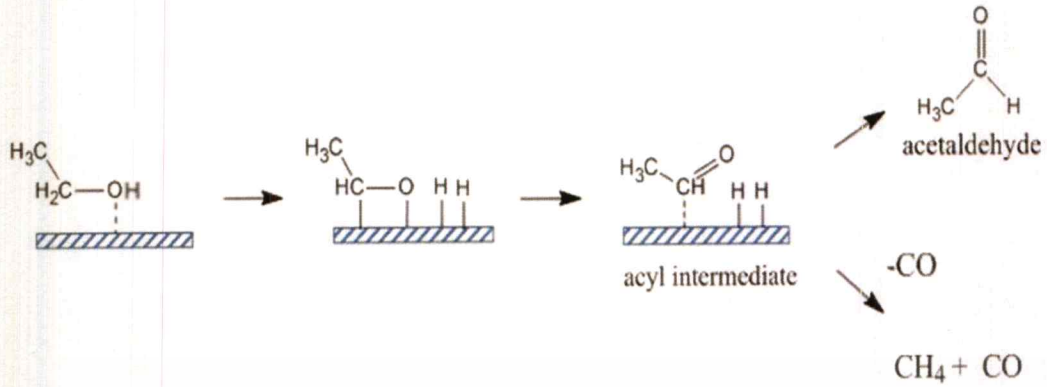

This is also the case for cobalt catalyst. 48 % selectivity to methane is observed accordingly. Hence, Ni/SiO_2 and Co/SiO_2 is not suitable for the dehydrogenation of ethanol to acetaldehyde.

In the case of Ag/SiO_2, a high selectivity to acetaldehyde is observed. It is possible that the ethanol adsorbed on metallic Ag surface as η^1 (O)-alcohol species forming alkoxide intermediate as shown below. The dehydrogenation of this species can lead only to the formation of acetaldehyde.

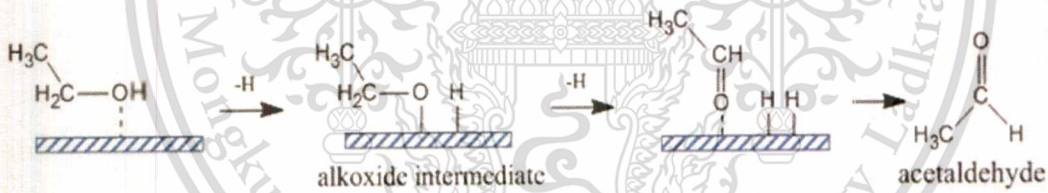

Accordingly, the selectivity of product appears to depend on adsorption mode of ethanol on metal surface, particularly the η^1 species, that leads only to the formation of acetaldehyde. The η^2 species lead to methane and carbon monoxide formation as demonstrated below.

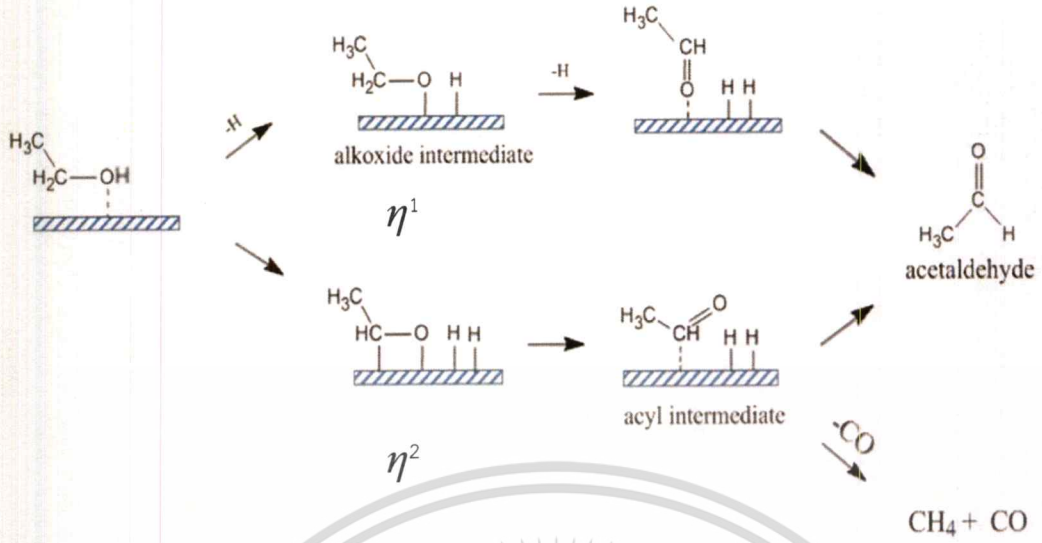

Nickel and cobalt catalysts favor to the formation of η^2 species while copper and silver catalyst promotes η^1 species. Since, no deactivation is observed for silver catalyst, it will be selected for further investigation.

4.2.2 The effect of temperature

The effect of temperature on ethanol conversion over Cu/SiO_2 and Ag/SiO_2 catalyst was investigated as shown in **Table 4.4** and **Figure 4.7**.

Table 4.4 The effect of reaction temperature with conversion of ethanol over Cu/SiO_2 catalyst.

Temperature (°C)	% Conversion	% Yield	
		CH_4	Acetaldehyde
400	34.9	0.4	34.5
500	57.0	5.0	52.0

(Reaction temperature: 400-500°C, Feed rate: 0.5523 g/h of absolute ethanol, W/F; 15 g.h/mol, 166 ml/min hydrogen, initial time on stream; 55 minutes)

From **Table 4. 4**, the conversion of ethanol and yield of methane and acetaldehyde was increased with temperature. As the reaction temperature increased, more methane is produced from ethanol decarbonylation resulting in declining of the selectivity of acetaldehyde. It suggests that at high temperature, the catalyst promotes decarbonulation as a undesired side reaction.

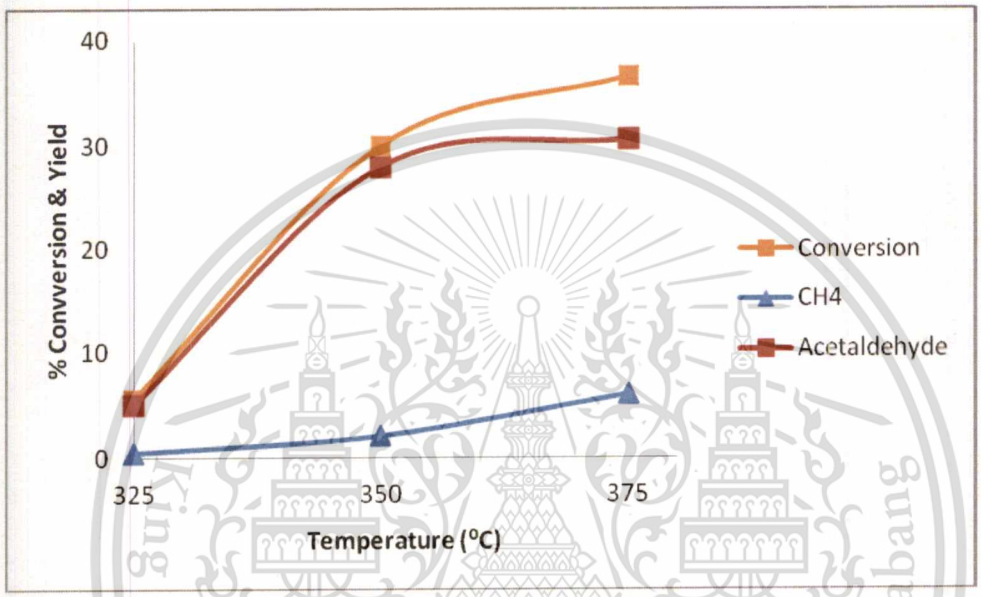

Figure 4.7 The effect of reaction temperature with conversion of ethanol over Ag/SiO_2 catalysts.

(Reaction temperature: 325-375°C, Feed rate: 0.3889 g/h of absolute ethanol, W/F; 12 g.h/mol, 30 ml/min nitrogen, Average time on stream; 150-230 minutes)

For Ag/SiO_2 catalyst (**Figure 4. 7**), the ethanol conversion to both acetaldehyde and methane is increased with the reaction temperature likewise Cu/SiO_2. At low temperature, ethanol is slightly converted to methane. Again, this is because the decarbonylation required relatively higher activation energy, as compared to the dehydrogenation. Therefore, the selectivity of acetaldehyde is high at low temperature. As both dehydrogenation and decarbonylation is endothermic, the reaction prefers at high temperature.

4.2.3 The effect of contact time

The conversion of ethanol and yield of products over Ag/SiO_2 catalyst at various contact times are shown in **Figure 4.8**.

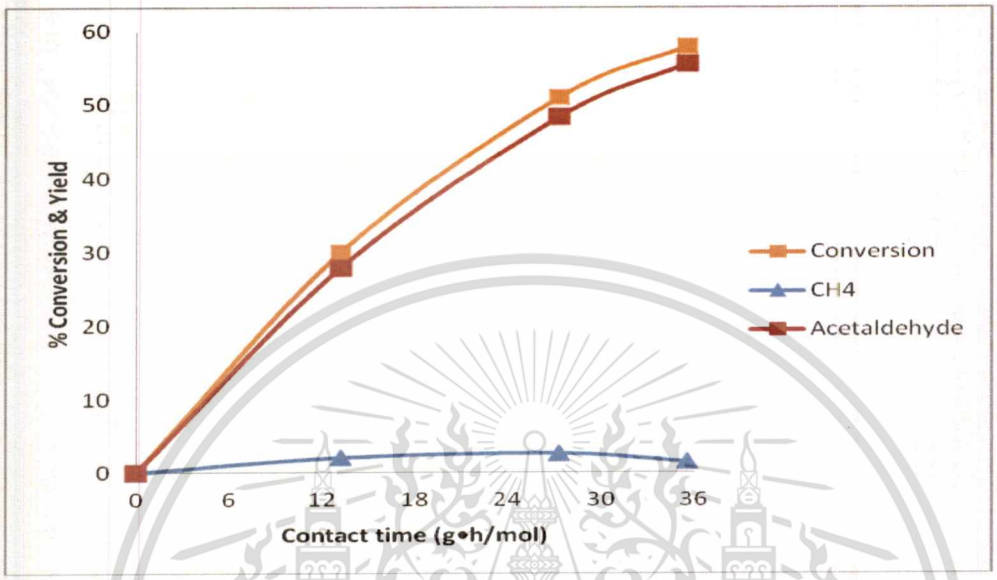

Figure 4.8 Conversion of ethanol and yields of product over Ag/SiO_2 catalysts.

(Reaction temperature: 350°C, Feed rate: 0.3889 g/h of absolute ethanol, W/F; 13.20 – 35.58 g.h/mol, 30 ml/min nitrogen)

From **Figure 4.8**, it can be seen that the conversion of ethanol is increased with contact time. The result is generally expected since increasing contact time allows a better chance for the reactant to interact with the catalyst active sites. Considering the products yield, it is observed that at low contact time, ethanol can be converted mainly to acetaldehyde and very small amount of methane. As discussed earlier, acetaldehyde is produced by dehydrogenation of η^1 (O)-alcohol species while methane is produced by decarbonylation of acyl intermediate derived from η^2 (C, O)-alcohol species. This suggests that over metallic Ag surface, ethanol preferentially adsorbed in η^1 mode, as compared to η^2 mode. However, some η^2- species is formed and hence; methane are generated in parallel

At contact time higher than 36 g.h/mol, the catalytic activity seems to approach saturated kinetics. No significant increase in conversion can be obtained [39]. Accordingly, the contact time of 36 g.h/mol is chosen for further study.

4.3 Ethanol conversion over H-ZSM-5

Although Ag/SiO_2 catalyst seems to be selective for the production of acetaldehyde, none of high molecular weights compounds can be observed over single silver catalyst. Hence, modification of the catalyst by the adding acid function is required to promote aldol condensation and oligomerization of the acetaldehyde produced. This shall lead to the subsequent formation of long chain hydrocarbon. However, acid catalyst alone can promote ethanol to hydrocarbons. Hence, the effect of acid site in H-ZSM-5 catalyst on the conversion of ethanol without metal catalyst is preliminarily evaluated.

4.3.1 The effect of contact time

The conversion of ethanol over H-ZSM-5 (12.5) was carried out at contact times of 5–15 g.h/mol at 400°C. The product distribution as a function of the contact time is shown in **Figure 4.9**

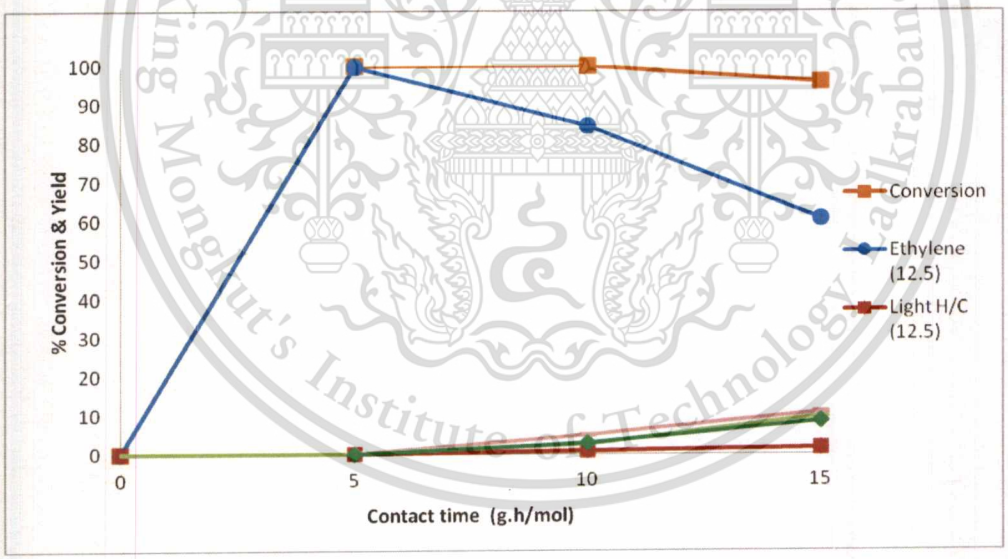

Figure 4.9 Product distributions from ethanol conversion over H-ZSM-5 (12.5)

(Reaction temperature: 400°C, Feed rate: 0.3889 g/h of absolute ethanol, W/F; 5 – 15 g.h/mol, 30 ml/min nitrogen, Average time on stream; 150-230 minutes)

The results reveal that despite the high conversion of ethanol is observed, only ethylene was produced at low contact time. Ethylene cannot be converted to higher hydrocarbons as the rate of ethylene oligomerization is relatively low, when compared to the rate of ethanol dehydration. This is because the ethylene oligomerization initially proceeds via the formation of primary carbocation [40]. As, the acid site is generally saturated with ethanol and water from dehydration, protonation of the ethylene formed is somewhat inhibited. However, as the contact time is increased, ethylene can oligomerized to mixture of higher hydrocarbon species (hydrocarbon pools) that undergo double bond isomerization, alkylation, cracking, cyclization and aromatization over H- ZSM- 5. Consequently, yield of ethylene is notably decreased, while yield of higher hydrocarbons such as light hydrocarbons (C_3-C_5), BTX aromatic, C_9 and C_{10} higher hydrocarbons is increased. The detail of product yield is tabulated in Appendix B. The reaction pathway for the production of long chain hydrocarbon and aromatic over H-ZSM-5 can be proposed as below:

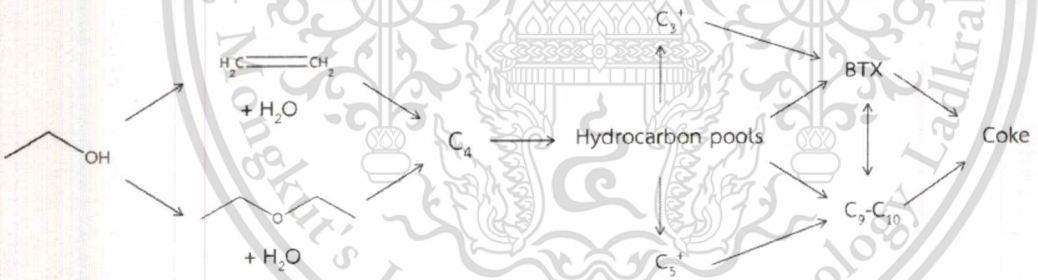

Since the contact time of 10 g. h/ mol initially shows activities for ethylene oligomerization, it is chosen for further study.

4.3.2 The effect of Si/Al ratio of H-ZSM-5

The effect of Si/Al ratio of H-ZSM-5 has been investigated using catalyst with Si/Al ratio of 12.5 and 28 as shown in **Table 4.5.**

Table4.5 Product distributions from ethanol conversion over H-ZSM-5 ratio 12.5 and 28

Si/Al ratio of H-ZSM-5	% Conversion	% Yields						
		Ethylene	Diethyl ether	Light H/C	BTX	C_7-C_8	C_9	C_{10}+
12.5	100	84	3.8	0.9	2.6	0.7	4.8	2.8
28	100	91	2.2	0.1	1.4	0	3.0	1.9

(Reaction temperature: 400°C, Feed rate: 0.3889 g/h of absolute ethanol, W/F of H^+; 10 g.h/mol, 30 ml/min nitrogen, Average time on stream; 150-230 minutes)

It can be seen that 100% conversion was observed for both catalysts. This means that those acid catalysts are active and in excess for ethanol conversion. However, hydrocarbon yield is decreased with decreasing acidity (higher Si/Al ratio) presumably due to the decrease in ethylene oligomerization. Again, this is because this reaction proceeds initially via the formation of primary carbocation that is activate over the acid site. As the acidity is decreased, the formation of intermediate hydrocarbons is suppressed. Moreover, the formation of hydrocarbon pools required close site proximity. Hence, as the acidity is decreased, appropriate site proximity for hydrocarbon production is also diminished. [41].

4.3.3 The effect of temperature

The effect of temperature on ethanol conversion over H-ZSM-5 (12.5) was investigated as shown in **Figure 4.10**.

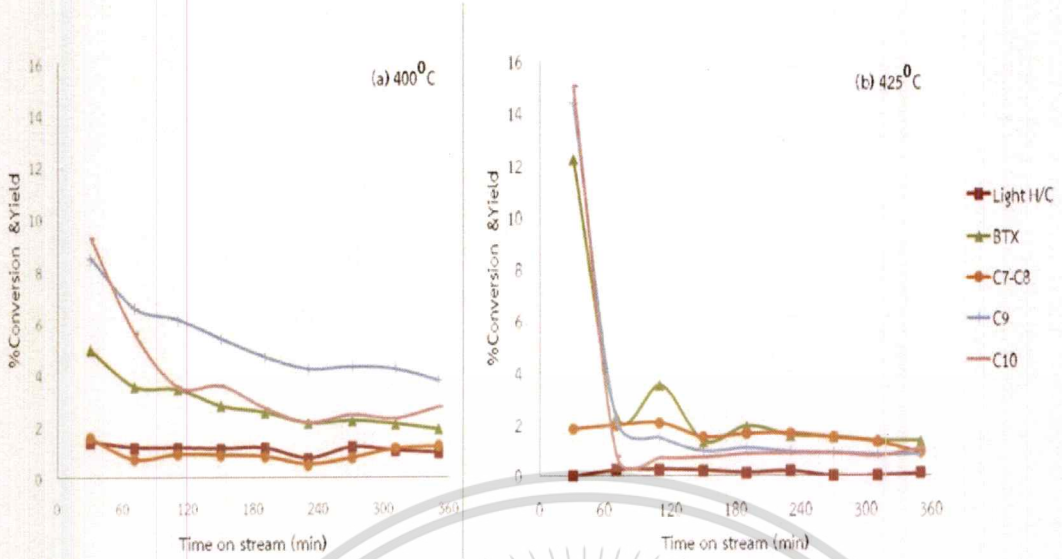

Figure 4.10 Hydrocarbon product distributions from ethanol conversion over HZSM-5 (12.5) at (a) 400°C and (b) 425°C

(Reaction temperature: 400-425°C, Feed rate: 0.3889 g/h of absolute ethanol, W/F of H^+; 10 g.h/mol, 30 ml/min nitrogen)

It is found that the 100 % conversion is obtained for both temperatures despite only contact time of 10 g.h/mol is used. However, a severe deactivation is observed at high temperature (425°C). This is presumably because at high temperature the formation of higher molecule weight deposit is largely promoted on the catalyst surface, blocking pores and access of the feed to strong acid sites [42]. This is in line with the observed high yield of BTX initially. Therefore, it can be considered that at lower temperature (400°C), the formation of coke can be somewhat suppressed.

4.4 Ethanol conversion over silver incorporated support

Although, H-ZSM-5 has excellent dehydration to ethylene but it is a poor catalyst for oligomerization and reforming to form higher hydrocarbons at this reaction condition. This is due to the lack of dehydrogenation activities. Therefore, the addition of metal species is required. From the result in **section 4.2**, metallic silver is chosen in this study for enhancing dehydrogenation activity of the catalyst.

4.4.1 The effect of metallic silver

The product distribution from ethanol conversion over H-ZSM-5 (28), physical mixture of Ag/SiO_2 + H-ZSM-5 (28) and silver impregnated H-ZSM-5 (28) catalyst were shown in **Table 4.6**

Table 4.6 Product distributions from ethanol conversion over H-ZSM-5 (28), physical mixture of 10%wt. Ag/SiO_2 + H-ZSM-5 (28) and impregnation Ag/H-ZSM-5 (28)

Catalyst	Ag content in the bed (mmol)	% Conversion	% Yields							
			Ethylene	Acetaldehyde	Diethyl ether	C_3-C_5	BTX	C_7-C_8	C_9	C_{10}+
H-ZSM-5 (28)	-	100	91	-	2.2	0.1	1.4	0	3.0	1.9
Ag/SiO_2 + H-ZSM-5 (28)	0.06	98	43	18	3.6	0.9	11	2.2	13	6.7
Ag/H-ZSM-5 (28)	0.02	98	48	14	3.5	0.9	11	2.4	12	5.0

(Reaction temperature: 400°C, Feed rate: 0.3889 g/h of absolute ethanol, W/F of H^+; 10 g.h/mol, 30 ml/min nitrogen, Average time on stream; 150-230 minutes)

Silver impregnated H-ZSM-5 (28) shows high conversion and hydrocarbon yields close to the physical mixed Ag/SiO_2 + H-ZSM-5 (28) despite the silver loading is much less. This suggests that Ag/H-ZSM-5 is more active than the physical mixed Ag/SiO_2 + H-ZSM-5, presumably due to the close proximity of silver and acid site. Moreover, it is clearly seen

that ethylene is significantly decreased while acetaldehyde and hydrocarbon yields are increased, as compared to H-ZSM-5 (28). This suggests that the presence of silver in the catalyst can promote dehydrogenation of ethanol to acetaldehyde and/ or ethylene oligomerization or both. Ethanol can be dehydrogenated to acetaldehyde over metallic silver. The acetaldehyde is readily coupled with other acetaldehyde through aldol condensation to higher aldehyde over acid site, followed by hydrogenation to higher alcohol. The higher alcohol can be readily dehydrated into unsaturated hydrocarbons. After that, the hydrocarbon is protonated then oligomerized with other unsaturated hydrocarbons to formed long chain hydrocarbons. It can be reformed to aromatic compounds as purposed below.

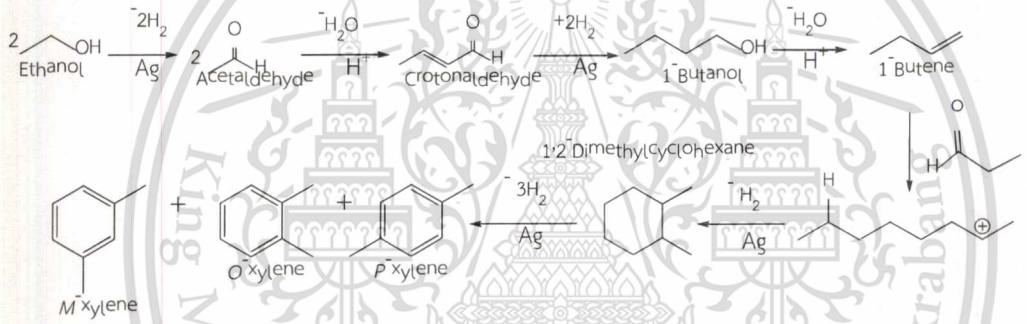

Alternatively, ethylene, formed by dehydration over acid site, can readily interact with metallic silver that also facilitate the oligomerization over a proximate acid site. Moreover, silver loaded catalyst can enhance C-H bond cleavage which would promote dehydrocyclization of long chain hydrocarbon to aromatics [43]. The systematic catalytic pathway was demonstrated as scheme below.

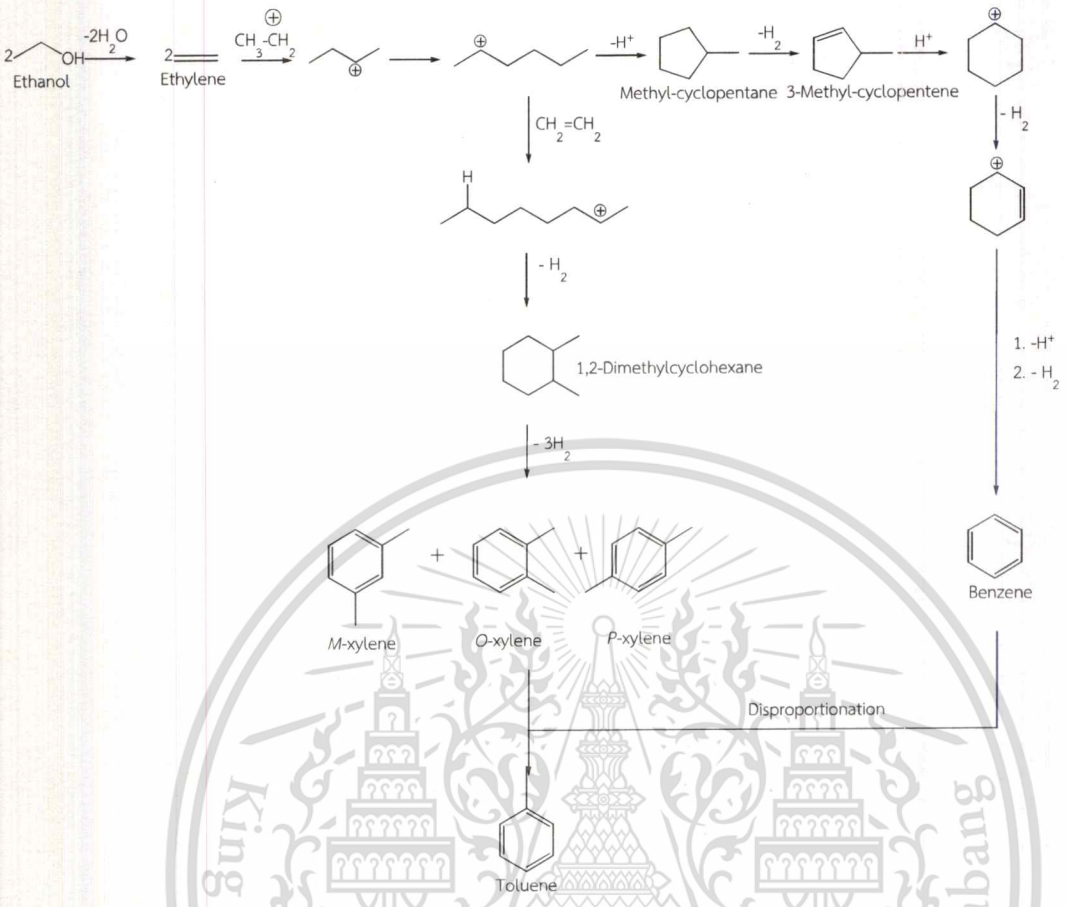

In line with above mentioned, high yield of aromatic hydrocarbon is largely observed over catalyst containing silver

4.4.2 The effect of contact time of Ag/H-ZSM-5 (28)

In order to verify the role of silver and reaction pathway, the conversion of ethanol over Ag/H-ZSM-5 (28) was carried out at contact times of 5–42 g.h/mol at 400°C. The product distribution as a function of the contact time is shown in **Figure 4.11**

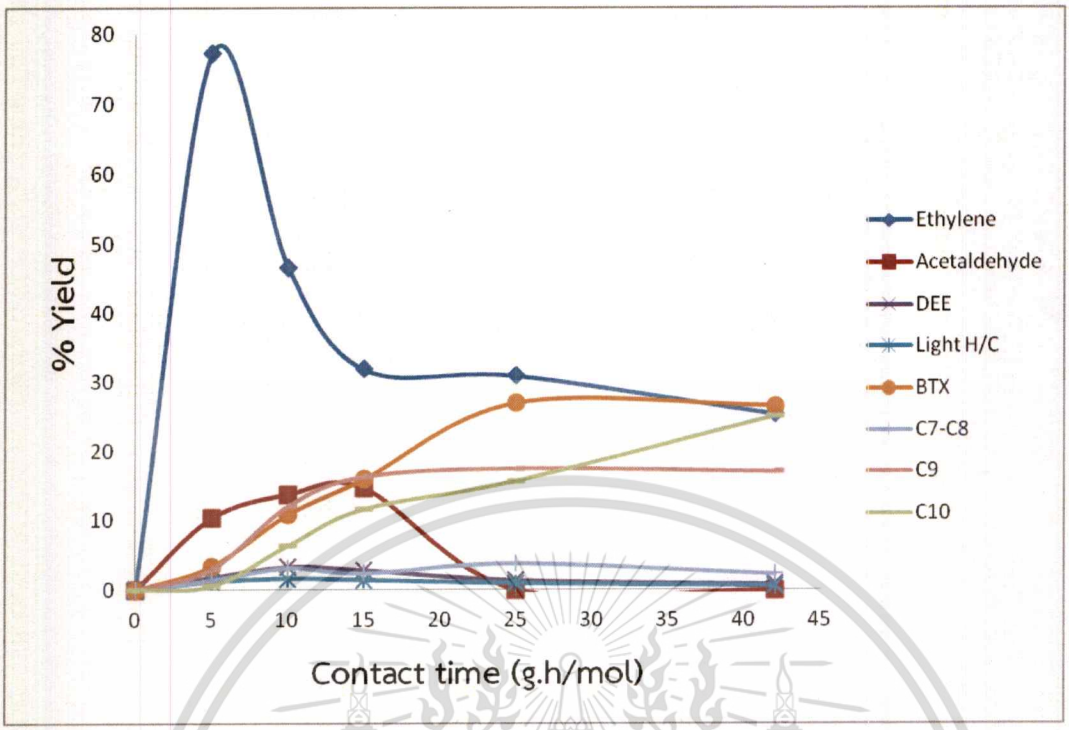

Figure 4.11 Conversion of ethanol and yields of product over Ag/H-ZSM-5 (28) catalyst.

(Reaction temperature: 400°C, Feed rate: 0.3889 g/h of absolute ethanol, W/F; 5 – 42 g.h/mol, 30 ml/min nitrogen)

At low contact time, ethanol is mainly dehydrated to ethylene and some is dehydrogenated to acetaldehyde. However, no significant yield of higher hydrocarbons is observed. This is because a limited number of acid sites for ethylene oligomerization and the aldol condensation of acetaldehyde cannot be readily facilitated. The available acid sites only activate ethanol dehydration to ethylene while silver promotes dehydrogenation to acetaldehyde. When the contact time is increased to 10-15 g.h/mol, ethylene is notably converted to higher hydrocarbons; C9, C10 and BTX as main products. From **Table 4.6**, it can be seen that, the hydrocarbon yields from Ag/H-ZSM-5 (28) are significantly higher than that over H-ZSM-5 (28). This is possibly due to dehydrogenation of ethanol to acetaldehyde enhanced the acid strength of Ag/H-ZSM-5 (28) (Figure 4.4), as compared to that H-ZSM-5, and conversion of both ethylene and acetaldehyde to higher hydrocarbons. The interaction of silver with the ethylene initially formed that promote oligomerization.

At the same time, the dehydrogenation of ethanol to acetaldehyde should also be enhanced as the amount of silver is increased. However, only small increase in acetaldehyde is observed. This suggests that some of acetaldehyde may convert to higher hydrocarbon via aldol condensation. Nevertheless, rate of aldol condensation is somewhat slower than that of ethylene oligomerization at this range of contact time. This is because ethylene is initially produced in larger fraction, as compared to acetaldehyde. Accordingly, there is a higher probability for the acid site to interact with ethylene. As the contact time is further increased (25-40 g.h/mol), ethylene consumption is somewhat limited while acetaldehyde is virtually converted to C_{10} and BTX. It is suggested that the increase silver content in the catalyst bed largely promotes ethanol dehydrogenation to acetaldehyde that undergo aldol condensation over the acid sites. At this range of contact time (25-40 g.h/mol) C_{10} and BTX is boosted with a complete conversion of acetaldehyde, while yield of C_9 and ethylene remain unchanged. Therefore, it is likely that C_{10} and some of BTX are derived from the aldol condensation of acetaldehyde, while C_9 is derived mainly from ethylene oligomerization. In addition, the catalyst seems to be more active for aldol condensation, at high contact time. This is because the activation of acetaldehyde to form the enol intermediate is readily facilitated, as compared to the deprotonation of ethylene to form a primary carbocation despite the oligomerization also promoted by silver, as discussed previously. The overall reaction pathway for conversion of ethanol to gasoline over Ag/H-ZSM-5 catalyst can be proposed below;

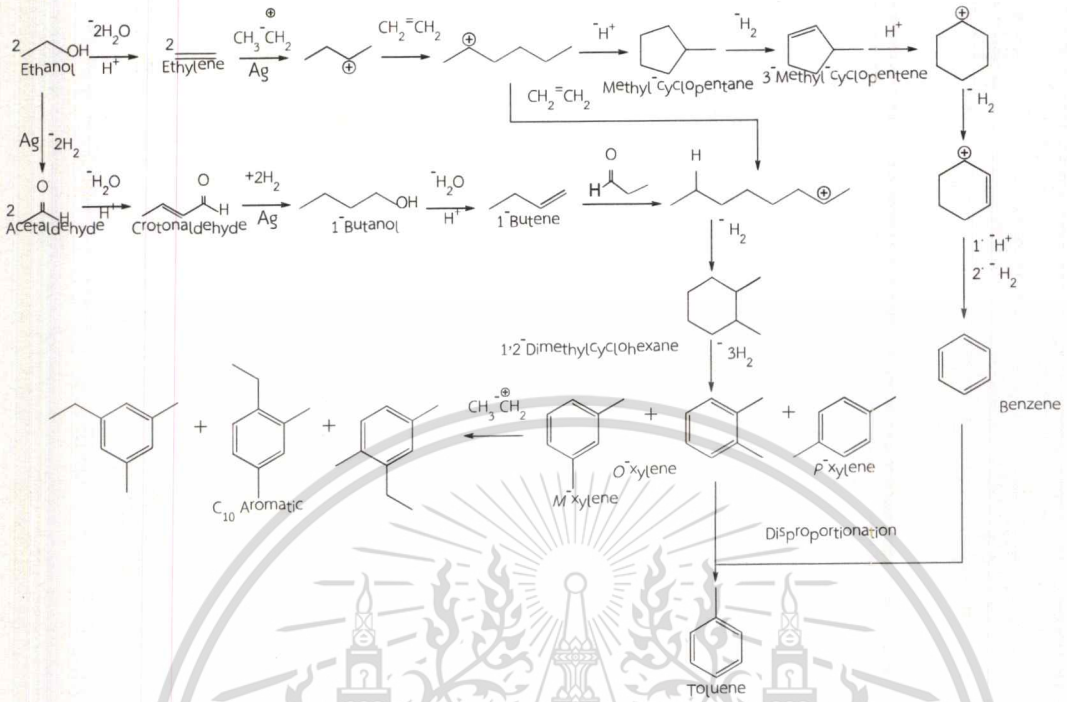

บทที่ 5
สรุปผลการวิจัยและข้อเสนอแนะ

5.1 Conclusions

The catalytic deoxygenation of glycerol to 1-propanol was studied using sequential bed system. In the upper bed, H-ZSM-5 (Si/Al=12.5) is used as a catalyst for dehydration of glycerol. Acolein and hydroxyacetone is a major and minor product, respectively. In the lowerbed, support ed Ni catalysts areused for su b sequently hydrogenation of acrolein to 1- It was found that propionaldehyde is .propanolan importantintermediat eto produce the major product propanol-1 via hydrogenation, while propanoic acid isa minor product obtained .from water reduction Interaction between metal and support significantly affects the hydrogenation activity and yield of 1-propanol in the lower catalytic bed. The orders of hydrogenation activity of supported Ni catalysts are as following: Ni/Al_2O_3 > Ni/TiO_2 > Ni/LDH > Ni/SiO_2 > Ni/MgO > Ni/C. The high activity of Ni/Al_2O_3 is due to the high Ni dispersion on the catalyst surface. The activity of Ni/TiO_2 catalyst can be also ascribed by high dispersion of Ni due to the strong metal support interaction effects (SMSI). Ni/LDH contains Al-O-Mg layers, which promotes the high dispersion of Ni on alumina phase. It is noted that activity of Ni/SiO_2 is due to its high surface area, while Ni/MgO possesses low surface area and low metal-support interaction. Ni/C presents poor Ni dispersion and hence, low activity. At low temperature (100°C), propionaldehyde is found as a main product because activation energy for C=O hydrogenation is insufficient. As the temperature is increased (120–200°C), it is noticed that yield of 1-propanol and propionaldehyde is similar for all tested temperature, presumably due to the saturated kinetics for hydrogenation-dehydrogenation over large Ni particle. However, at temperature > 200°C the decarbonylation of propionaldehyde yielding ethylene and carbon monoxides is promoted. The deactivation of catalyst is observed due to deposition of high molecular weight product on the catalysts.

5.2 Suggestions for Future Studies

5.2.1) The elimination of silanol group of H-ZSM-5 from glycerol dehydration in the first bed likely increases yield of acrolein that is major product.

5.2.2) Changing feed solvent from water to others is interested to decrease the yield of by-product propanoic acid from water reduction in second bed.

บรรณานุกรม

[1] Enrlque Costa,' Angeles Ugulna, JosC Aguado, and Pedro J. Herndndez. "**Ethanol to Gasoline Process: Effect of Variables, Mechanism, and Kinetics**", Ind. Eng. Chem. Process Des. Dev. 1985, 24, 239-244.

[2] Anup K. Talukdar, Krishna G. Bhattacharyya, S. Sivasanker. "**HZSM-5 catalysed conversion of aqueous ethanol to hydrocarbons**", Applied Catalysis A: General 148 (1997) 357-371.

[3] Alice M. de Lima, Adilson J. de Assis, Carla E. Hori, Miria H. E. Reis, Antonio E. H. Machado. "**Thermodynamic Analysis of Ethanol Dehydration to Ethylene through Equilibrium Constant Method Using Classic Thermodynamics and Quantum Chemistry**", I.RE.CH.E.(2012), Vol. 4, N.5 ISSN 2035-1755.

[4] Robert R. Frame, Paul T. Barger, "**Process for the oligomerization of olefins and a catalyst thereof**" US4795852 A (1989).

[5] Nagabhatla Viswanadham, Sandeep K. Saxena, Jitendra Kumar, Peta Sreenivasulu, Devaki Nandan. "**Catalytic performance of nano crystalline H-ZSM-5 in ethanol to gasoline (ETG) reaction.**" Fuel 95 (2012) 298–304.

[6] Junming Sun, Yong Wang. "**Recent Advances in Catalytic Conversion of Ethanol to Chemicals.**" ACS Catal. 2014, 4, 1078−1090.

[7] Artit Ausavasukhi. "**The Production of Gasoline and Aromatics From Ethanol.**" KMITL (2001).

[8] Jacqueline l. Kroschwitz, "**Executive Editor. Encyclopedia of Chemical Technology vol. 1.**" 4th Ed. New York : John Wiley & Son 1991.

[9] Shelly Minteer. "**Alcoholic Fuels.**" 6000 Broken Sound Parkway, NW Suite 300, Boca Raton, FL 33487 : CRC Press Taylor & Francis Group 2006.

[10] Wang, M., Saricks, C., Wu, M., "**Fuel-Cycle Fossil Energy Use and Greenhouse Gas Emission of Fuel ethanol.**" Illinois Department of Commerce and Community Affairs, Center for transportation Research, Argonne Natiional Laboratory, 1997.

[11] Mahy, H., Szabo, C. and Woods, L., "**200 Proof Transportation: the potential for Ethanol as an Alternative Fuel,**" University of Washington, Global commercialization of Environmental Technologies ENVIR 550/BBUS 550, Hund, G. and Laverty, K., Eds., 2003.

[12] Leong, S.T., Muttamara, S. and Laortanakul, P., "**Applicability of gasoline containing ethanol as Thailand' s alternative fuel to curb toxic VOC pollutants from automobile emission.**" Atmospheric Environment, 2002.

[13] U.S. EPA, "**Motor vehicle-related air toxic study.**" U.S. Environmental Protection Agency, Office of Mobile Source, Ann Arbor, MI, EPA Report No. EPA 420-R-93-005, April 1993.

[14] Surapas Sitthisa, Trung Pham, Teerawit Prasomsri, Tawan Sooknoi, Richard G. Mallinson, Daniel E. Resasco. "**Conversion of furfural and 2-methylpentanal on Pd/SiO_2 and $Pd–Cu/SiO_2$ catalysts.**" Journal of Catalysis 280 (2011) 17–27.

[15] Surapas Sitthisa, Tawan Sooknoi, Yuguang Ma, Perla B. Balbuena, Daniel E. Resasco. "Kinetics and mechanism of hydrogenation of furfural on Cu/SiO2 catalysts". Journal of Catalysis 277 (2011) 1–13.

[16] "**Aldol Condensation.**" [Online]. Available : http://en.wikipedia.org/wiki/Aldol_condensation. 2015.

[17] T.W. GRAHAM SOLOMONS. "**Organic Chemistry.**" 4th Ed. U.S.: John Wiley & Son, INC. 2011.

[18] "**Hydrogenation.**" [Online]. Available : http://en.wikipedia.org/wiki/Hydrogenation. 2015.

[19] "**Oligomerization.**" [Online]. Available : https://www.ihs.com/products/chemical-technology-pep-reviews-oligomerization-for- gasoline-2009.html. 2009.

[20] George A. Olah, Árpád Molnár. "**Hydrocarbon Chemistry.**" New York: John Wiley & Son. 1995.

[21] "**MFI.**" [Online]. Available : http://izasc-mirror.la.asu.edu/fmi/xsl/IZA-SC/ftc_fw.xsl?-db=Atlas_main&-lay=fw&-max=25&STC=MFI&-find. 2007.

[22] Chen N. Y., William E. Garwood. and Francis G. Dwyer. "**Shape Selective Catalysis in Industrial Applications.**" 2nd Ed. New York : Marcel Dekker. 1996.

[23] Subhash Bhatia. "**Zeolite Catalysis: Principles and Applications.**" Florida : CRC Press. 1990.

[24] Bruce C. Gates. "**Catalytic Chemistry.**" New York : John Wiley & Son. 1992.

[25] Hegedus L. Louis, Editor. "**Catalyst Design Progress and Perspective.**" New York : John Wiley & Son. 1987.

[26] Bekkum H. Van, Editors. **" Introduction to Zeolite Science and practice. "** Amsterdam : Elsevier Science. 1991.

[27] Kokotailo G. T., Lawton S. L. and Olson D. H. **"Structure of Synthetic Zeolite ZSM-5."** Vol. 272, March 1978. Pp. 473-438.

[28] Robert J. Arganer., Kansington M., George R. Landolt. And Audbon N. J. **"Crystalline Zeolite ZSM-5 and Method of Preparing the Same."** U.S patent no. 3702886, November 1972.

[29] Xianlong Zhang, Ziwei Liu, Xingliang Xu, Huijuan Yue, Ge Tian, and Shouhua Feng. **" Hydrothermal Synthesis of 1- Butanol from Ethanol Catalyzed with Commercial Cobalt Powder."** ACS Sustainable Chem. Eng. 2013, 1, 1493−1497

[30] S. Totong, K. Faungnawakij, N. Laosiripojana. **" Hydrogen Production from Dehydrogenation of Ethanol over Ag- Based Catalysts. "** World Academy of Science, Engineering and TechnologyInternational Journal of Chemical, Nuclear, Metallurgical and Materials Engineering Vol:8 No:2, 2014

[31] XUE Jingjing, CUI Fang, HUANG Zhiwei, ZUO Jianliang, CHEN Jing, XIA Chungu. **"Effect of Metal Additives on Structure and Properties of a Co/SiO_2 Hydrogenation Catalyst."** CHINESE JOURNAL OF CATALYSIS Volume 33, Issue 10, 2012

[32] N. M. Deraz, M. M. Selim, M. Ramadan. **" Processing and properties of nanocrystalline Ni and NiO catalysts"** Materials Chemistry and Physics 113 (2009) 269–275

[33] Miranda L. Smith, Andrew Campos, James J. Spivey. " Reduction processes in Cu/SiO2, Co/SiO_2, and CuCo/SiO_2 catalysts". Catalysis Today 182 (2012) 60–66.

[34] G. V. Mamontov, T. I. Izaak, O. V. Magaev, A. S. Knyazev, and O. V. Vodyankina **" Reversible Oxidation/ Reduction of Silver Supported on Silica Aerogel: Influence of the Addition of Phosphate" ISSN 0036-0244, Russian Journal of Physical Chemistry A, Vol. 85, No. 9, 2011**

[35] Ali A. Rownaghi and Jonas Hedlund **"Methanol to Gasoline-Range Hydrocarbons: Influence of Nanocrystal Size and Mesoporosity on Catalytic Performance and Product Distribution of ZSM-5", Ind. Eng. Chem. Res. 2011, 50, 11872–11878**

[36] Franke, M. E.; Simon, U. **"Solvate-supported proton transport in zeolites."** Chem. Phys. Chem. 2004, 5, 465–472.

[37] Luz Rodrı´guez-Gonza´lez, Florian Hermes, Marko Bertmer , Enrique Rodrı´guez-Castello´n, Antonio Jime´nez-Lo´pez, Ulrich Simona. **"The acid properties of H-ZSM-5 as studied by NH_3-TPD and 27Al-MAS-NMR spectroscopy".** Applied Catalysis A: General 328 (2007) 174–182.

[38] Ching-Shiun Chena, Wu-Hsun Chengb, Shou-Shiun Lin. **"Study of iron-promoted Cu/SiO2 catalyst on high temperature reverse water gas shift reaction".** Applied Catalysis A: General 257 (2004) 97–106

[39] Bruce C. Gates. **"Catalytic Chemistry".** New York : John Wiley & Sons. 1992.

[40] George A. Olah., Arpad Molnar. **"Hydrocarbon Chemistry".** New York : John Wiley & Sons. 1995.

[41] Filipa Ferreira Madeiraa, Karima Ben Tayebb, Ludovic Pinarda, Hervé Vezinb, Sylvie Mauryc, Nicolas Cadranc **"Ethanol transformation into hydrocarbons on ZSM-5 zeolites: Influence of Si/Al ratio on catalytic performances and deactivation rate. Study of the radical species role".** Applied Catalysis A: General 443– 444 (2012) 171– 180

[42] M. Guisnet, P. Magnoux **"Organic chemistry of coke formation".** Applied Catalysis A: General 212 (2001) 83–96

[43] Weitkamp J, Editor. **"Zeolites and Related Microporous Materials"**: State of the Art 1994. Amsterdam: Elsevier Science. 1994

ภาคผนวก

ภาคผนวก ก

CHARACTERIZATION OF CATALYSTS

1. X-ray diffraction

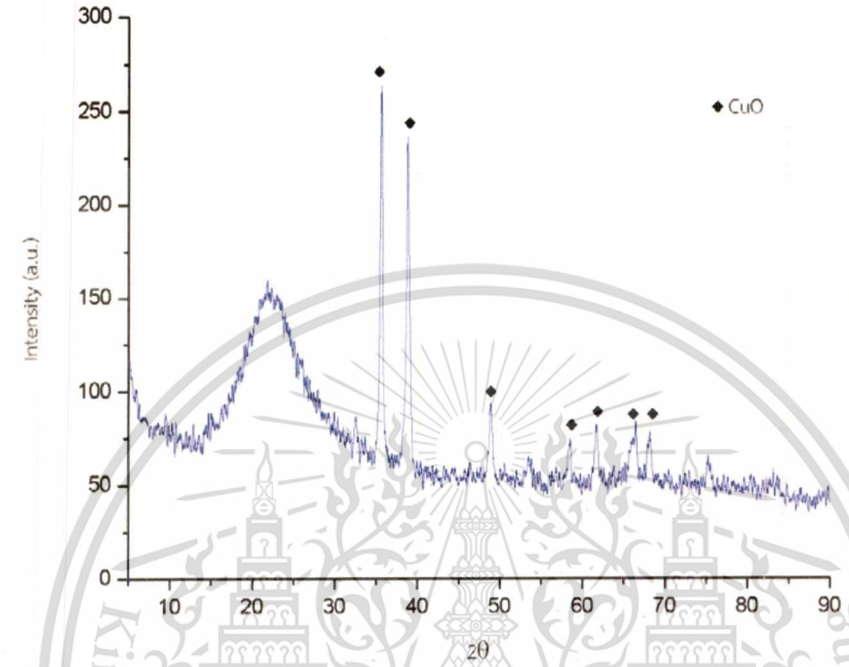

Fig.A1 X-ray pattern of 10%wt. CuO/SiO_2

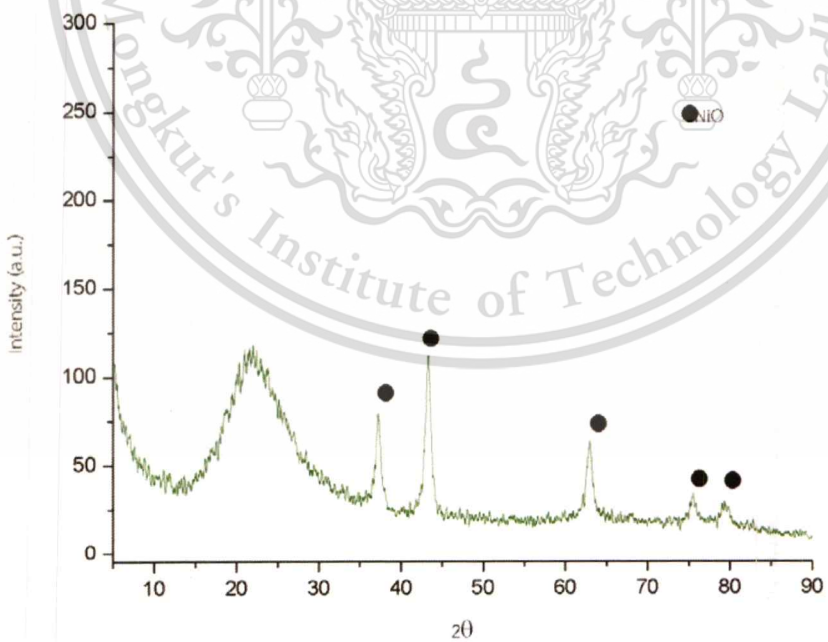

Fig.A2 X-ray pattern of 10%wt. NiO/SiO_2

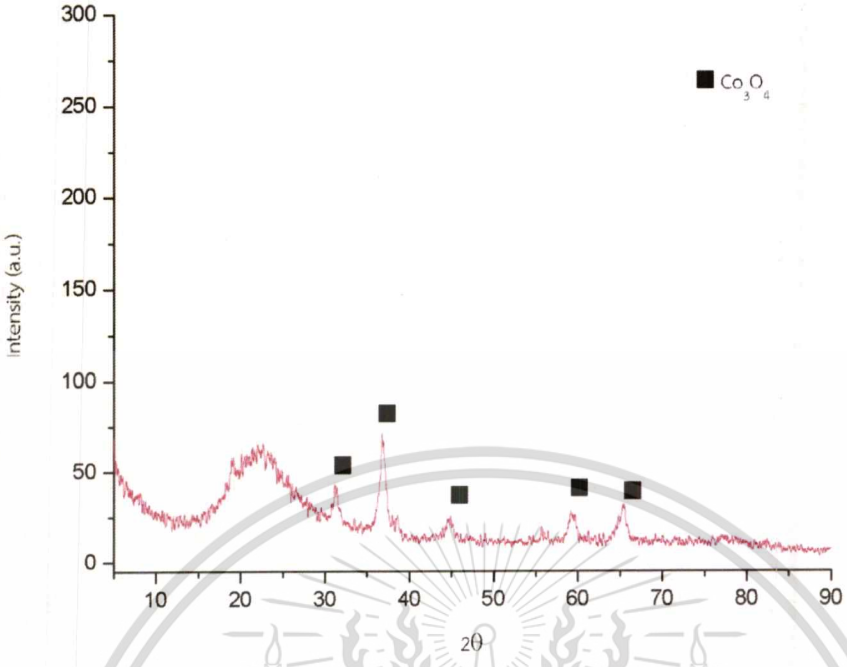

Fig.A3 X-ray pattern of 10%wt. Co_3O_4/SiO_2

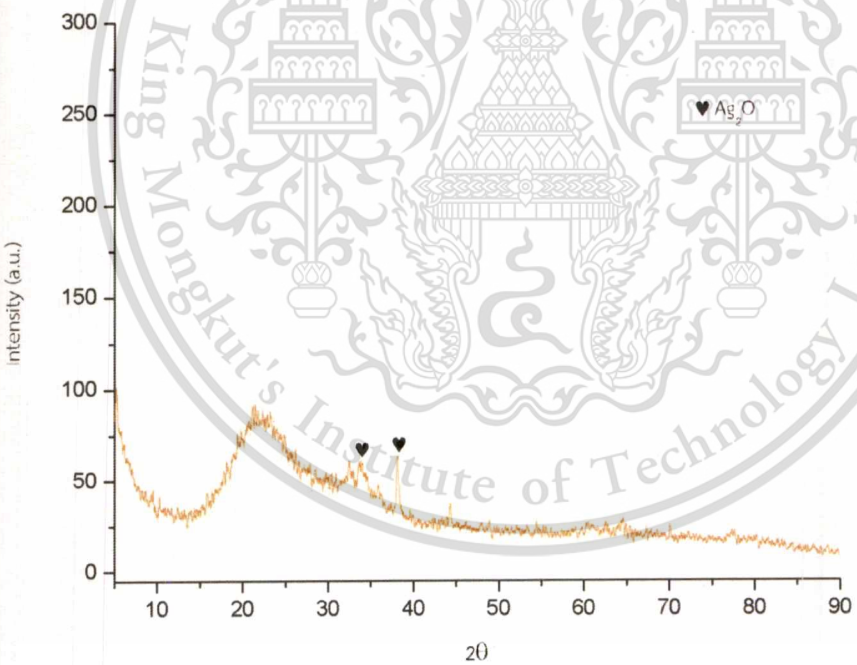

Fig.A4 X-ray pattern of 10%wt. Ag_2O/SiO_2

2. X-ray fluorescence

Table A1 Elemental composition of 10%wt. CuO/SiO_2 catalyst

SiO_2	CuO	Intensity Scal
70.9 KCps	211.4 KCps	
89.70%	9.76%	0.9165

Table A2 Elemental composition of 10%wt. NiO/SiO_2 catalyst

SiO_2	NiO	Intensity Scal
972.7 KCps	4157.3 KCps	
84.80%	14.50%	0.9150

Table A3 Elemental composition of 10%wt. Co_3O_4/SiO_2 catalyst

SiO_2	CoO	Intensity Scal
999.6 KCps	3019.5 KCps	
86.50%	12.80%	0.9595

Table A4 Elemental composition of 10%wt. Ag_2O/SiO_2 catalyst

SiO_2	AgO	Intensity Scal
1044.5 KCps	277.2 KCps	
85.50%	13.80%	0.9272

Table A5 Elemental composition of Ag_2O/H-ZSM-5 ratio 28 catalyst

SiO_2	Al_2O_3	AgO	Intensity Scal
65.7 KCps	2.1 KCps	27.9 KCps	
80.70%	2.44%	2.34%	

Example of elemental composition calculation from **Table A1**

Mole of each compositions:

SiO_2 = 89.70 g / (60.080 g/mol) = 1.4930 mol

CuO = 9.760 g / (79.545 g/mol) = 0.1227 mol

Weight of each elementals:

Si = 1.4930 mol × (28 g/mol) = 41.8040 g

Cu = 0.1227 mol × (63.55 g/mol) = 7.7975 g

Example of elemental composition calculation from **Table A5**

Normalize of each composition:

$SiO_2 = SiO_2 / (SiO_2 + Al_2O_3 + AgO)$

= 80.70 / (80.70 + 2.44 + 2.34)

= 94.40%

$Al_2O_3 = Al_2O_3 / (SiO_2 + Al_2O_3 + AgO)$

= 2.44 / (80.70 + 2.44 + 2.34)

= 2.85%

$AgO = AgO / (SiO_2 + Al_2O_3 + AgO)$

= 2.34 / (80.70 + 2.44 + 2.34)

= 2.73%

Mole of each compositions:

SiO_2 = 94.40 g / (60.080 g/mol) = 1.5712 mol

Al_2O_3 = 2.85 g / (101.960 g/mol) = 0.0279 mol

AgO = 2.73 g / (139.87 g/mol) = 0.0195 mol

Weight of each elementals:

Si = 1.5712 mol × (28 g/mol) = 43.9936 g

Al = 0.0279 mol × (2 × 27 g/mol) = 1.5066 g

Ag = 0.0195 mol × (107.87 g/mol) = 2.1034 g

Si/Al ratio of H-ZSM-5 support:

Si/Al = 1.5712 mol / (0.0279 mol × 2) = 28.1577

3. Gas adsorption analysis

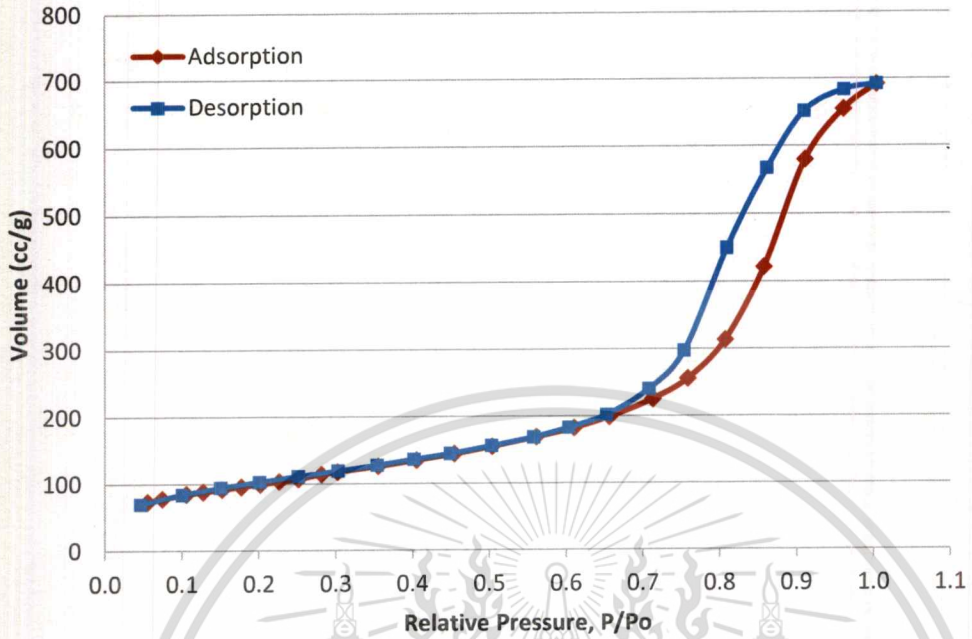

Area 363.33 m^2/g

Fig.A5 Isotherm of SiO_2

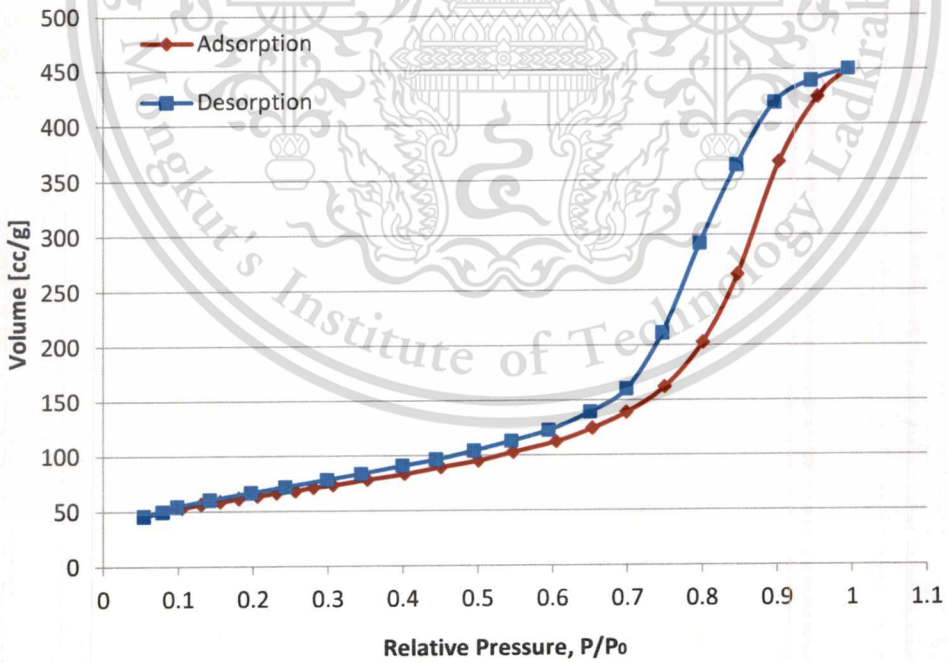

Area 228.61 m^2/g

Fig.A6 Isotherm of 10%wt. Cu/SiO_2

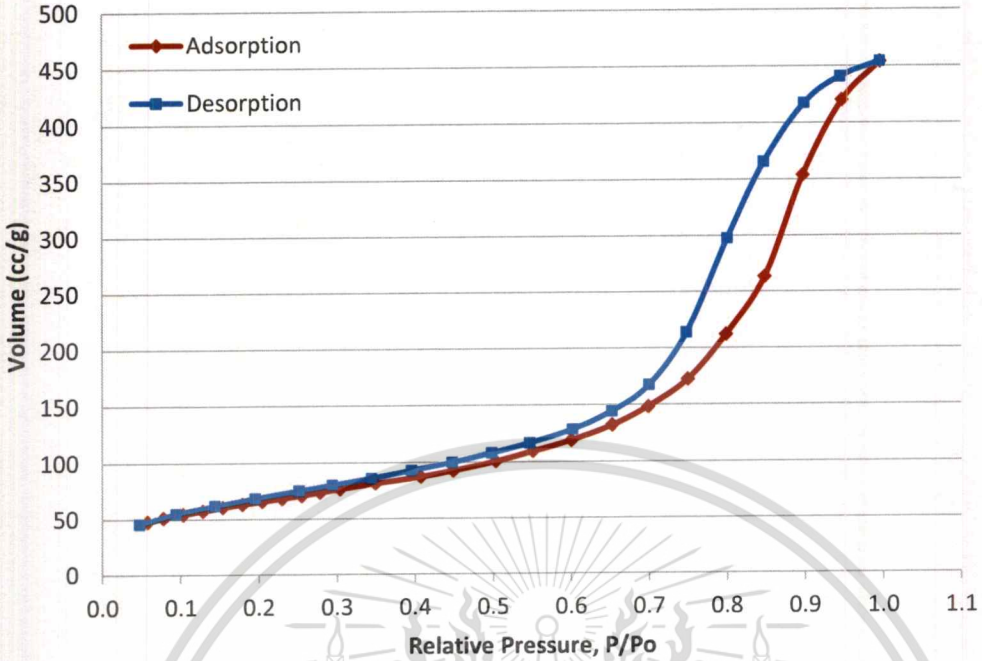

Area 239.68 m^2/g

Fig.A7 Isotherm of 10%wt. Ni/SiO_2

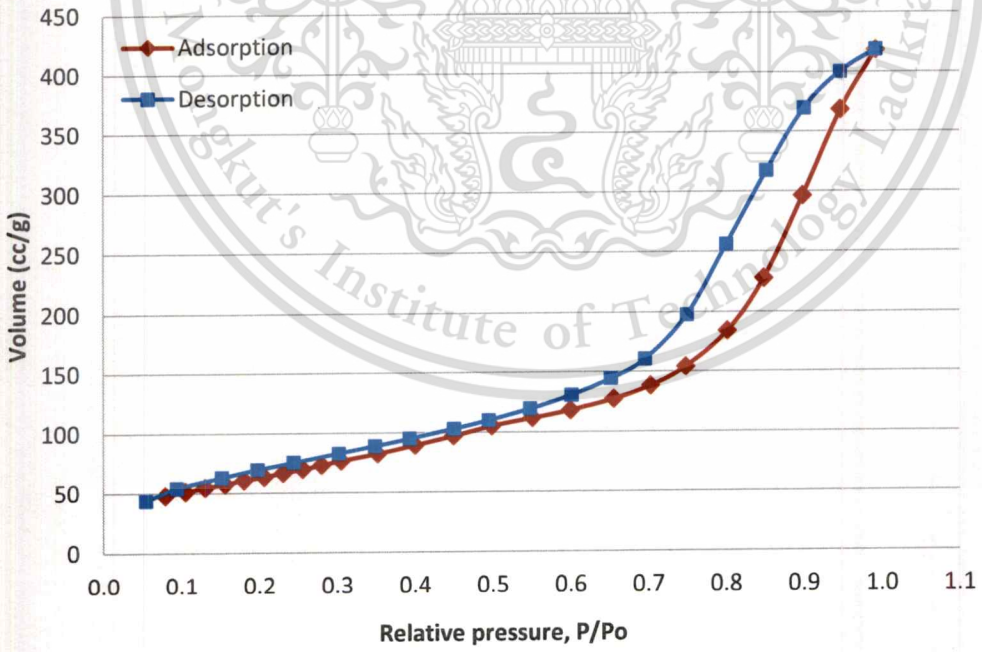

Area 242.19 m^2/g

Fig.A8 Isotherm of 10%wt. Co/SiO_2

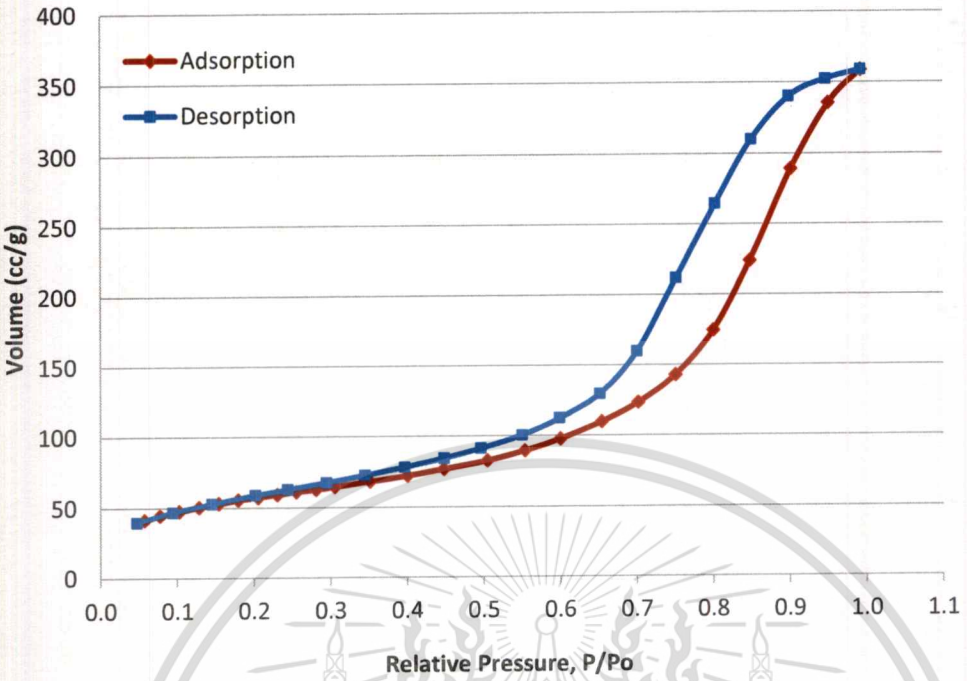

Area 206.03 m^2/g

Fig.A9 Isotherm of 10%wt. Ag/SiO_2

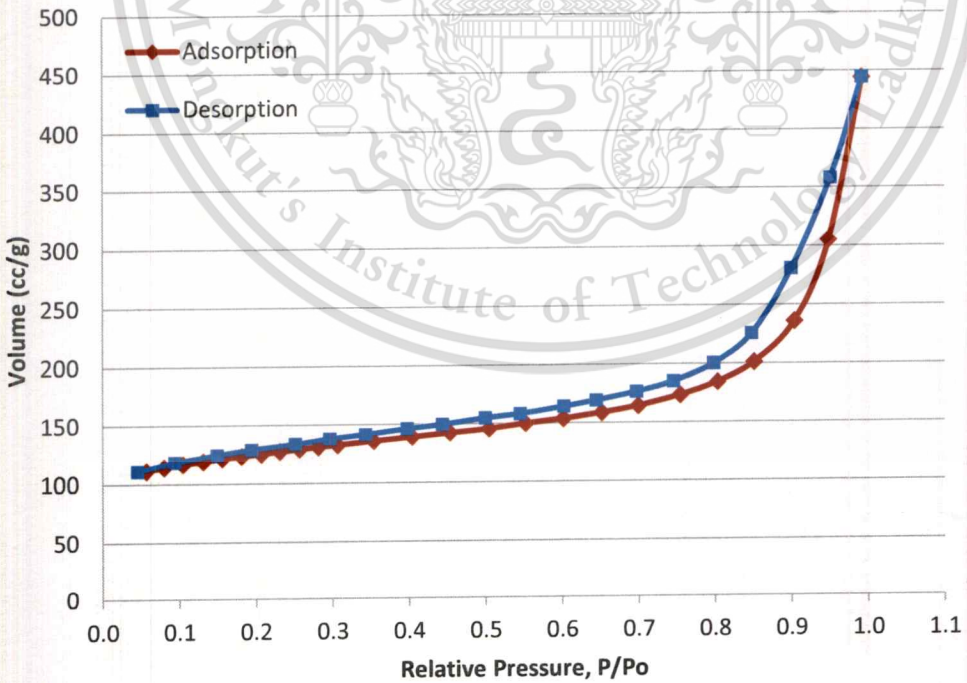

Area 403.48 m^2/g

Fig.A10 Isotherm of H-ZSM-5 ratio 12.5

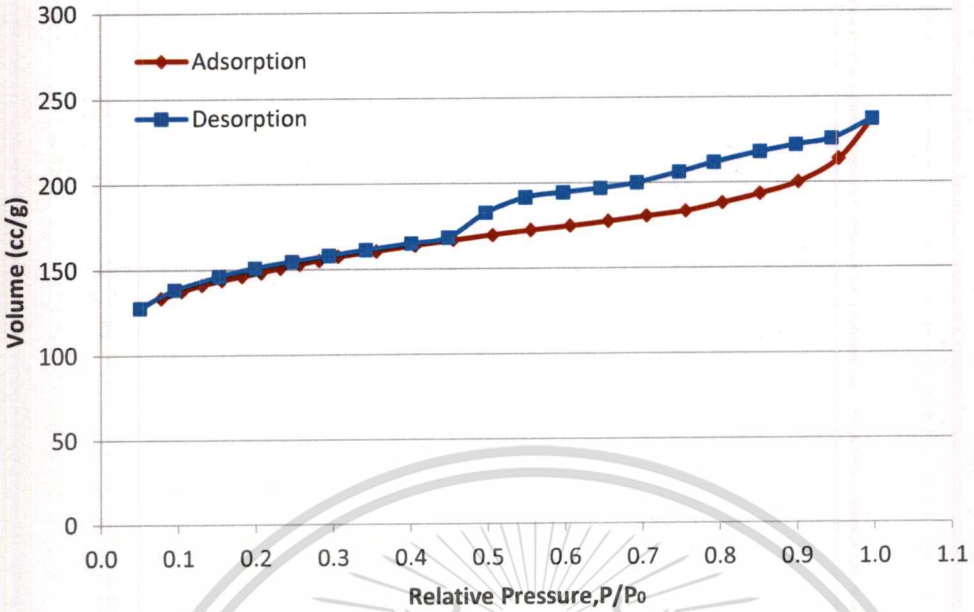

Area 479.18 m²/g

Fig.A11 Isotherm of H-ZSM-5 ratio 28

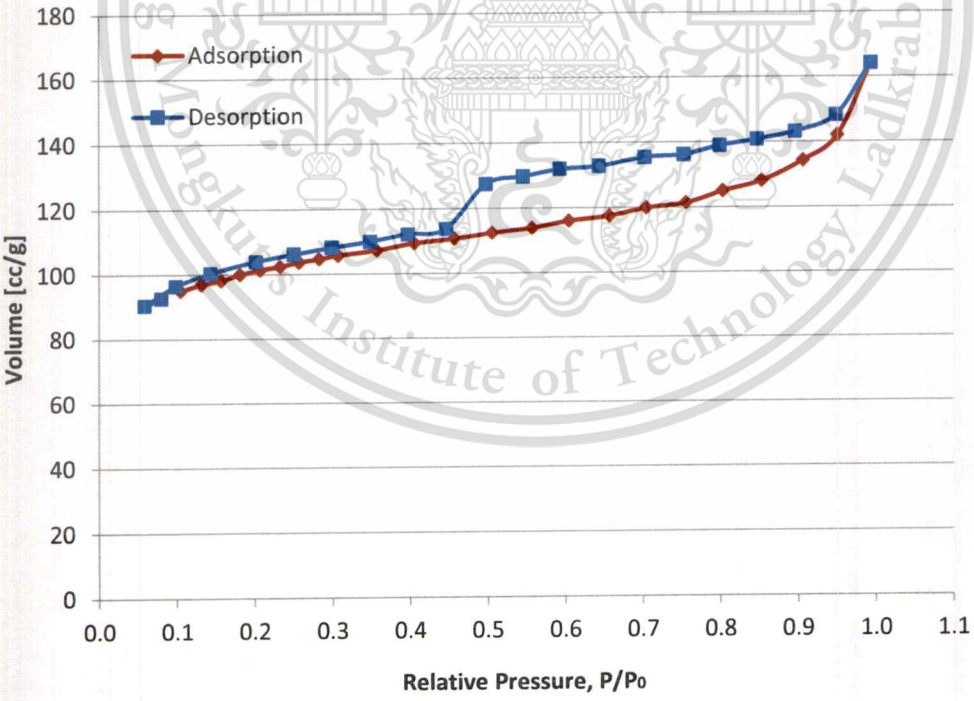

Area 321.57 m²/g

Fig.A12 Isotherm of Ag/H-ZSM-5 ratio 28

4. Temperature programmed reduction

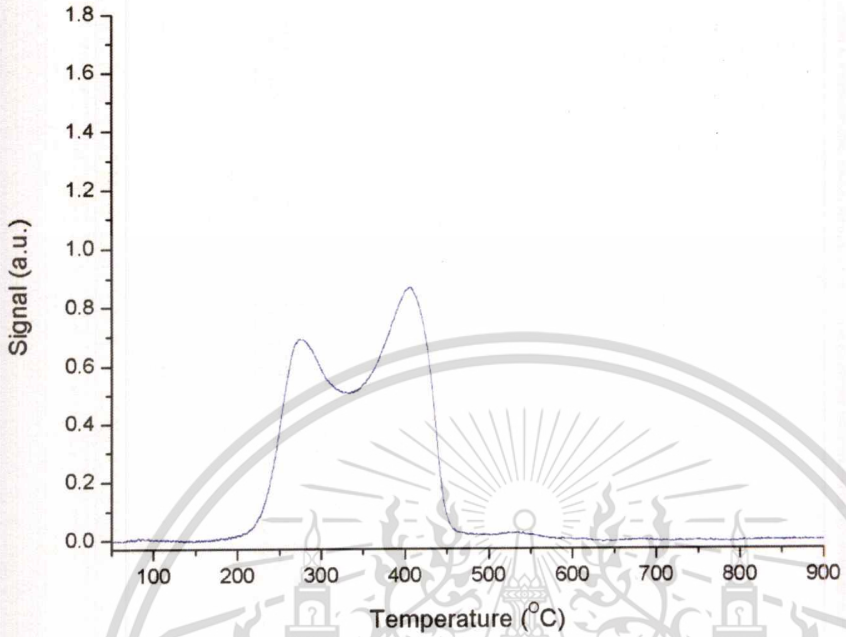

Fig.A13 Temperature programmed reduction of 10%wt. Cu/SiO_2

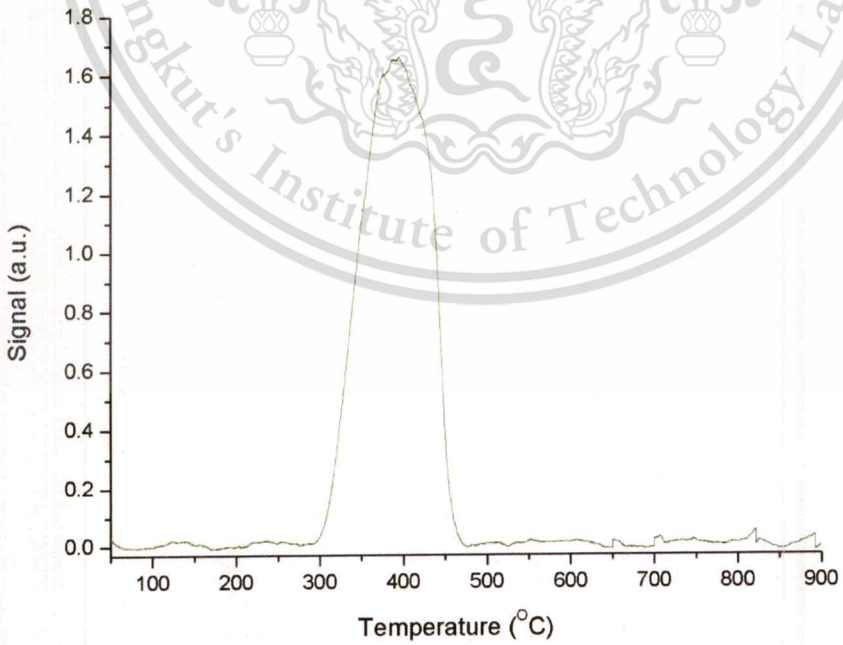

Fig.A14 Temperature programmed reduction of 10%wt. Ni/SiO_2

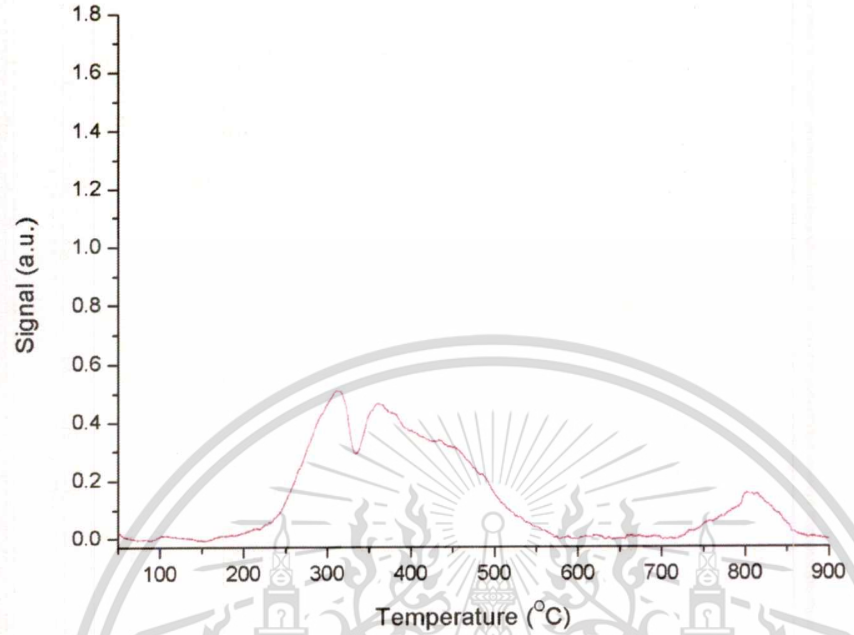

Fig.A15 Temperature programmed reduction of 10%wt. Co/SiO_2

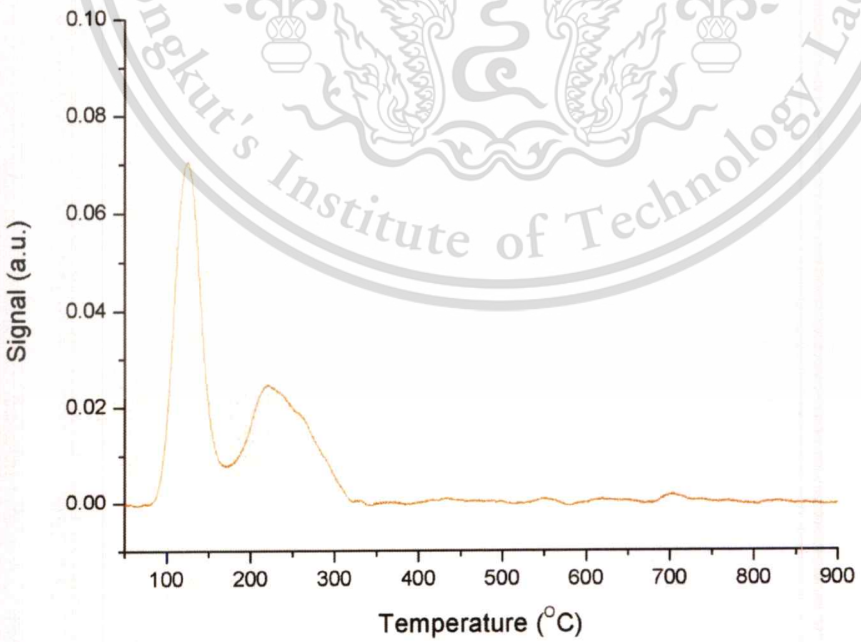

Fig.A16 Temperature programmed reduction of 10%wt. Ag/SiO_2

5. Temperature programmed desorption

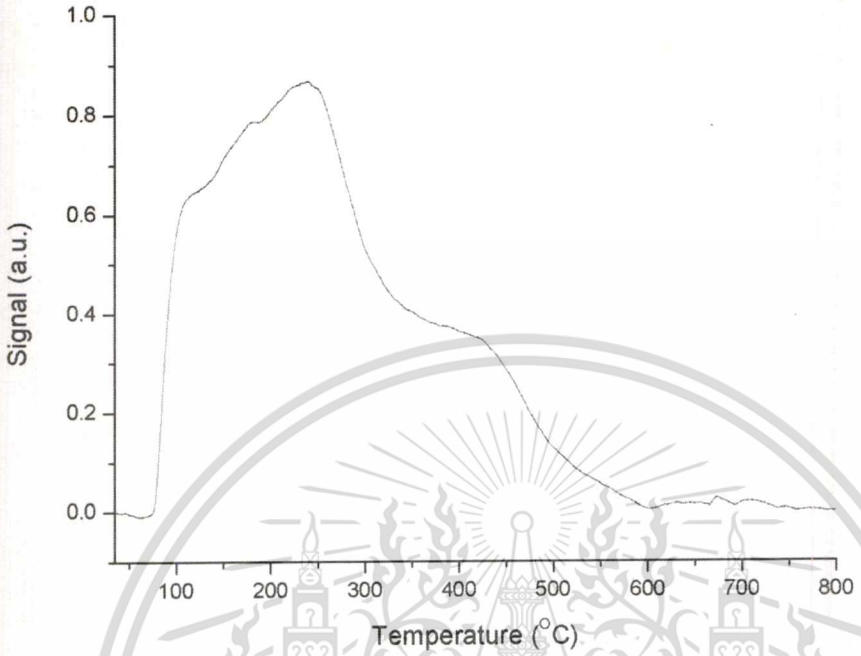

Fig.A17 Temperature programmed desorption of H-ZSM-5 ratio 12.5

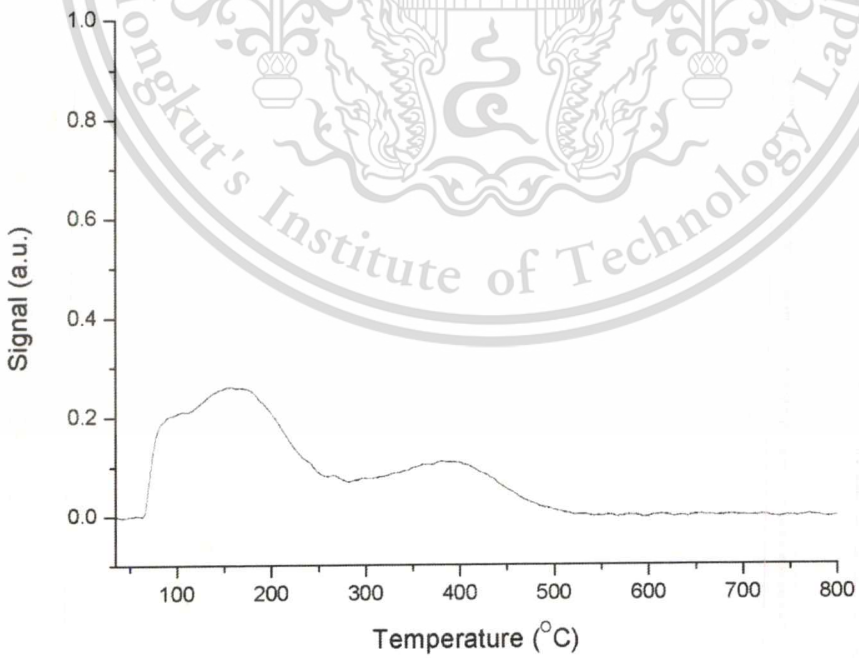

Fig.A18 Temperature programmed desorption of H-ZSM-5 ratio 28

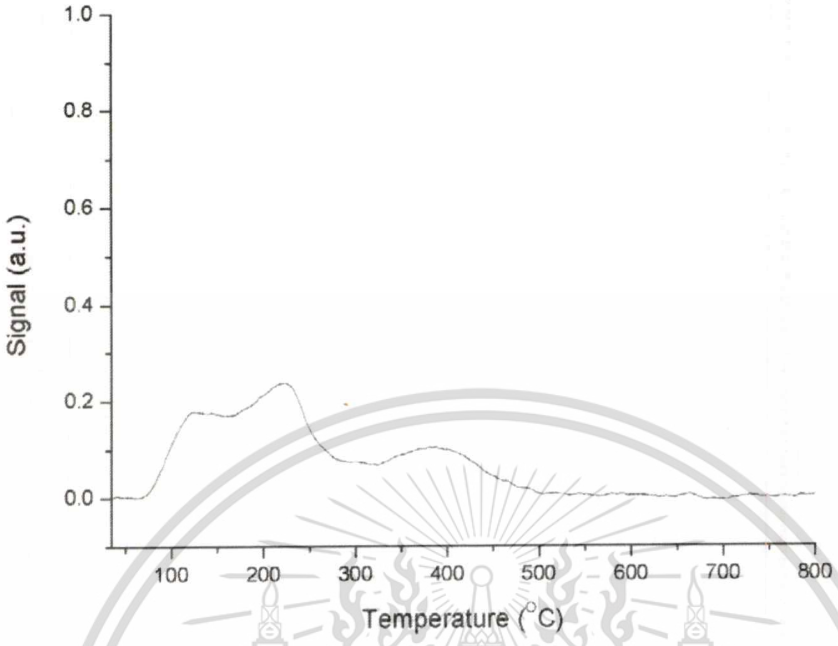

Fig.A19 Temperature programmed desorption of Ag/H-ZSM-5 ratio 28

6. Transmission electron microscopy

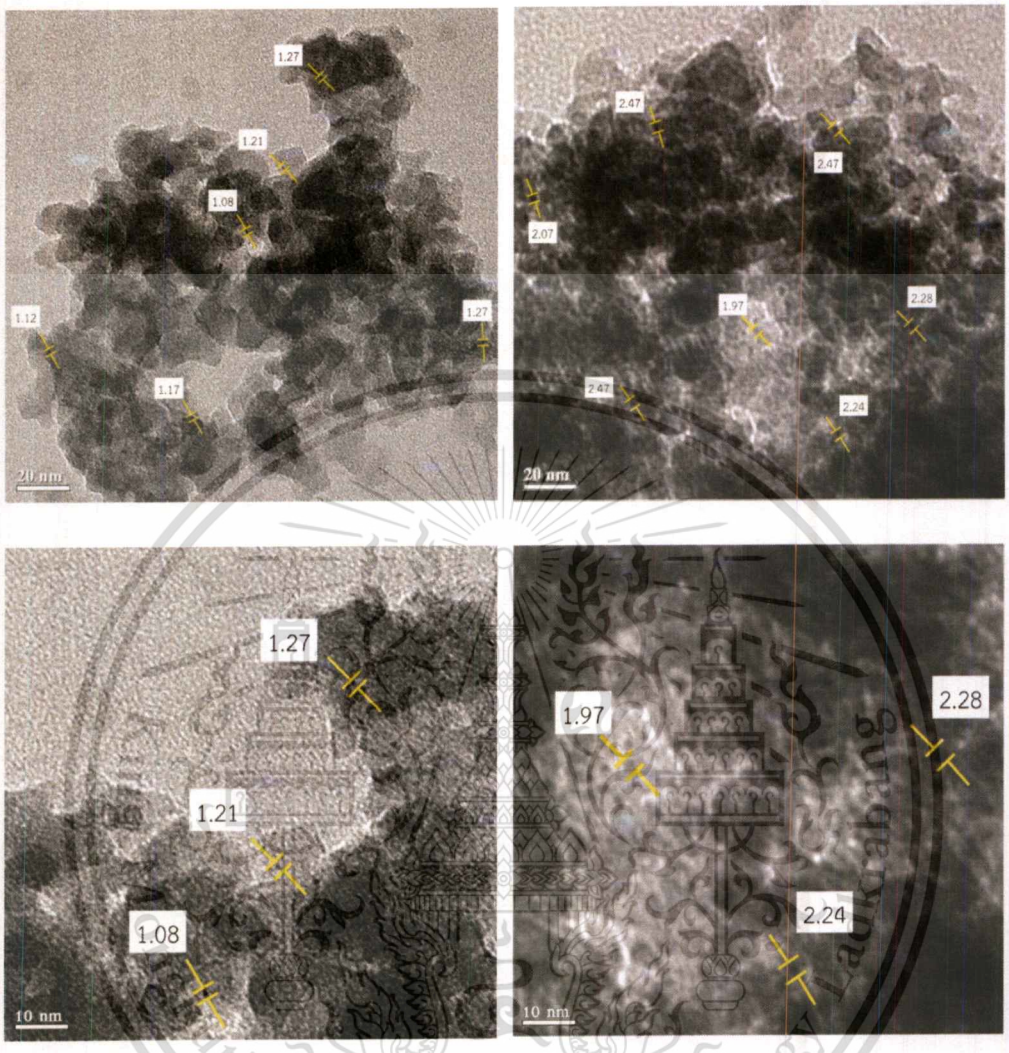

Fig.A20 Transmission electron microscope of fresh 10%wt. Cu/SiO_2 catalyst (A, C) and spent 10%wt. Cu/SiO_2 catalyst (B, D)

ภาคผนวก ข

GAS CHROMATOGRAM

Analysis gas product from gas chromatography

Prior analysis, GC-MS (gas chromatography with mass spectrometer detector) was used to identify the structure of products in the sample and the GC-FID (gas chromatography with flam ionization detector) was used to determine the quantitative of the product with the condition expressed in **Table B1.**

Table B1 The GC condition for quantitative analysis

Column	HP-5, 30 m x 0.32 mm x 0.25 µm
Temperature program	35°C (5 min hold) to 85°C (2 min hold) at 15°/min and ramp to 220°C (3 min hold) at 10°/min
Carrier gas	Nitrogen gas, flow rate 30ml/min
Injector temperature	150 °C
Detector temperature	FID at 230 °C

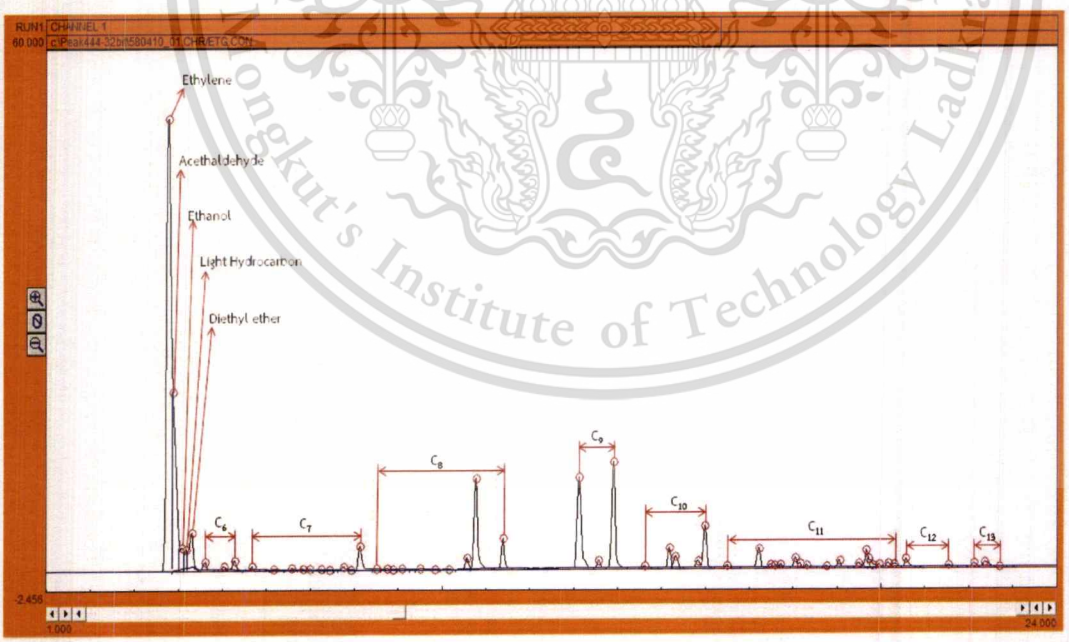

Fig. B1 Chromatogram of hydrocarbon products at contact time 10 g.h/mol

Reaction condition; Catalyst: Ag/H-ZSM-5, Temperature: 400°C,

Carrier gas; 30ml/min of nitrogen, Feed rate: 0.3889 g/h of absolute ethanol,

Ambient pressure

Table B2 Chromatogram data of standard product and feed

Component	Retention time	Structure of Product
Ethylene	3.766	 ethylene
Acetaldehyde	3.85	 acetaldehyde
Ethanol	4.066	 ethanol
Light Hydrocarbon	4.166	
Diethyl ether	4.283	 diethylether
C_6	4.583 – 5.266	(4.583)  2-methyl-pentane (5.016)  methyl-cyclopentane (5.266)  benzene
C_7	5.65 – 8.116	(5.65)  1,1-dimethyl-cyclopentane (6.566) 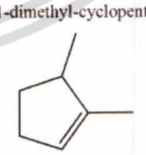 1,5-dimethyl-cyclopentene (6.816) 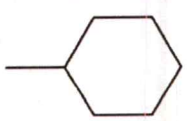 methyl-cyclohexane (7.233) 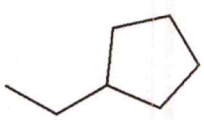 ethyl-cyclopentane

		(7.733) 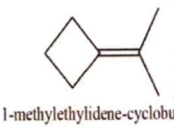 1-methylethylidene-cyclobutane (8.116) 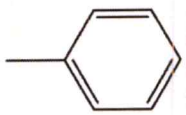 toluene
C_8	9.066 – 11.366	(9.066) 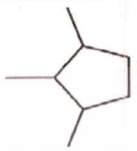 1,2,3-trimethyl cyclopentane (10.55)  p-xylene (10.75)  m-xylene (11.36)  o-xylene
C_9	13.1 – 13.883	(13.1)  1-ethyl-2-methyl-benzene (13.216) 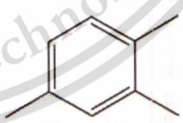 1,2,4-trimethyl-benzene 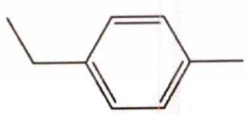 (13.55) 1-ethyl-4-methyl-benzene (13.883) 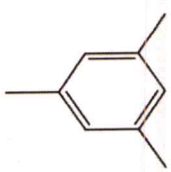 mesitylene

C_{10}	14.6 – 15.966	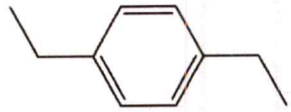 1,4-diethyl-benzene (14.6) 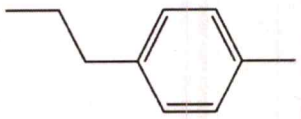 1-methyl-4-propyl-benzene (15.166) 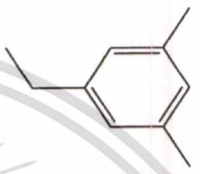 (15.3) 1-ethyl-3,5-dimethyl-benzene (15.816) 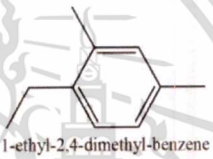 1-ethyl-2,4-dimethyl-benzene (15.966) 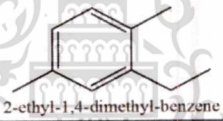 2-ethyl-1,4-dimethyl-benzene
C_{11}	16.466 – 20.283	 1-ethyl-2,4,5-trimethyl-benzene (16.466) 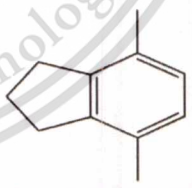 2,3-dihydro-4,7-dimethyl-1H-Indane (18.033) 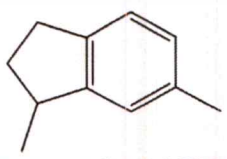 2,3-dihydro-1,6-dimethyl-1H-Indane (18.283)

		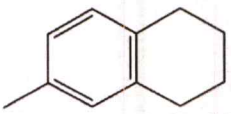 1,2,3,4-tetrahydro-6-methyl-naphthalene (18.733) 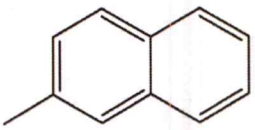 2-methyl-naphthalene (19.65)
C_{12}	20.55 – 21.516	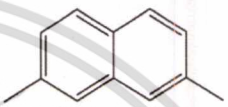 2,7-dimethyl-naphthalene (20.55) 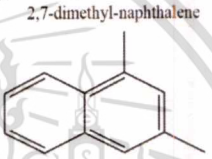 1,3-dimethyl-naphthalene (21.516)
C_{13}	22.1 – 22.683	

ภาคผนวก ค

CALCULATION

Calculation of catalytic parameters

Contact time **(W/F)**

$$W/F = \frac{\text{Weight of catalysts (g)}}{\text{Mole of reactant feed (mol/h)}}$$

Example

In the reaction using 0.0085 mol/h of ethanol in feed and using 0.3092 grams of catalyst, the W/F is calculated as follow:

$$W/F = [0.3092\ (g)\ /0.0085\ (mol/h)]$$

$$= 36\ g.h/mol$$

In similar manner; W/F of catalyst with different catalyst weight and different feed rate are calculated.

Calculation of % yield of products from gas chromatography

Table C1 the summation of the peak area for products.

Product	Peak area
Methane	12.7010
Acetaldehyde	100.3280
Ethanol (Feed)	289.1000
Total	402.129

*In formation of 10%Ag/SiO_2, Temperature 350 °C, Contact time 36 g.h/mol, time on steam = 30 minutes

In normalization method, the areas of all eluted peak were computed areas for differences in the detector response to different compound types. The concentration of the analyzed was found from the ratio of its area to the total area of all peaks.

Calculate the percent yield of each component in sample as follows:

$$\%\text{Yield in each product} = \frac{\textbf{Peak area of Y x 100}}{\textbf{Total area}}$$

When Y is each product.

For example;

$$\%\text{Yield of Acetaldehyde} = \frac{\textbf{100.328 x 100}}{\textbf{402.129}}$$

$$= 25$$

The percent yield of each product obtained from above calculation is shown in **Table C2.**

Table C2 %Yield of product derived by normalization method.

Product	% Yield
Methane	3.1
Acetaldehyde	25
Ethanol (Feed)	72
Total	100

Conversion

%Conversion can be calculated from the following equation:

$$\%\text{Conversion} = \frac{\textbf{(Area total}-\textbf{Areafeed x 100)}}{\textbf{Area total}}$$

For example;

$$\%\text{Conversion} = \frac{\textbf{(402.129}-\textbf{289) x 100}}{\textbf{402.129}}$$

$$= 28$$

Selectivity

%Selectivity can be obtained from the following equation:

$$\%\text{Selectivity in each product} = \frac{\%\text{Yield of each product x 100}}{\%\text{Conversion}}$$

For example;

$$\%\text{Selectivity of acetaldehyde} = \frac{25 \times 100}{28}$$

$$= 89$$

ภาคผนวก ง

REACTION DATA

D1 : Ethanol dehydrogenation over metal supports catalysts.

D1.1 Effect of metal

Table D1 Product distribution from the reaction of ethanol over 10%wt. Ag supported SiO_2

Time on stream (h)	Conversion (%)	Yield of acetaldehyde (%)	Yield of CH_4 (%)
30	5.5	5.1	0.4
60	5.3	4.9	0.4
90	4.5	4.3	0.2
120	4.4	4.2	0.2
150	5.1	4.9	0.2
180	5.0	4.6	0.4
210	5.0	4.7	0.3
240	4.8	4.5	0.3
270	4.6	4.3	0.3
300	4.5	4.3	0.2
330	4.4	4.1	0.4
360	4.1	4.0	0.2

Reaction condition; Temperature: 325°C, W/F; 12.7508 g.h/mol, Feed rate: 0.3889 g/h of absolute ethanol, Carrier gas; 30ml/min of nitrogen, Ambient pressure

Table D2 Product distribution from the reaction of ethanol over 10%wt. Ni supported SiO_2

Time on stream (h)	Conversion (%)	Yield of acetaldehyde (%)	Yield of CH_4 (%)
30	10.5	3.3	7.2
60	6.5	3.1	3.4
90	5.6	2.6	2.9
120	5.8	2.4	3.3
150	5.8	2.4	3.4
180	5.6	2.3	3.3
210	5.8	2.4	3.4
240	6.3	2.3	4.0
270	7.4	2.7	4.7
300	7.6	2.7	4.9
330	7.9	2.7	5.2
360	6.7	2.1	4.5

Reaction condition; Temperature: 325°C, W/F; 12.4788 g.h/mol, Feed rate: 0.3889 g/h of absolute ethanol, Carrier gas; 30ml/min of nitrogen, Ambient pressure

Table D3 Product distribution from the reaction of ethanol over 10%wt. Co supported SiO_2

Time on stream (h)	Conversion (%)	Yield of acetaldehyde (%)	Yield of CH_4 (%)
30	2.0	1.1	1.0
60	2.5	1.5	1.0
90	2.4	1.4	1.0
120	2.4	1.3	1.0
150	2.2	1.2	1.0
180	1.7	0.9	0.8
210	2.2	1.2	1.0
240	2.1	1.2	0.9
270	2.1	1.2	0.9
300	2.0	1.2	0.9
330	2.1	1.2	0.9
360	1.5	0.8	0.7

Reaction condition; Temperature: 325°C, W/F; 11.8992 g.h/mol, Feed rate: 0.3889 g/h of absolute ethanol, Carrier gas; 30ml/min of nitrogen, Ambient pressure

Table D4 Product distribution from the reaction of ethanol over 10%wt. Cu supported SiO_2

Time on stream (h)	Conversion (%)	Yield of acetaldehyde (%)	Yield of CH_4 (%)
30	35.5	35.5	0.0
60	32.0	32.0	0.0
90	35.1	35.1	0.0
120	26.2	26.2	0.0
150	22.6	22.6	0.0
180	20.4	20.4	0.0
210	14.9	14.9	0.0
240	9.7	9.7	0.0
270	7.7	7.7	0.0
300	6.6	6.6	0.0
330	5.4	5.4	0.0
360	4.7	4.7	0.0

Reaction condition; Temperature: 325°C, W/F; 12.2540 g.h/mol, Feed rate: 0.3889 g/h of absolute ethanol, Carrier gas; 30ml/min of nitrogen, Ambient pressure

D1.2 : Effect of Reaction Temperature

D1.2.1 : Ag/SiO_2

Table D5 The yield of ethanol dehydrogenation at 325°C

Time on stream (h)	Conversion (%)	Yield of acetaldehyde (%)	Yield of CH_4 (%)
30	5.5	5.1	0.4
60	5.3	4.9	0.4
90	4.5	4.3	0.2
120	4.4	4.2	0.2
150	5.1	4.9	0.2
180	5.0	4.6	0.4
210	5.0	4.7	0.3
240	4.8	4.5	0.3
270	4.6	4.3	0.3
300	4.5	4.3	0.2
330	4.4	4.1	0.4
360	4.1	4.0	0.2

Reaction condition; Catalyst: 10%wt. Ag supported SiO_2, W/F; 12.7508 g.h/mol, Carrier gas; 30ml/min of nitrogen, Feed rate: 0.3889 g/h of absolute ethanol, Ambient pressure

Table D6 The yield of ethanol dehydrogenation at 350°C

Time on stream (h)	Conversion (%)	Yield of acetaldehyde (%)	Yield of CH_4 (%)
30	30.0	27.9	2.1
60	32.6	31.2	1.4
90	32.1	30.3	1.8
120	30.1	28.5	1.6
150	31.4	29.9	1.6
180	31.8	30.7	1.1
210	31.1	29.6	1.5
240	31.5	30.2	1.4
270	32.1	30.6	1.6
300	32.2	30.6	1.6
330	30.7	29.0	1.7
360	31.5	30.0	1.5

Reaction condition; Catalyst: 10%wt. Ag supported SiO_2, W/F; 13.2003 g.h/mol, Carrier gas; 30ml/min of nitrogen, Feed rate: 0.3889 g/h of absolute ethanol, Ambient pressure

Table D7 The yield of ethanol dehydrogenation at 375°C

Time on stream (h)	Conversion (%)	Yield of acetaldehyde (%)	Yield of CH_4 (%)
30	36.6	30.5	6.0
60	33.3	29.9	3.4
90	33.5	30.0	3.5
120	35.9	31.8	4.1
150	35.1	30.4	4.7
180	32.4	29.4	3.0
210	35.3	31.3	3.9
240	38.5	34.7	3.7
270	37.9	34.5	3.4
300	33.9	31.3	2.6
330	39.5	34.6	5.0
360	34.9	32.3	2.6

Reaction condition; Catalyst: 10%wt. Ag supported SiO_2, W/F; 13.2594 g.h/mol, Carrier gas; 30ml/min of nitrogen, Feed rate: 0.3889 g/h of absolute ethanol, Ambient pressure

D1.2.2 : Cu/SiO_2

Table D8 The yield of ethanol dehydrogenation at 400°C

Time on stream (h)	Conversion (%)	Yield of acetaldehyde (%)	Yield of CH_4 (%)
55	34.9	34.5	0.4
95	30.4	30.1	0.3
135	25.4	25.1	0.3
175	21.6	21.4	0.2
215	20.8	20.6	0.2
255	17.4	17.2	0.2
295	13.8	13.6	0.2
335	11.5	11.3	0.2
375	10.7	10.5	0.2
415	9.9	9.7	0.2
455	8.4	8.3	0.1

Reaction condition; Catalyst: 10%wt. Cu supported SiO_2, W/F; 15.1751 g.h/mol, Carrier gas; 166ml/min of nitrogen, Feed rate: 0.5523 g/h of absolute ethanol, Ambient pressure

Table D9 The yield of ethanol dehydrogenation at 500°C

Time on stream (h)	Conversion (%)	Yield of acetaldehyde (%)	Yield of CH_4 (%)
15	67.4	61.6	5.8
55	56.9	52.0	4.9
95	53.2	48.0	5.2
135	50.0	46.3	3.7
175	47.2	42.3	4.9
215	49.9	45.3	4.6
255	49.1	44.6	4.5
295	48.5	44.1	4.4

Reaction condition; Catalyst: 10%wt. Cu supported SiO_2, W/F; 15.1418 g.h/mol, Carrier gas; 166ml/min of nitrogen, Feed rate: 0.5523 g/h of absolute ethanol, Ambient pressure

D1.3 Effect of Contact time

Table D10 The yield of ethanol dehydrogenation at contact time 13 g.h/mol

Time on stream (h)	Conversion (%)	Yield of acetaldehyde (%)	Yield of CH_4 (%)
30	30.0	27.9	2.1
60	32.6	31.2	1.4
90	32.1	30.3	1.8
120	30.1	28.5	1.6
150	31.4	29.9	1.6
180	31.8	30.7	1.1
210	31.1	29.6	1.5
240	31.5	30.2	1.4
270	32.1	30.6	1.6
300	32.2	30.6	1.6
330	30.7	29.0	1.7
360	31.5	30.0	1.5

Reaction condition; Catalyst: 10%wt. Ag supported SiO_2, Temperature: 350°C, Carrier gas; 30ml/min of nitrogen, Feed rate: 0.3889 g/h of absolute ethanol, Ambient pressure

Table D11 The yield of ethanol dehydrogenation at contact time 27 g.h/mol

Time on stream (h)	Conversion (%)	Yield of acetaldehyde (%)	Yield of CH_4 (%)
30	50.6	48.0	2.6
60	50.3	48.9	1.4
90	49.5	47.9	1.6
120	56.2	54.2	2.0
150	53.4	51.6	1.8
180	52.9	51.3	1.5
210	52.9	50.8	2.1
240	52.6	51.2	1.4
270	37.3	36.4	0.9
300	39.7	38.5	1.2
330	52.7	50.7	2.0

Reaction condition; Catalyst: 10%wt. Ag supported SiO_2, Temperature: 350°C, Carrier gas; 30ml/min of nitrogen, Feed rate: 0.3889 g/h of absolute ethanol, Ambient pressure

Table D12 The yield of ethanol dehydrogenation at contact time 36 g.h/mol

Time on stream (h)	Conversion (%)	Yield of acetaldehyde (%)	Yield of CH_4 (%)
30	57.1	55.6	1.5
60	56.8	54.9	1.9
90	56.2	54.7	1.5
120	57.8	56.6	1.2
150	55.2	54.0	1.2
180	55.9	54.5	1.4
210	55.3	53.7	1.7
240	57.1	55.9	1.2
270	56.5	55.5	0.9
300	45.3	44.5	0.8
330	56.1	55.1	1.0
360	53.5	52.1	1.4

Reaction condition; Catalyst: 10%wt. Ag supported SiO_2, Temperature: 350°C, carrier gas; 30ml/min of nitrogen, Feed rate: 0.3889 g/h of absolute ethanol, Ambient pressure

D2 : Ethanol dehydration over H-ZSM-5 catalysts.

D2.1 : Effect of Reaction Temperature

Table D13 The yield of ethanol dehydration at 400°C

Time on steam	% Conversion	% Yields						
		Ethylene	DEE	Light H/C	BTX	C6-C8	C9	C10+
30	97.7	66.9	4.1	1.4	4.9	2.9	8.4	9.1
70	98.3	76.2	3.5	1.2	3.5	1.8	6.5	5.6
110	98.1	78.0	3.9	1.3	3.4	2.0	6.0	3.5
150	98.1	79.0	4.2	1.4	2.7	1.9	5.3	3.5
190	98.0	81.3	3.7	1.3	2.5	1.9	4.6	2.7
230	98.2	83.5	3.6	1.5	2.1	1.2	4.1	2.1
270	98.0	82.2	3.8	1.3	2.2	1.9	4.2	2.4
310	97.9	81.7	4.2	1.5	2.0	2.1	4.1	2.3
350	97.8	81.8	4.3	1.4	1.8	2.1	3.7	2.7
390	97.8	82.4	4.3	1.5	1.8	2.3	3.6	1.8

Reaction condition; Catalyst: H-ZSM-5 Si/Al ratio 12.5, W/F; 10 g.h/mol, Carrier gas; 30ml/min of nitrogen, Feed rate: 0.3889 g/h of absolute ethanol, Ambient pressure

Table D14 The yield of ethanol dehydration at 425°C

Time on steam	% Conversion	% Yields						
		Ethylene	DEE	Light H/C	BTX	C6-C8	C9	C10+
30	100.0	55.5	0.9	0.3	12.2	1.8	14.3	15.0
70	100.0	88.3	3.1	1.3	2.2	2.2	2.1	0.8
110	100.0	89.7	2.3	0.0	3.5	2.3	1.5	0.7
150	100.0	91.7	2.5	1.1	1.3	1.7	0.9	0.7
190	100.0	90.8	2.8	0.9	1.9	1.7	1.1	0.8
230	98.7	89.4	3.1	1.0	1.5	1.8	0.9	0.9
270	100.0	92.2	2.4	0.8	1.5	1.5	0.9	0.9
310	100.0	92.6	2.4	0.8	1.3	1.3	0.8	0.8
350	100.0	92.9	2.1	0.9	1.3	1.0	0.8	1.0
390	-	-	-	-	-	-	-	-

Reaction condition; Catalyst: H-ZSM-5 Si/Al ratio 12.5, W/F; 10 g.h/mol, Carrier gas; 30ml/min of nitrogen, Feed rate: 0.3889 g/h of absolute ethanol, Ambient pressure

D2.2 Effect of contact time

Table D15 The yield of ethanol dehydration at contact time 5.2 g.h/mol

Time on steam	% Conversion	% Yields						
		Ethylene	DEE	Light H/C	BTX	C6-C8	C9	C10+
30	100	99.1	0.4	0	0.2	0	0.4	0
70	100	99.7	0.3	0	0	0	0	0
110	100	99.7	0.3	0	0	0	0	0
150	100	99.8	0.2	0	0	0	0	0
190	100	99.8	0.2	0	0	0	0	0
230	100	99.7	0.3	0	0	0	0	0
270	100	99.7	0.3	0	0	0	0	0
310	100	99.8	0.2	0	0	0	0	0
350	100	99.8	0.2	0	0	0	0	0
390	100	99.8	0.2	0	0	0	0	0

Reaction condition; Catalyst: H-ZSM-5 Si/Al ratio 12.5, Temperature: 400°C, Carrier gas; 30ml/min of nitrogen, Feed rate: 0.3889 g/h of absolute ethanol, Ambient pressure

Table D16 The yield of ethanol dehydration at contact time 10 g.h/mol

Time on steam	% Conversion	% Yields						
		Ethylene	DEE	Light H/C	BTX	C6-C8	C9	C10+
30	97.7	66.9	4.1	1.4	4.9	2.9	8.4	9.1
70	98.3	76.2	3.5	1.2	3.5	1.8	6.5	5.6
110	98.1	78.0	3.9	1.3	3.4	2.0	6.0	3.5
150	98.1	79.0	4.2	1.4	2.7	1.9	5.3	3.5
190	98.0	81.3	3.7	1.3	2.5	1.9	4.6	2.7
230	98.2	83.5	3.6	1.5	2.1	1.2	4.1	2.1
270	98.0	82.2	3.8	1.3	2.2	1.9	4.2	2.4
310	97.9	81.7	4.2	1.5	2.0	2.1	4.1	2.3
350	97.8	81.8	4.3	1.4	1.8	2.1	3.7	2.7
390	97.8	82.4	4.3	1.5	1.8	2.3	3.6	1.8

Reaction condition; Catalyst: H-ZSM-5 Si/Al ratio 12.5, Temperature: 400°C, Carrier gas; 30ml/min of nitrogen, Feed rate: 0.3889 g/h of absolute ethanol, Ambient pressure

Table D17 The yield of ethanol dehydration at contact time 15 g.h/mol

Time on steam	% Conversion	% Yields						
		Ethylene	DEE	Light H/C	BTX	C6-C8	C9	C10+
30	96.8	53.7	3.2	1.8	11.2	2.9	12.1	12.0
70	96.9	58.0	3.2	1.5	11.0	2.6	11.4	9.2
110	96.4	56.9	3.3	1.5	11.1	3.0	12.0	8.5
150	96.5	59.0	3.4	1.6	9.9	3.0	10.7	8.8
190	96.7	59.4	3.5	1.6	9.8	2.5	10.8	9.0
230	96.6	61.1	3.6	1.7	9.7	2.9	10.2	7.4
270	96.6	59.1	3.4	1.6	10.0	3.4	10.9	8.3
310	96.9	56.5	3.3	1.8	9.7	2.8	11.0	11.7
350	96.5	60.9	3.3	0.0	9.1	3.2	9.4	10.6
390	97.6	46.0	3.6	1.5	14.4	11.7	10.3	10.0

Reaction condition; Catalyst: H-ZSM-5 Si/Al ratio 12.5, Temperature: 400°C, Carrier gas; 30ml/min of nitrogen, Feed rate: 0.3889 g/h of absolute ethanol, Ambient pressure

Table D18 The yield of ethanol dehydration at contact time 5.1 g.h/mol

Time on steam	% Conversion	% Yields						
		Ethylene	DEE	Light H/C	BTX	C6-C8	C9	C10+
30	100	98.2	0.1	0.0	0.8	0.0	0.9	0
70	100	99.9	0.1	0.0	0.0	0.0	0.0	0
110	100	99.7	0.0	0.0	0.0	0.3	0.0	0
150	100	99.6	0.1	0.0	0.0	0.3	0.0	0
190	-	-	-	-	-	-	-	-
230	100	99.9	0.0	0.1	0.0	0.1	0.0	0
270	100	99.7	0.1	0.0	0.0	0.3	0.0	0
310	100	99.7	0.1	0.0	0.0	0.2	0.0	0
350	100	99.7	0.0	0.0	0.0	0.2	0.0	0
390	100	99.6	0.0	0.0	0.0	0.0	0.4	0

Reaction condition; Catalyst: H-ZSM-5 Si/Al ratio 28, Temperature: 400°C, Carrier gas; 30ml/min of nitrogen, Feed rate: 0.3889 g/h of absolute ethanol, Ambient pressure

Table D19 The yield of ethanol dehydration at contact time 10 g.h/mol

Time on steam	% Conversion	% Yields						
		Ethylene	DEE	Light H/C	BTX	C6-C8	C9	C10+
30	100.0	67.1	2.0	0.7	4.6	0.3	7.1	18.1
70	100.0	77.2	1.8	0.8	3.3	0.1	6.0	10.7
110	98.3	81.0	4.7	1.9	1.6	3.2	2.2	3.7
150	100.0	86.2	2.2	0.8	2.3	0.1	4.2	4.2
190	100.0	92.7	1.9	0.8	1.0	0.0	2.7	0.8
230	100.0	93.0	2.3	1.0	0.9	0.2	2.2	0.5
270	100.0	93.4	2.2	0.9	0.9	0.0	2.2	0.4
310	100.0	94.2	2.0	0.9	0.7	0.0	2.0	0.2
350	100.0	95.6	1.9	0.7	0.5	0.0	1.3	0.0
390	100.0	96.3	1.9	0.0	0.5	0.0	1.3	0.0

Reaction condition; Catalyst: H-ZSM-5 Si/Al ratio 28, Temperature: 400°C, Carrier gas; 30ml/min of nitrogen, Feed rate: 0.3889 g/h of absolute ethanol, Ambient pressure

Table D20 The yield of ethanol dehydration at contact time 15 g.h/mol

Time on steam	% Conversion	% Yields						
		Ethylene	DEE	Light H/C	BTX	C6-C8	C9	C10+
30	98.7	46.9	3.3	1.2	8.0	2.2	13.3	23.8
70	98.5	55.3	4.0	1.2	6.7	2.7	10.7	17.9
110	98.4	63.3	4.6	1.8	5.9	3.6	9.1	10.0
150	98.5	66.4	4.8	1.5	5.0	3.4	8.2	9.2
190	98.4	65.9	4.7	1.8	4.6	3.4	7.8	10.2
230	97.9	67.2	5.3	1.7	4.7	4.7	7.5	6.8
270	98.0	68.2	5.2	1.6	4.8	4.4	7.1	6.6
310	98.5	66.5	4.7	1.8	5.1	3.8	8.5	8.1
350	97.9	70.7	5.1	1.9	4.1	4.3	6.3	5.5
390	98.1	72.3	5.3	2.0	3.8	4.4	6.0	4.4

Reaction condition; Catalyst: H-ZSM-5 Si/Al ratio 28, Temperature: 400°C, Carrier gas; 30ml/min of nitrogen, Feed rate: 0.3889 g/h of absolute ethanol, Ambient pressure

D3: Ethanol conversion over silver incorporated support.

Table D21 Product distribution from ethanol conversion over 10% wt. Ag/SiO_2 + H-ZSM-5(28)

Time on steam	% Conversion	% Yields							
		Ethylene	Acetaldehyde	DEE	Light H/C	BTX	C6-C8	C9	C10+
30	98.5	38.9	13.9	3.3	1.6	11.8	1.5	15.5	12.0
70	98.5	38.3	20.0	2.9	1.5	11.2	2.6	14.1	7.8
110	98.4	43.6	17.3	3.0	1.6	10.6	3.1	13.0	6.1
150	97.6	41.7	19.1	3.6	1.8	10.0	2.9	12.2	6.3
190	98.3	41.8	18.0	3.8	1.8	10.5	2.9	12.9	6.5
230	98.2	42.3	15.4	3.3	1.4	11.4	3.6	13.7	7.1
270	97.9	39.7	18.4	3.5	2.1	11.4	3.3	13.5	6.1
310	98.1	33.6	18.2	3.2	1.6	12.9	3.5	15.8	9.3
350	98.7	36.4	12.5	2.9	1.2	13.6	3.8	16.4	11.8
390	98.6	32.0	14.9	3.2	1.1	14.1	3.7	17.5	12.1

Reaction condition; Catalyst: Temperature: 400°C, , W/F of H-ZSM-5; 10 g.h/mol Carrier gas; 30ml/min of nitrogen, Feed rate: 0.3889 g/h of absolute ethanol, Ambient pressure

D3.1 Effect of contact time

Table D22 Product distribution from ethanol conversion at contact time 5.3 g.h/mol

Time on steam	% Conversion	% Yields							
		Ethylene	Acetaldehyde	DEE	Light H/C	BTX	C6-C8	C9	C10+
30	99.1	68.4	8.5	1.6	0.8	5.2	0.1	9.2	5.3
70	98.9	74.5	10.0	1.7	0.8	3.6	1.1	5.8	1.5
110	99.2	78.3	8.6	1.6	0.8	3.4	1.1	4.4	0.9
150	98.9	75.0	11.1	1.8	0.8	4.0	1.6	3.9	0.7
190	99.1	79.8	9.3	1.9	0.8	3.0	1.2	2.5	0.5
230	98.9	77.1	10.7	1.8	1.8	3.2	1.5	2.6	0.3
270	98.9	79.1	10.7	1.8	0.8	2.5	1.6	2.2	0.2
310	98.5	77.7	12.0	1.6	0.9	2.7	1.1	1.7	0.7
350	98.8	76.4	12.4	2.0	0.9	2.7	1.5	1.8	1.1
390	98.7	77.7	11.8	1.9	0.9	2.7	1.3	1.7	0.7

Reaction condition; Catalyst: Ag/H-ZSM-5, Temperature: 400°C, Carrier gas; 30ml/min of nitrogen, Feed rate: 0.3889 g/h of absolute ethanol, Ambient pressure

Table D23 Product distribution from ethanol conversion at contact time 10 g.h/mol

Time on steam	% Conversion	% Yields							
		Ethylene	Acetaldehyde	DEE	Light H/C	BTX	C6-C8	C9	C10+
30	98.3	40.3	13.3	2.8	1.1	11.4	2.3	14.7	12.3
70	97.8	47.1	16.4	3.8	1.6	9.6	2.8	11.6	4.9
110	97.9	46.3	13.8	3.2	1.4	10.8	2.7	12.8	6.8
150	97.6	47.4	14.0	3.5	1.4	10.8	3.2	12.3	5.0
190	-	-	-	-	-	-	-	-	-
230	-	-	-	-	-	-	-	-	-
270	97.9	47.6	11.6	3.0	1.6	11.4	3.3	12.7	6.7
310	97.5	43.7	16.3	3.3	1.4	10.8	2.9	12.3	6.9
350	97.6	48.5	13.4	3.7	1.8	10.4	3.2	11.2	5.4
390	98.1	42.9	16.7	3.4	1.6	10.9	3.6	12.7	6.3

Reaction condition; Catalyst: Ag/H-ZSM-5, Temperature: 400°C, Carrier gas; 30ml/min of nitrogen, Feed rate: 0.3889 g/h of absolute ethanol, Ambient pressure

Table D24 Product distribution from ethanol conversion at contact time 15 g.h/mol

Time on steam	% Conversion	% Yields							
		Ethylene	Acetaldehyde	DEE	Light H/C	BTX	C6-C8	C9	C10+
30	97.9	23.2	15.9	2.5	1.2	15.0	1.5	17.8	20.9
70	97.8	30.4	13.6	2.5	1.5	16.5	1.9	18.0	13.6
110	97.2	32.1	14.1	2.6	1.4	16.1	2.2	17.2	11.6
150	96.7	31.3	15.8	3.1	1.7	15.8	2.4	15.7	10.9
190	97.5	29.8	14.4	2.8	1.3	16.4	2.1	17.7	13.0
230	97.1	34.6	13.8	2.7	1.1	15.7	2.8	15.5	10.9
270	97.7	26.6	14.2	2.6	1.2	15.5	1.6	15.3	20.7
310	97.4	29.0	15.9	2.6	1.3	16.8	2.4	16.4	13.0
350	97.7	32.3	11.7	2.3	1.4	18.7	3.2	16.8	11.3
390	96.4	33.4	14.7	3.0	1.6	15.6	4.1	14.4	9.5

Reaction condition; Catalyst: Ag/H-ZSM-5, Temperature: 400°C,
Carrier gas; 30ml/min of nitrogen, Feed rate: 0.3889 g/h of absolute ethanol,
Ambient pressure

Table D25 Product distribution from ethanol conversion at contact time 25 g.h/mol

Time on steam	% Conversion	% Yields							
		Ethylene	Acetaldehyde	DEE	Light H/C	BTX	C6-C8	C9	C10+
30	97.2	29.0		1.2	0.7	28.1	3.6	17.3	17.3
70	97.5	29.0		1.4	0.9	26.3	3.9	18.6	17.4
110	97.6	28.1		1.2	0.8	26.3	3.6	18.0	19.7
150	97.3	30.1		1.3	0.9	27.4	3.7	18.3	15.7
190	96.9	32.0		1.4	1.0	26.7	3.9	17.1	14.9
240	97.2	30.7		1.5	1.0	26.7	3.8	17.0	16.4
280	96.9	30.8		1.4	1.0	27.0	3.7	17.1	15.9
320	97.7	27.6		1.1	0.9	29.1	3.6	18.5	17.0
360	97.2	29.0		1.2	0.7	28.2	3.4	17.2	17.4
400	97.3	28.8		1.1	0.9	29.1	3.5	18.6	15.4

Reaction condition; Catalyst: Ag/H-ZSM-5, Temperature: 400°C,
Carrier gas; 30ml/min of nitrogen, Feed rate: 0.3889 g/h of absolute ethanol,
Ambient pressure

Table D26 Product distribution from ethanol conversion at contact time 42 g.h/mol

Time on steam	% Conversion	% Yields							
		Ethylene	Acetaldehyde	DEE	Light H/C	BTX	C6-C8	C9	C10+
30	97.8	18.6		0.8	0.6	20.2	1.5	13.9	42.3
70	96.9	24.6		1.0	0.8	22.5	2.0	14.3	31.7
110	97.1	22.9		1.0	0.6	23.1	1.8	15.5	32.1
150	96.3	26.3		1.1	0.9	27.1	2.6	16.7	21.5
190	96.8	26.2		0.9	0.8	27.6	2.3	17.8	21.1
240	100.0	23.7		0.5	0.0	24.9	1.9	16.6	32.5
280	96.7	24.4		0.8	0.7	25.9	2.5	16.3	26.0
320	96.4	24.6		1.1	1.0	27.0	2.7	16.8	23.2
360	96.6	24.1		0.9	0.6	27.4	2.4	17.7	23.5
400	96.6	24.1		0.9	0.6	27.4	2.4	17.7	23.5

Reaction condition; Catalyst: Ag/H-ZSM-5, Temperature: 400°C, Carrier gas; 30ml/min of nitrogen, Feed rate: 0.3889 g/h of absolute ethanol, Ambient pressure

ภาคผนวก จ

สรุปค่าใช้จ่ายการดำเนินโครงการวิจัย

บันทึกรายการรับ-จ่ายเงิน โครงการวิจัย สัญญาเลขที่ .....2560-01-05-065..... ตั้งแต่วันที่ .....1 ต.ค. 59..... ถึงวันที่ .....30 ก.ย. 60.....

แหล่งทุน: คณะวิทยาศาสตร์

ชื่อโครงการ : การศึกษาประสิทธิภาพของตัวเร่งปฏิกิริยาเพื่อเปลี่ยนเอทานอลเป็นแก๊สโซลีน

ชื่อหัวหน้าโครงการ: รศ.ดร.ดะวัน สุขน้อย

ว/ด/ป	รายการ	เลขที่อ้างถึง	รายการรับ - จ่าย			รายรับ	รายจ่าย						รวม
			รับ	จ่าย	คงเหลือ	ดอกเบี้ยรับ	งบบุคลากร	งบดำเนินงาน				งบลงทุน	รายจ่าย
							ค่าจ้างชั่วคราว	ค่าตอบแทน	ค่าใช้สอย	ค่าวัสดุ	ค่าสาธารณูปโภค	ค่าครุภัณฑ์	
	งบประมาณที่ได้รับการอนุมัติ (ตามแผน)												-
	จำนวนเงินที่ได้รับ (งวดที่ 1 = 85%)		127,500.00										
	จำนวนเงินที่ได้รับ (งวดที่ 2 = 15%)		22,500.00										
	จำนวนเงินที่ได้รับ (งวดที่ 3)												
	หัก ค่าใช้จ่าย (ครั้งที่ 1)			88,782.50			46,800.00	-	15,937.50	26,013.00	32.00	-	88,782.50
	ค่าใช้จ่าย (ครั้งที่ 2)			61,217.77			-	-	7,800.00	53,417.77	-	-	61,217.77
	งบประมาณคงเหลือ		150,000.00	-	0.27	9.00							
	รายละเอียดค่าใช้จ่าย												
ครั้งที่ 1													
6 ก.พ. 60	ค่าวิเคราะห์ XRD	00843							1,720.00				1,720.00
7 ก.พ. 60	Teflon tape	1158								200.00			200.00
16 ก.พ. 60	Fittings									1,020.00			1,020.00
28 ก.พ. 60	ค่าจ้างชั่วคราว						15,600.00						15,600.00
7 มี.ค. 60	ค่าไปรษณีย์	3822									32.00		32.00
16 มี.ค. 60	Heating tape	1386								3,852.00			3,852.00
17 มี.ค. 60	ค่าวิเคราะห์ TEM	LSU60001959							7,687.50				7,687.50
31 มี.ค. 60	ค่าวิเคราะห์ XRF	00749							1,370.00				1,370.00
31 มี.ค. 60	ค่าจ้างชั่วคราว						15,600.00						15,600.00
4 เม.ย. 60	Nitrogen and Hydrogen gas	17000466 RP								9,951.00			9,951.00
21 เม.ย. 60	ค่าวิเคราะห์ XRD	00852							5,160.00				5,160.00
30 เม.ย. 60	ค่าจ้างชั่วคราว						15,600.00						15,600.00
2 พ.ค. 60	Flow meter	IV0600277								10,700.00			10,700.00
16 พ.ค. 60	ค่าถ่ายเอกสาร									290.00			290.00
													-
													-
	รวมครั้งที่ 1						46,800.00	-	15,937.50	26,013.00	32.00	-	88,782.50
ครั้งที่ 2													
2 มิ.ย. 60	ค่าวิเคราะห์ SEM	23							7,800.00				7,800.00
18 ก.ย. 17	Lab accessories	5022173304								933.00			933.00
19 ก.ย. 17	ค่าถ่ายเอกสาร	13367								500.00			500.00
19 ก.ย. 17	Air with cylinder	RC6009190005								6,473.50			6,473.50
20 ก.ย. 17	Regulator	17001154 RP								4,066.00			4,066.00
21 ก.ย. 17	Nickel nitrate	IV17-091051								1,369.60			1,369.60
29 ก.ย. 17	Fittings (Reducing 1/8 to 8mm)	07632								2,495.67			2,495.67
29 ก.ย. 17	stainless sheet	IV00038								8,560.00			8,560.00
29 ก.ย. 17	Heating cement	IV00043								9,095.00			9,095.00
29 ก.ย. 17	Insulator blocks	IV00037								9,630.00			9,630.00
29 ก.ย. 17	Motors	IV00041								10,165.00			10,165.00
29 ก.ย. 17	Zip bag									130.00			130.00
	รวมครั้งที่ 2						-	-	7,800.00	53,417.77	-	-	61,217.77

ประวัตินักวิจัย

หัวหน้าโครงการวิจัย

1. ชื่อ - นามสกุล (ภาษาไทย)

   รศ.ดร.ตะวัน สุขน้อย

2. ชื่อ - นามสกุล (ภาษาอังกฤษ)

   Assoc.Prof.Tawan Sooknoi

3. ตำแหน่งปัจจุบัน

   รองศาสตราจารย์

4. หน่วยงานและสถานที่อยู่ที่ติดต่อ

   ภาควิชาเคมี คณะวิทยาศาสตร์ สถาบันเทคโนโลยีพระจอมเกล้าเจ้าคุณทหารลาดกระบัง 10520 แขวงลาดกระบัง เขตลาดกระบัง กรุงเทพ ช.ฉลองกรุง1 1

   โทรศัพท์ 02 329 8400-11 ต่อ 6250 โทรสาร 02 329 8428 โทรศัพท์มือถือ 081 929 8288

   อีเมล์ kstawan@gmail.com

5. ประวัติการศึกษา

   2530-2534 วท.บ. สถาบันเทคโนโลยีพระจอมเกล้าเจ้าคุณทหารลาดกระบัง

   2536-2535 M.Sc. University of Manchester Institute of Science and Technology, UK

   2536-2537 Ph.D. University of Manchester Institute of Science and Technology, UK

6. สาขาวิชาการที่มีความชำนาญพิเศษ (แตกต่างจากวุฒิการศึกษา) ระบุสาขาวิชาการ

   Applied Chemistry, Zeolite and Heterogeneous Catalysis

7. ประสบการณ์ที่เกี่ยวข้องกับการบริหารงานวิจัยทั้งภายในและภายนอกประเทศ

<u>ปี 2558</u>

(i) Aligned CNTs/Polymer Composites Membrane for Selective Gas Separation, ทุนนักศึกษาโครงการปริญญาเอกกาญจนาภิเษก, สำนักงานกองทุนสนับสนุนการวิจัย (5 ปี)

(ii) Oxidative approach for methane conversion under SCG-KMITL Catalyst Innovation Program, SCG Chemicals Co.,Ltd. (1.5 year)

(iii) Heterolytic C-H activation of Methane using single site heterogeneous catalysts under SCG-KMITL Catalyst Innovation Program, SCG Chemicals Co.,Ltd. (1.5 year)

(iv) Methane activation over metal loaded zeolites under SCG-KMITL Catalyst Innovation Program, SCG Chemicals Co.,Ltd. (1.5 year)

ปี 2557

(i) SCG-KMITL Catalyst Innovation Program, SCG Chemicals Co.,Ltd.

ปี 2556

(i) Decarbonylation / Decarboxylation of fatty acid to produce renewable long chain α-olefin, ทุนวิจัยองค์ความรู้ใหม่ที่เป็นพื้นฐานต่อการพัฒนา (วุฒิเมธีวิจัย สกว.), สำนักงานกองทุนสนับสนุนการวิจัย (3 ปี).

(ii) Swift response catalytic testing system for innovative approach, Research & Development Grant, SCG Chemicals Co.,Ltd. (1 year).

(iii) Glycerol conversion to C3 alcohols, Research & Development Grant, PTT Public Co.,Ltd. (1.2 year).

งานวิจัยที่ทำเสร็จแล้ว :

(i) Extending the basic function of lattice oxygen in lepidocrocite titanate – The conversion of intercalated fatty acid to liquid hydrocarbon fuels, Tosapol Maluangnont, Pornanan Arsa, Tawan Sooknoi, Journal of Solid State Chemistry, 256 (2017) 219–226

(ii) Production of liquid fuel from palmitic acid over nanocrystalline CeO_2-based catalysts with minimal use of H_2, Tosapol Maluangnont, Chalinee Dararat, Teerapong Kulrat, Surachet Soontontawesub, Thitima Anothaiwalaikul, Piyawadee Bunprechawong, Rawipot Chanda, Jarin Kanchanawarin, Pinit Kidkhunthod, and Tawan Sooknoi, Catalysis Communications, 102 (2017) 123–126

(iii) Enhancing the Acylation Activity of Acetic Acid by Forming an Intermediate Aromatic Ester, Nhung N. Duong, Bin Wang, Tawan Sooknoi, Steven P. Crossley, Daniel E. Resasco, ChemSusChem, 10, Issue 13 (2017) 2823–2832

(iv) Improvement of Water Vapor Permeability of LLDPE/EVA Film with Zeolite A as Filler, S Rukchonlatee, N Jaisomboon, T Sooknoi, Key Engineering Materials, 730 (2017) 31-36

(v) Simultaneous upgrading of furanics and phenolics via hydroxyalkylation/aldol condensation reactions, Tuong V. Bui, Tawan Sooknoi, Daniel E. Resasco, ChemSusChem, 10, Issue 7 (2017) 1631–1639

(vi) Reaction mechanism of aqueous-phase conversion of γ-valerolactone (GVL) over a Ru/C catalyst, Abigail Rozenblit, Adam J. Avoian, Qiaohua Tan, Tawan Sooknoi, Daniel E. Resasco, Journal of Energy Chemistry, 25 (6) (2016) 1008–1014

(vii) Generation of reductive Zn species over Zn/HZSM–5 catalysts for n–pentane aromatization, Sikarin Tamiyakul, Tawan Sooknoi, Lance L. Lobban, Siriporn Jongpatiwut, Applied Catalysis A: General, 525, (2016) 190–196

(viii) Selective ketonization of acetic acid over HZSM-5: The importance of acyl species and the influence of water, Abhishek Gumidyala, Tawan Sooknoi, Steven Crossley, Journal of Catalysis, 340 (2016) 76–84

(ix) Surface and interlayer base-characters in lepidocrocite titanate: The adsorption and intercalation of fatty acid, Tosapol Maluangnont, Pornanan Arsa, Kanokporn Limsakul, Songsit Juntarachairot, Saithong Sangsan, Kazuma Gotoh, Tawan Sooknoi, Journal of Solid State Chemistry, 238, (2016) 175–181

(x) Synthesis of C4 and C8 Chemicals from Ethanol on MgO-Incorporated Faujasite Catalysts with Balanced Confinement Effects and Basicity, Lu Zhang, Tu N. Pham, Jimmy Faria,Daniel Santhanaraj, Tawan Sooknoi, Qiaohua Tan, Zheng Zhao, Daniel E. Resasco, ChemSusChem, 9, Issue 7 (2016) 736-748

(xi) Selective Hydrodeoxygenation of Bio-Oil Derived Products: Acetic acid to propylene over hybrid CeO_2-Cu/zeolite catalysts, Ayut Witsuthammakul and **Tawan Sooknoi**, Catalysis Science & Technology, 6 (2016) 1737-1745

(xii) Selective Hydrodeoxygenation of Bio-Oil Derived Products: Ketones to Olefins, Ayut Witsuthammakul and **Tawan Sooknoi,** Catalysis Science & Technology, 5 (2015) 3639-3648

(xiii) Role of Keto Intermediates in the Hydrodeoxygenation of Phenol over Pd on Oxophilic Supports, Priscilla M. de Souza, Raimundo C. Rabelo-Neto, Luiz E. P. Borges, Gary Jacobs, Burtron H. Davis, **Tawan Sooknoi,** Daniel E. Resasco, and Fabio B. Noronha, *ACS Catalysis*, 5 (2015) pp 1318–1329.

(xiv) Oxidation of tetrahydrofuran to butyrolactone catalyzed by iron-containing clay, Artit Ausavasukhi and **Tawan Sooknoi,** Green Chemistry, 17 (2015) 435-441

(xv) Catalytic activity enhancement by thermal treatment and re-swelling process of natural containing Fe-clay for Fenton oxidation, Artit Ausavasukhi, **Tawan Sooknoi,** Journal of Colloid and Interface Science, 436 (2014) 37–40

(xvi) Selective conversion of m-cresol to toluene over bimetallic Ni–Fe catalysts Lei Nie, Priscilla M. de Souza, Fabio B. Noronha, Wei An, **Tawan Sooknoi,** Daniel E. Resasco,Journal of Molecular Catalysis A: Chemical, 388–389 (2014) 47–55

(xvii) Hydrophobic Zeolite-Filled Polymeric Films with High Ethylene Permselectivity for Fresh Produce Packaging Applications, Fuongfuchat, A., Sirikittikul, D., Booncharoen, W., Raksa, P., Ritvirulh, C., **Sooknoi,** T. Packaging Technology and Science Volume 27, Issue 10, pages 763–773, October 2014

(xviii) Tunable activity of [Ga]HZSM-5 with H2 treatment: Ethane dehydrogenation, Artit Ausavasukhi, **Tawan Sooknoi,** Catalysis Communications, 45 (2014) 63–68

(xix) Ketonization of Carboxylic Acids: Mechanisms, Catalysts, and Applications in Bio-oil Upgrading, Tu N Pham , **Tawan Sooknoi** , Steven Crossley, Daniel E. Resasco, ACS Catalysis, 3 (2013), 2456–2473

(xx) Aqueous-phase ketonization of acetic acid over Ru/TiO2/carbon catalysts, Tu Nguyet Pham, Dachuan Shi, **Tawan Sooknoi,** Daniel E. Resasco, Journal of Catalysis, 295 (2012), 169–178

(xxi) Aromatization of Cyclopentane Over ZSM-5 Catalysts: A Proposal of Reaction Pathway, N. Peamaroon, **T. Sooknoi**, Petroleum Science and Technology, Volume 30(16) (2012), 1647-1655.

(xxii) Hydrodeoxygenation of m-cresol over gallium-modified beta zeolite catalysts, Artit Ausavasukhi, Yi Huang, Anh T. To, **Tawan Sooknoi**, Daniel E. Resasco, Journal of Catalysis, 290 (2012), 90-100.

(xxiii) Direct conversion of glycerol to acrylic acid via integrated dehydration-oxidation bed system, Ayut Witsuthammakul and **Tawan Sooknoi**, Applied Catalysis A: General, 413–414 (2012) 109–116

(xxiv) Effect of extra-framework cesium on the deoxygenation of methylester over CsNaX zeolites, Tanate Danuthai, **Tawan Sooknoi**, Siriporn Jongpatiwut, Thirasak Rirksomboon, Somchai Osuwan, Daniel E. Resasco, Applied Catalysis A:General, 409-410 (2011) 74-81

(xxv) Selective ethylene-permeable zeolite composite double-layered film for novel modified atmosphere packaging, P. Monprasit, C. Ritvirulh, **T. Sooknoi**, S. Rukchonlatee, A. Fuongfuchat, D. Sirikittikul, Polymer Engineering & Science, 51(7) (2011) 1264–1272

(xxvi) Conversion of furfural and 2-methylpentanal on Pd/SiO2 and Pd-Cu/SiO2 catalysts, Surapas Sitthisa, Trung Pham, Teerawit Prasomsri, **Tawan Sooknoi**, Richard G. Mallinson, Daniel E. Resasco, Journal of Catalysis, 280 (2011) 17-27

ผลงานวิจัยจดทะเบียนสิทธิบัตร 5 ปีย้อนหลัง

(i) Australian Patent, AU 2011293914 B2, *Master Batch for preparing plastic films with high ethylene permselectivity and the plastic films produced therefrom*, December 4th, 2014

(ii) เลขที่คำขอจดทะเบียน 1401006098 กระบวนการขจัดออกซิเจนออกจากกรดคาร์บอกซิลิกด้วยกระบวนการคีโต-ไฮโดรดีออกซิจีเนชั่น 8 ตุลาคม 2557

(iii) เลขที่คำขอจดทะเบียน 1301007386 กระบวนการเปลี่ยนชีวมวลลิกโนเซลลูโลสเป็นเชื้อเพลิงและสารประกอบเคมีพื้นฐานที่มีออกซิเจนต่ำ 26 ธันวาคม 2556

(iv) เลขที่คำขอจดทะเบียน 1101000205 การผลิตไฮโดรคาร์บอนสายยาวจากปฏิกิริยาดีคาร์บอกซิเลชันของกรดปาล์มมิติกโดยใช้โลหะออกไซด์เป็นตัวเร่งปฏิกิริยา, 15 กุมภาพันธ์ 2554

(v) เลขที่คำขอจดทะเบียน 6284 อนุสิทธิบัตร ตัวตรวจวัดแก๊สชนิดฟิล์มบางโลหะออกไซด์ที่เคลือบด้วยแผ่นเยื่อ

-ซิลิกาไลต์1ชนิดเด่นระนาบ 010, 2554